

# The introduction of Poly(3,4-ethylenedioxythiophene) into a bicontinuous interfacially jammed emulsion gel as an electrical conductor for various applications

Ing. Stefan Bouts<sup>1</sup>

Supervisors: Dr. M. F. Haase<sup>1</sup> and M. T. Alting MSc<sup>1</sup>

<sup>1</sup>Debye Institute for Nanomaterials Science, University of Utrecht, Padualaan 8, Utrecht Science Park, Physical Colloid Chemistry, Van 't Hoff Laboratory, Netherlands.

January 20<sup>th</sup> 2023.

## Abstract

The International Energy Agency (IEA) shows that energy produced by solar power has greatly increased and that the need for grid energy storage with batteries also has greatly increased. Dye-sensitized solar cells (DSSCs) are a low cost and environmentally friendly solar cell. The limited surface area of these solar cells results in fast recombination of electrons thus reducing the efficiency. The relative small surface area of lithium-ion batteries increases the diffusion limitations of these batteries; resulting in a limited charging performance at high current. Bicontinuous interfacially jammed emulsion gels (Bijels) could be a low cost, high surface area template for a solar cell or battery with the ability to exchange chemicals between phases. The common ground is the need for an electrical conductor; therefore, the research question will be: to which extent can we introduce Poly(3,4-ethylenedioxythiophene) (PEDOT) into a silica bijel system forming a conductive bijel? This research question was investigated by using a model system and a bijel system which were investigated using timelapse, zeta-potential, Scanning Electron Microscope (SEM) Energy Dispersive X-ray (EDX), confocal and conductivity measurements. The model system found that the polymerization speed of PEDOT and change in zeta-potential of the silica particles is dependent on the oxidizer. The SEM-EDX confirmed the formation and electrostatic adsorption on the silica particles. The polymerization from the water phase of the bijel resulted in a decrease of polarity of the silica surface. The addition of pre-polymerized EDOT was sufficient to keep the structure open and increase the conductivity significantly. The concentration increase of an oil-soluble oxidizer increased the conductivity and gave more control over the polymerization. This research extends our knowledge of the introduction of PEDOT into the bijel system and is an experimental stepping stone for future fundamental research. Considerably more work will need to be done to determine the effects of PEDOT polymerization to the bijel system.

**Keywords:** Bijels, PEDOT, DSSCs, Batteries



# Contents

Abbreviations	4
<b>1 Introduction</b>	<b>5</b>
<b>2 Theoretical background</b>	<b>6</b>
2.1 Emulsion behavior . . . . .	6
2.2 Stabilized emulsions . . . . .	6
2.2.1 Surfactant stabilized emulsions . . . . .	6
2.2.2 Nanoparticle stabilized emulsions . . . . .	7
2.3 Bicontinuous interfacially jammed emulsion gels (Bijels) . . . . .	9
2.4 Poly(3,4-ethylenedioxythiophene) (PEDOT) . . . . .	11
2.4.1 General . . . . .	11
2.4.2 Polymerization . . . . .	11
<b>3 Experimental setup</b>	<b>14</b>
3.1 Chemicals & materials . . . . .	14
3.2 Model system . . . . .	14
3.2.1 Timelapse . . . . .	14
3.2.2 Zeta-potential . . . . .	15
3.2.3 Scanning Electron Microscope (SEM) Energy Dispersive X-ray (EDX) . . . . .	17
3.3 Bijel system . . . . .	18
3.3.1 Precursor dispersion preparation . . . . .	18
3.3.2 Microfluidic devices . . . . .	19
3.3.3 Device coating . . . . .	19
3.3.4 Bijel fiber printing . . . . .	20
3.3.5 TEOS treatment . . . . .	20
3.3.6 Polymerization EDOT to PEDOT in bijel fibers for confocal analysis . . . . .	20
3.3.7 Conductivity measurement . . . . .	21
3.4 Characterization . . . . .	22
3.4.1 Timelapse experiments . . . . .	22
3.4.2 Zeta-potential experiments . . . . .	22
3.4.3 Scanning electron microscope (SEM) - Energy Dispersive X-ray (EDX) experiments	22
3.4.4 Confocal microscope experiments . . . . .	23
3.4.5 Conductivity experiments . . . . .	23
<b>4 Results and discussion</b>	<b>24</b>
4.1 Model system . . . . .	24
4.1.1 Timelapse . . . . .	24
4.1.2 Zeta-potential . . . . .	27
4.1.3 SEM-EDX . . . . .	30
4.2 Bijel system . . . . .	33
4.2.1 Confocal microscope . . . . .	33
4.2.2 SEM-EDX . . . . .	37
4.2.3 Conductivity measurement . . . . .	40
<b>5 Conclusions and outlook</b>	<b>43</b>
<b>6 Acknowledgements</b>	<b>44</b>
References	45
Appendices	48

---

## Abbreviations

Abbreviations	Meaning
Bijels	Bicontinuous interfacially jammed emulsion gels
CTAB	Hexadecyltrimethylammonium bromide
DEP	Diethyl phthalate
DSSCs	Dye Sensitized Solar Cells
EDOT	3,4-ethylenedioxythiophene
EDX	Energy Dispersive X-ray
Fe(III)(OTs) <sub>3</sub>	Iron(III) p-toluenesulfonate hexahydrate
ID	Inner Diameters
IEA	International Energy Agency
OD	Outer Diameters
OTS	Octadecyltrichlorosilane
PEDOT	Poly(3,4-ethylenedioxythiophene)
PV	Photovoltaics
SEM	Scanning Electron Microscope
ST-IPS	Solvent Transfer Induced Phase Separation
TEOS	Tetraethyl orthosilicate

# 1 Introduction

The cumulative solar Photovoltaics (PV) capacity surpassed 2% of the world's power production in 2017, according to the IEA (International Energy Agency), which also predicted that PV will dominate the increase of renewable energy capacity over the following five years [1]. It also anticipates that global investment in battery energy grid storage reaches 20 billion in 2022. This is an important factor for the stability of the grid when excess renewable energy is generated when not required by the grid [2, 3].

The energy generation with renewable energy and the energy storage coincide and rely on each other to function. One prominent example for renewable energy generation are solar cells, more specifically Dye Sensitized Solar Cells (DSSCs) which are low cost solar cells. DSSCs have a lot of advantages over conventional silicon based solar cells. This is because of its cost effectiveness and its ability to work under low light and indoor light conditions while being not as harmful for the environment as conventional solar cells. However, in practice it is difficult to get a good price to performance because of its low efficiency. [4-6]. The modern DSSCs are based on titanium dioxide covered in a dye which is in contact with an electrolyte. There are various issues affecting the performances of DSSCs; light scattering capability, interfacial contact and dye/electrolyte sealing. By increasing the interfacial contact the electron collection is increased, thus reducing the recombination reaction of the electrons. This increases efficiency and thus the cost effectiveness [6].

The other half of electrification is the storage of the generated energy which can be done in batteries. Lithium-ion battery research focuses on extending lifetime, boosting energy density, enhancing safety, cutting costs, and quickening charging. To decrease charging time one could increase the current applied when charging. When the 4.2 volt limit of a lithium-ion battery is reached, charging slows down significantly. A significant process here is diffusion, which is connected to the battery's kinetics. Because of the diffusion of lithium ions from the anodic to the cathodic sides of the battery, which takes the form of an electrochemical potential gradient. For batteries increasing the surface area could increase the charging performance by decreasing the diffusion limitations [7, 8].

One could use Bicontinuous interfacially jammed emulsion gels (Bijels) as an template with high interfacial contact for DSSCs, decreasing electron recombination thus increasing the efficiency. The bijel also does not limit the electrolyte diffusion to the dye, thus allowing for a closed circuit to be possible. The bijel template still allows for the diffusion of lithium ions while also decreasing the diffusion distance because of its high interfacial area, thus increasing the charging performance at higher current. Bijels were first mentioned as a hypothetical new class of soft materials in 2005 [9, 10]. Bijels are formed by taking two immiscible liquids and mixing them with a solvent and surface active nanoparticles making a precursor dispersion. By removing the solvent from this to a continuous phase, spinodal decomposition is triggered. The surface active nanoparticles arrest the structure in place by interfacially jamming, creating a bicontinuous structure this process is also called Solvent Transfer Induced Phase Separation (STriPS) [11]. The common ground for DSSCs and batteries is the need for an electrical conductor; therefore, the research question will be: to which extend can we introduce Poly(3,4-ethylenedioxythiophene) (PEDOT) into a silica bijel system forming a conductive bijel? Here the PEDOT is a conductive polymer acting as an electrical conductor. The first hypothesis is; the introduction of EDOT into the precursor dispersion will be a viable way to introduce PEDOT into a bijel. The second hypothesis is; the introduction of PEDOT after the bijel has already been formed will be a viable way to introduce PEDOT into the bijel. Here the PEDOT should electrostatically adsorb onto the silica of the nanoparticles at the interface of the bijel. This should allow for a conductive layer to form around it and reinforce the structure. To obtain a better understanding of the PEDOT introduction into a bijel system, a model system was set up based around silica particles. Timelapses are used to investigate the polymerization rate and to investigate where the polymerization takes place. Zeta-potential measurements are used to see if PEDOT can electrostatically adsorb onto the silica particles. The SEM-EDX measurements are done to visually see if PEDOT is adsorbed onto the silica and confirm this with EDX. Finally, the bijel system itself will be investigated. This was done by confocal microscopy and SEM-EDX which allowed us to see how the structure changes based on the various polymerization conditions and also confirm the PEDOT adsorption by looking at the structure. Conductivity measurements are used to confirm that the PEDOT can become conductive by the introduction of PEDOT.

## 2 Theoretical background

### 2.1 Emulsion behavior

An emulsion is defined as a system with two liquids where spherical droplets of an immiscible liquid are dispersed in a continuous phase. First, the system has to be aggregated to form an emulsion as shown in figure 2. Any emulsion system's interfacial property determines the colloid stability and instability if no stabilizers are added. This is because the energy per molecule for each liquid is higher at the interface than in the bulk. To lower the interfacial area and consequently the total interfacial energy between the two phases, the mixture is often pushed by thermodynamics to phase separation [12, 13]. This causes emulsion coalescence, which can happen via various ways: flocculation, sedimentation, creaming & Ostwald ripening. This all happens to reduce the interfacial area of the interface, thus reducing the interfacial free energy. To prevent the phase separation an energy barrier needs to be introduced which can be done by stabilizing agents such as surfactants, which will be discussed in the next chapter [14, 15].

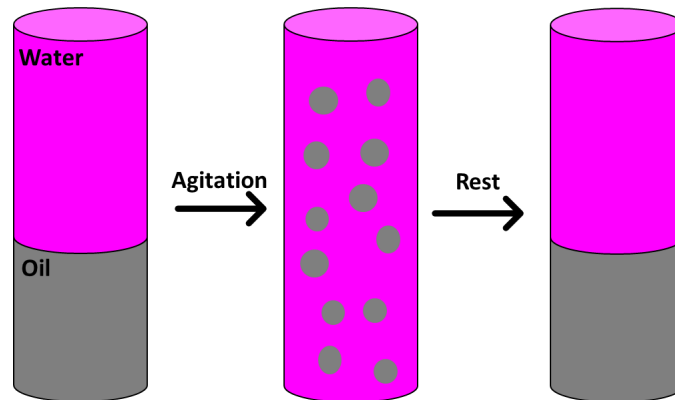


**Fig. 1:** A phase separated composition of oil (black) and water (magenta) forming an emulsion after agitation, which phase separated after a period of rest.

### 2.2 Stabilized emulsions

#### 2.2.1 Surfactant stabilized emulsions

Amphiphilic molecules like surfactants are inclined to bind to the oil-water interface. They lower the tension between the oil and the water at the interface, which lowers the energy needed to produce an emulsion. Surfactant molecules that have been adsorbed at the interface function as steric or electrostatic barriers to slow down droplet coalescence and improve emulsion stability (see figure 2) [16].

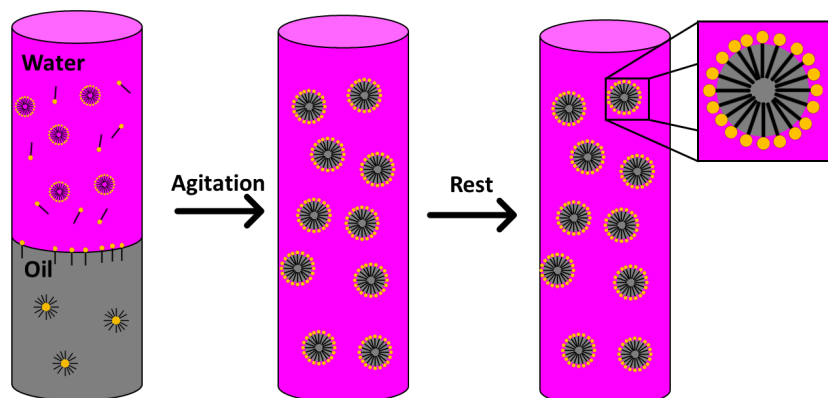


**Fig. 2:** A phase separated composition of oil (black) and water (magenta) containing surfactant forming an emulsion after agitation, which forms a stable emulsion after rest.

The emulsion stabilization with surfactants is highly dependent on various factors which can limit the applications of using surfactants to create, for example, a bicontinuous structure. This is because surfactants are sensitive to various parameters. This results in surfactants that can be easily detach from the oil-water interface and rearrange. To circumvent this issue, one could use nanoparticles to stabilize the emulsion, which in many ways similar to a conventional surfactant stabilized emulsion which will be discussed in the next chapter [17, 18].

### 2.2.2 Nanoparticle stabilized emulsions

Emulsions stabilized by particles (see figure 3) was first described by S. U. Pickering in 1907 thus, finding the name Pickering emulsion [19]. However, W. Ramsden first recognized the effect of nanoparticles stabilizing the emulsion [20].

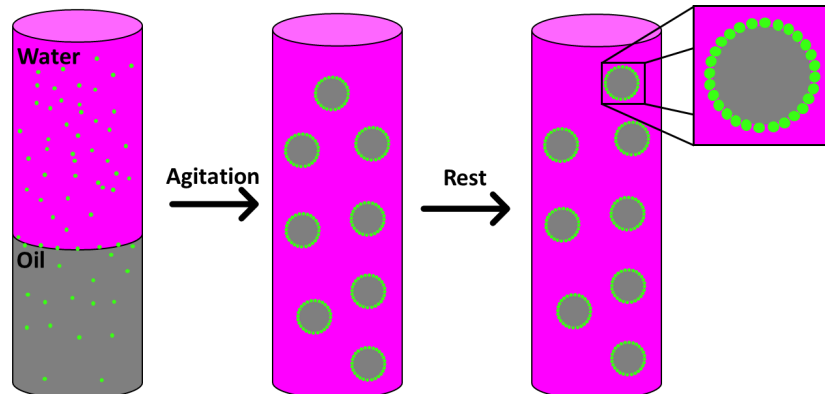


**Fig. 3:** A phase separated composition of oil (black) and water (magenta) containing surface active nanoparticles (green) forming an emulsion after agitation, which forms a stable emulsion after rest.

The stabilization of emulsions with nanoparticles happens because of adhesion of the nanoparticles to the interface of the two phases. Normally, for example, silica nanoparticles are hydrophilic and don't have a strong interaction with the oil phase. One could change this interaction strength to be more favored by the oil phase. This can be done by adsorbing a hydrophobic surfactant onto the surface area of the nanoparticle. A surfactant with an opposite charge of the nanoparticle can, for example, be used to change the wettability of the nanoparticle. When the wettability of the particle changes (also referred to as the contact angle) to above 90 degrees ( $\theta_{w/o} > 90^\circ$ ), it will result in a W/O emulsion. If not enough or no surfactant is adsorbed to the nanoparticle, then, the contact angle will be below 90 degrees ( $\theta_{o/w} < 90^\circ$ ). This change in wettability of the particle and thus contact angle, results in an O/W emulsion. If the contact angle is 90 degrees the particle has equal affinity with the oil and water phase, creating a neutrally wetting particle [17]. To vary the adsorption of the surfactant onto the nanoparticle, the change in surfactant concentration can result in different wettability as shown in figure 4.

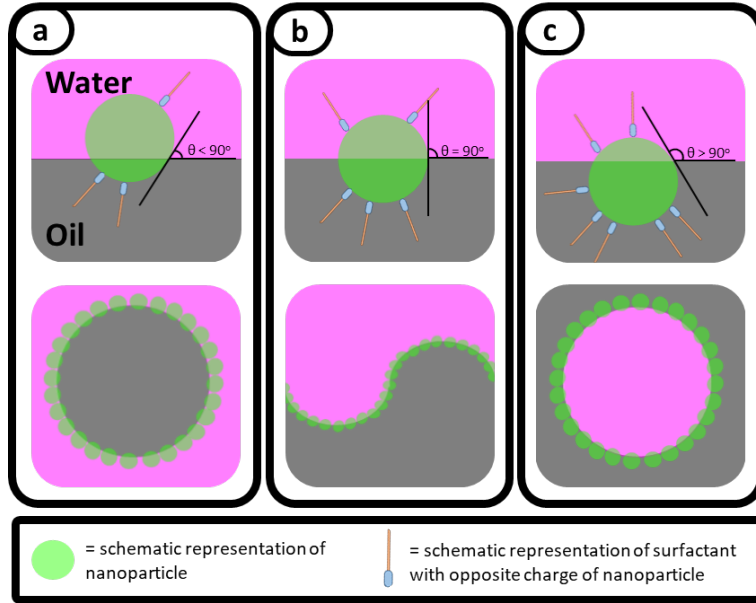


**Fig. 4:** Effect of surfactant adsorption onto nanoparticle (green) and contact angle. **a)** With a contact angle smaller than 90 degrees the particle is more hydrophilic and thus have more interaction with the water (magenta) and create an O/W emulsion. **b)** When the contact angle is equal to 90 degrees the particle has an equal interaction with the oil (black) and water and thus creating a curved interface. **c)** If more surfactant is added, the particle becomes more hydrophobic and thus has more interaction with the oil and creating a W/O emulsion

The hydrophobic tails increase the affinity of the particle to the hydrophobic oil phase. As mentioned before, the surfactant concentration is an important factor to contact angle; however, the variation of pH can also result in difference of contact angle [21]. An important factor of contact angles ( $\theta$ ) is understanding the energy difference of moving a particle from 1 phase to the interface. The contact angle is dependent on the free energy of the surface of the various interfaces with specific interfacial tensions: particle-water ( $\gamma_{p/w}$ ), particle-oil ( $\gamma_{p/o}$ ) and oil-water ( $\gamma_{o/w}$ ) forming Young's equation (1) [17, 22, 23].

$$\gamma_{p/o} - \gamma_{p/w} = \gamma_{o/w} \cos(\theta) \quad (1)$$

If a small spherical particle is at the oil-water interface it is in equilibrium state "i", here the surface free energy  $E^i$  is at it's minimum giving equation 2.

$$E^i = \gamma_{o/w} A_{o/w}^i + \gamma_{p/w} A_{p/w}^i + \gamma_{p/o} A_{p/o}^i \quad (2)$$

Here  $A^i$  describes the area of the respective interface where the sum equals the surface area of the particle ( $A_p$ ) as shown by equation 3.

$$A_p = A_{p/w}^i + A_{p/o}^i \quad (3)$$

If a particle at the final state "j" in the bulk of a certain phase the surface free energy becomes  $E^j$ . Here the surface free energy of a particle in the oil bulk phase ( $E_o^j$ ) gives equation 4.

$$E_o^j = \gamma_{o/w} A_{o/w}^j + \gamma_{p/o} A_{p/o}^j \quad (4)$$

Here the  $A_{o/w}^j$  is the area of the oil-water interface after the detachment, where  $A_{p/o}^j$  is equal to  $A_p$ . Taking into account equations 1,3 and subtracting equation 2 from equation 4 the equation of particle detachment  $\Delta E_{d/o}$  is obtained (see equation 5).



$$\Delta E_{d/o} = \gamma_{o/w}(A_c + A_{p/w}^i \cos\theta) \quad (5)$$

Here the  $A_c$  is equal to  $A_{o/w}^j - A_{o/w}^i$  which is the area of the oil-water interface that is engaged by the particle. Doing the same derivation for the water phase results in equation 6.

$$\Delta E_{d/w} = \gamma_{o/w}(A_c + A_{p/o}^i \cos\theta) \quad (6)$$

Using equation 3 and equation 6 we get an expression of equation 5 yields equation 7.

$$\Delta E_{d/o} = \Delta E_{d/w} + \gamma_{o/w} A_c \cos\theta \quad (7)$$

For the spherical particles with radius  $R$ , combining  $A_c = \pi(R \sin\theta)^2$  and  $A_{p/w} = 2\pi R^2(1 + \cos\theta)$  with equations 6,7 result in equation 8 and equation 9.

$$\Delta E_{d/w} = \pi R^2 \gamma_{o/w} (1 - \cos(\theta))^2 \quad (8)$$

$$\Delta E_{d/o} = \pi R^2 \gamma_{o/w} (1 + \cos(\theta))^2 \quad (9)$$

Combining equation 8 and equation 9 where  $\Delta E_d$  is equal to  $\Delta E_{d/w}$  for  $0 \leq \theta \leq 90^\circ$  and is equal to  $\Delta E_{d/o}$  for  $90 \leq \theta \leq 180^\circ$  results in equation 10.

$$\Delta E_d = \pi R^2 \gamma_{o/w} (1 - |\cos(\theta)|)^2 \quad (10)$$

Here the attachment energy to the interface  $\Delta E_a$  is equal to the negative detachment energy  $-\Delta E_d$  resulting in equation 11.

$$\Delta E_a = -\pi R^2 \gamma_{o/w} (1 - |\cos(\theta)|)^2 \quad (11)$$

The attachment energy  $\Delta E_a$  (see equation 11) is maximized and detachment energy  $\Delta E_d$  (see equation 10) is minimized if  $\cos(\theta) = 0$ . This is the case if  $\theta = 90^\circ$ , thus meaning that enough surfactant needs to be adsorb onto the particle making it neutrally wetting. To summarize, the importance of a neutrally wetting particle is because of curvature of the oil water interface and having a high attachment energy to the interface. The next chapter will discuss Bicontinuous interfacially jammed emulsion gels (Bijels), which rely on these properties of the neutrally wetting particle.

### 2.3 Bicontinuous interfacially jammed emulsion gels (Bijels)

The particle stabilization is a very important factor for bicontinuous interfacially jammed emulsion gels (bijels). Bijels were first mentioned as a hypothetical new class of soft materials in 2005 [9, 10]. Bijels have been demonstrated to form using spherical surface-active colloidal particles [24]. As shown in figure 5, the starting dispersion is a homogeneous dispersion with oil, water, solvent and surface active nanoparticles indicated by the red dot (i). This specific composition, where the dispersion is allowed to go through spinodal decomposition is called the plait point. By the diffusion of the solvent to a continuous phase, the system shifts its composition in the ternary phase diagram as indicated by the blue arrow. This process is referred to Solvent Transfer Induced Phase Separation (STrIPS), which is the process of phase separation by the extraction of a solvent. This change in composition allows for the solution to go through spinodal decomposition resulting in the bicontinuous structure which is arrested by the surface-active nanoparticles. The dispersion follows the tie lines connecting to a specific composition which connects to the binodal line. Which results in water-rich (ii) and oil-rich (iii) phase, resulting in a composition only containing oil and water. If the precursor dispersion has a different phase composition than indicated by the red dot. The dispersion will not go through spinodal decomposition first, but through binodal decomposition, resulting in nucleation and growth [9, 25].

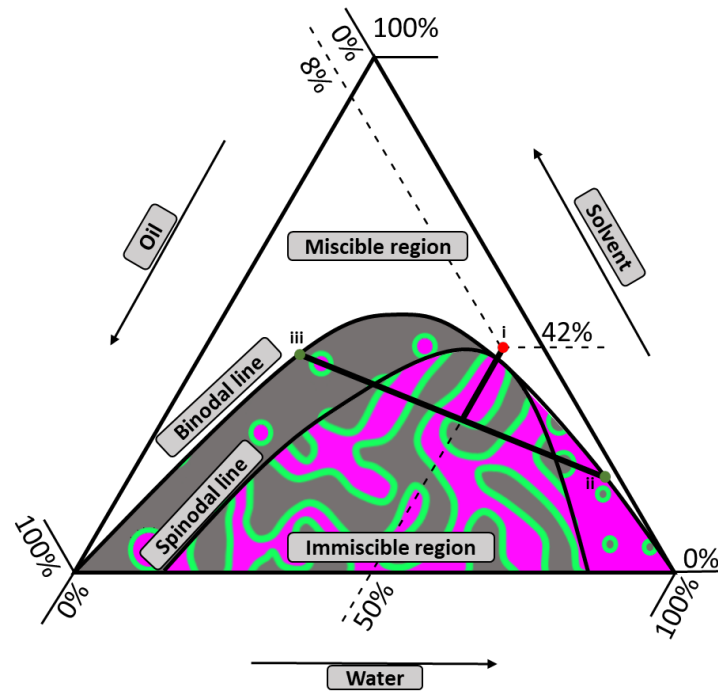


**Fig. 5:** Here the schematically portrayed ternary phase diagram consists of oil, water and a solvent. Here, for example, the red dot (i) is a composition of  $\%_{\text{oil}} = 8$ ,  $\%_{\text{solvent}} = 42$ ,  $\%_{\text{water}} = 50$ . This composition is just above the binodal and spinodal line in the miscible region. The black line indicates the change in composition of the red dot (i) due to solvent transfer into a continuous phase. Which results in a composition only containing oil and water.

The usage of a flow device made from glass capillaries allows for a defined size of bijel (see figure 6). If the flow is correct of both phases, the formation of a continuous fiber can be achieved [11]. The solvent close on the outside of the bijel and thus closed to the continuous phase diffuses relatively quickly; after this the solvent diffusion slows down because of the created structure on the outside. Which allows for coarsening to take place of the structure deeper inside of the bijel structure, thus resulting in a pore-size gradient [26]. The bijel can be used as a template for the introduction of a conductive polymer which will be discussed next.

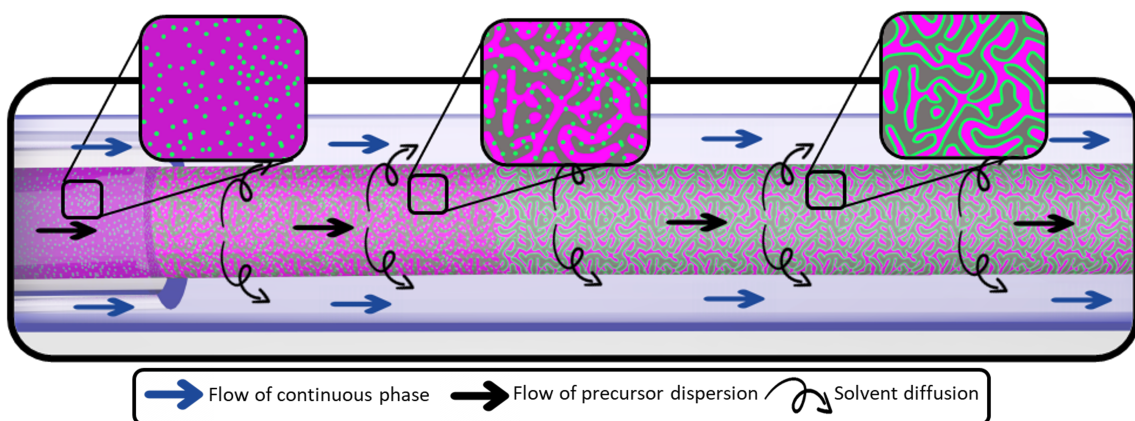


**Fig. 6:** The precursor dispersion starts from the inner capillary, while in the outer capillary flows a continuous phase for the solvent to diffuse into. The evolution of the bijel formation is schematically shown in the inserts.

## 2.4 Poly(3,4-ethylenedioxythiophene) (PEDOT)

### 2.4.1 General

One of the first important instances of a conducting polymer was a publication in 1977 of doped polyacetylene, which later was honored with a Nobel prize in 2000 [27]. The conductivity of conjugated polymers has a wide range. Ranging from semi-conductors with a conductivity of  $10^{-8}$  to  $10^3$  S/cm or even metallic conductors with a conductivity of  $10^6$  S/cm or higher. This shows, depending on the conductivity of the polymer, it can be used for a specific application where a semi-conductor or a metallic conductor is needed [28]. The conductivity of metals and semiconductors come from the excitation of electrons into the conduction band giving the electrons mobility [29]. Conjugated polymers have a  $\pi$  system in their backbone. An energy gap between a fully filled  $\pi$  band and an empty  $\pi^*$  band is the outcome of the nature of the alternating  $\pi$  bonds. The energy cost of rearranging the carbon atoms is outweighed by the energy savings brought on by the new band gap. Purified conjugated polymers are normally semiconductors because there are no partially filled bands. However, similar to inorganic semiconductors, these polymers can be ‘doped’ with a counter ion changing their electronic properties. This ‘doping’ is normally not the correct wording, but it refers to the chemical oxidation or reduction of the polymers [28, 30, 31].

### 2.4.2 Polymerization

One of those conducting- (conjugated-) polymers is Poly(3,4-ethylenedioxythiophene) (PEDOT). The polymerization from the monomer 3,4-ethylenedioxythiophene (EDOT) to the conjugated polymer Poly(3,4-ethylenedioxythiophene) was first introduced by Bayer AG in 1989 [32]. There are several ways to polymerize the monomer; the main ways are electrochemical polymerization and chemical polymerization [31, 33]. Electrochemical polymerization is the polymerization through an applied potential. Here usually the electrolyte solution contains certain electrolytes which can form as counter agents to dope the PEDOT increasing the polymerization rate [31]. However, this process often results in the spontaneous propagation of the polymerization, resulting in various branches growing from the electrodes [34].

The second widely used method is chemical polymerization, which relies on an oxidator. Here an oxidating agent such as Fe(III) can be used to polymerize EDOT, which is very unstable to oxidizing agent, so oxidizers such as nitric acid are too strong. The possibilities of oxidizers are very vast; however, the most common used oxidizer is Fe(III)Cl<sub>3</sub>. The addition of Na<sub>2</sub>S<sub>2</sub>O<sub>8</sub> allows for the rapid polymerization of EDOT. The Fe(III) here acts as a catalyst to decompose the peroxodisulfate [35, 36]. The decomposition of the peroxodisulfate creates radicals which can initiate the polymerization as shown in figure 7.

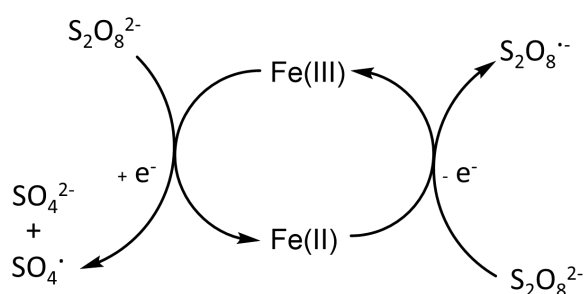


**Fig. 7:** The Fe(III) is reduced to Fe(II) creating a sulfate radical from the Na<sub>2</sub>S<sub>2</sub>O<sub>8</sub>. The Fe(II) can be oxidized again creating a Na<sub>2</sub>S<sub>2</sub>O<sub>8</sub> with a radical. Image adapted from Haizhou Liu *et al.* [36].

The combination of these two allows for the rapid radical generation and thus the rapid polymerization. This polymerization can also be acid catalyzed, but this does not achieve high conductivity [31, 35]. The polymerization mechanism based on FeCl<sub>3</sub> is shown in figure 8.

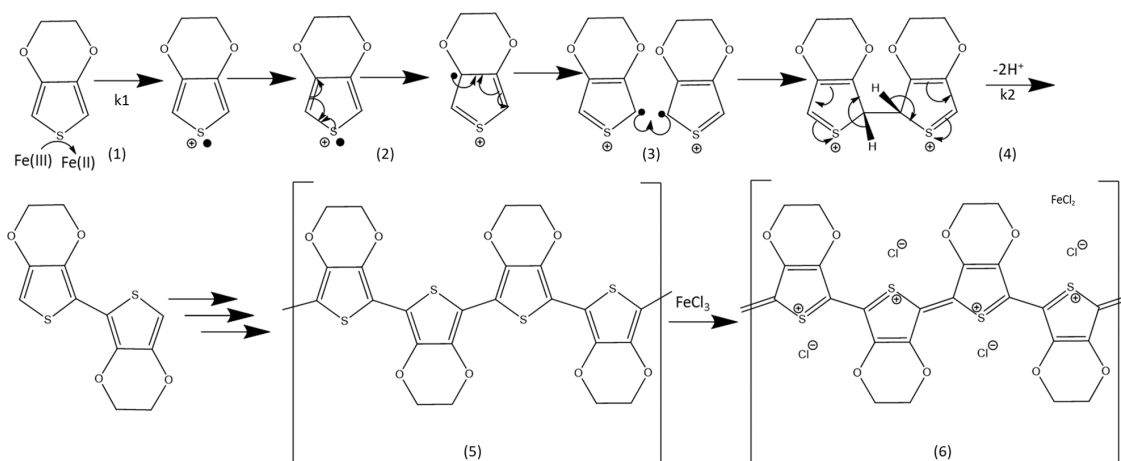


**Fig. 8:** In this figure the proposed mechanism is shown according to Sakunpongpitiporn *et al.* [37] and Mueller *et al.* [38] based on  $\text{FeCl}_3$ . (1) Here the oxidizing agent gets reduced by taking up electrons from EDOT. (2) After this, the EDOT can delocalize the charge with in the monomeric EDOT [33]. (3) This brings a radical to two alpha hydrogen positions of the EDOT after this two radicals of two monomers of EDOT can form a dimer where (4) 2 molar equivalents of  $\text{H}^+$  is formed. (5) This then forms neutrally charged PEDOT. (6) After another oxidation, the PEDOT becomes charged and is doped by the available counter-ions.

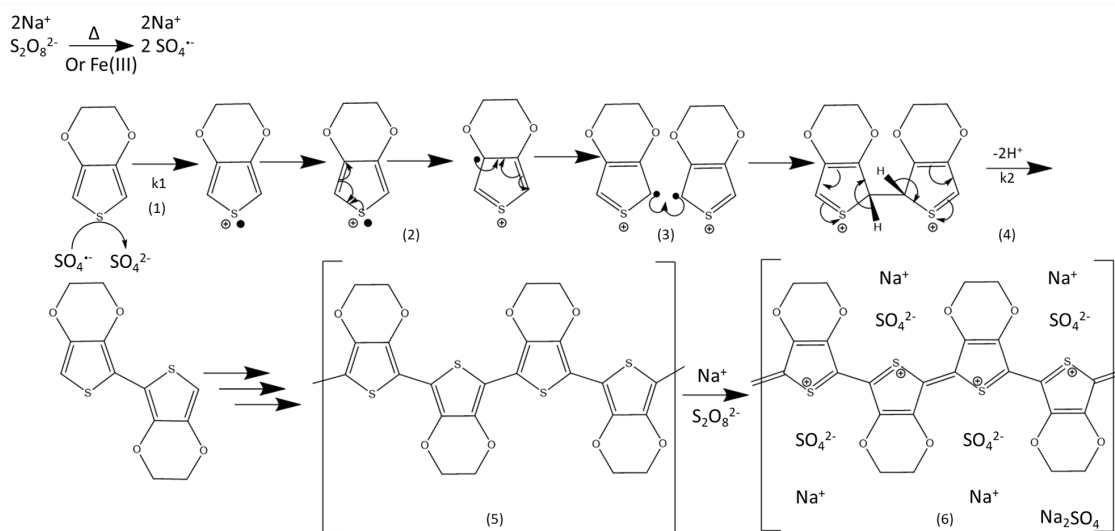


**Fig. 9:** In this figure the proposed mechanism is shown according to Sakunpongpitiporn *et al.* [18] based on  $\text{Na}_2\text{S}_2\text{O}_8$ . (1) Here the oxidizing agent gets reduced by taking up electrons from EDOT. (2) After this, the EDOT can delocalize the charge with in the monomeric EDOT [33]. (3) This brings a radical to two alpha hydrogen positions of the EDOT after this two radicals of two monomers of EDOT can form a dimer where (4) 2 molar equivalents of  $\text{H}^+$  is formed. (5) This then forms neutrally charged PEDOT. (6) After another oxidation, the PEDOT becomes charged and is doped by the available counter-ions.

These oxidizers are normally also the doping agents of PEDOT because these salts can act as the counter ion thus doping it. Such oxidizers can be iron(III) chloride, iron(III) tosylate, or sodiumperoxodisulfate resulting in chloride, tetrachloroferrate, tosylate, or sulfate as counterions. First, the oxidizers polymerizes the EDOT creating a neutral, undoped, polymer. The excess oxidizer can oxidize it again charging

---

and doping the polymer [31] as shown in figure 8. Here the doped PEDOT has a much higher conductivity compared to the neutrally charged variant [39]. The slowest reaction rate of the polymerization is the oxidation and radical creation ( $k_1 = 0.16 \text{ L}^3 \text{ mol}^{-3} \text{ h}^{-1}$ ) of the EDOT monomer, after this it forms a dimer and trimer relatively fast ( $k_2 = 10^8\text{--}10^9 \text{ L mol}^{-1} \text{ h}^{-1}$ ).

This can result in a highly conductive polymer; however, a lot of factors influence the conductivity of the polymer. The following factors can change the conductivity: humidity [40], counter ion [31], ratio PEDOT to counterion [31], solvent [41], reaction temperature [31] and more. This is great for all the different applications it can be used for such as: electrodes [42, 43], OLEDs [43], dye-sensitized solar cells (DSSCs) [44], oxygen reduction reaction reactions [44] and more. However, this also means the PEDOT is highly sensitive to various reaction conditions which could influence conductivity. The next chapter describes the procedures and methods used in this research.

## 3 Experimental setup

### 3.1 Chemicals & materials

**Table 1** Chemicals used in the experiments with their purity, type of chemical and supplier.

Chemicals	Purity	Supplier
Stöber silica (dispersion in ethanol, ca. 400 nm)	N/A	Synthesized by Haran
LUDOX <sup>®</sup> TMA (34wt% aqueous dispersion, ca. 20 nm)	N/A	Grace
Toluene	>99%	Thermos scientific
Diethyl phthalate (DEP)	99%	ACROS Organics
n-Hexane	>99%	Biosolve BV
3,4-Ethylenedioxythiophene (EDOT)	100%	ChemCruz <sup>®</sup>
Iron chloride hexa-hydrate (FeCl <sub>3</sub> )	100 %	Sigma-Aldrich
Sodium persulfate (Na <sub>2</sub> S <sub>2</sub> O <sub>8</sub> )	>98%	Fisher bioreagents
Iron(III) p-toluenesulfonate hexahydrate (Fe(III)(OTs) <sub>3</sub> )	100%	Sigma-Aldrich
Sodium chloride	N/A	Sigma-Aldrich
1-propanol	≥99.5%	Sigma-Aldrich
1-pentanol	≥99.0%	Sigma-Aldrich
Glycerol	>99%	Thermo scientific
Mineral oil	100%	Sigma-Aldrich
Octadecyltrichlorosilane (OTS)	N/A	ChemCruz <sup>®</sup>
Tetraethyl orthosilicate (TEOS)	≥99%	Sigma-Aldrich
Nile red	99%	Sigma-Aldrich
Hexadecyltrimethylammonium bromide (CTAB)	>99%	Sigma-Aldrich

### 3.2 Model system

To obtain a better understanding of the PEDOT introduction into a bijel system, a model system was set up based around silica particles. This was done because a bijel system is difficult to investigate because of its complex nature. There were two model systems set up based around two different silica particles. The first model was with the Ludox TMA which also used in the formation of a bijel. This was done to understand the effects on the physical properties of the particles that underwent reaction with EDOT. The second was based around Stöber silica which was used to visualize and analyse the spatial distribution of the PEDOT. These were used because individual particles could be visually observed because of their submicron size.

#### 3.2.1 Timelapse

To study the first model system timelapse were done. These were done to study the effects of FeCl<sub>3</sub>, Na<sub>2</sub>S<sub>2</sub>O<sub>8</sub> and Ludox TMA on the polymerization of EDOT (molar weight: 142.17 g/mol, density: 1.34 g/cm<sup>3</sup>). Here we look at the reaction speeds with the oxidizers and the interaction of PEDOT and the particles. This is based on the principle that PEDOT is black and the surrounding environment is white, thus allowing for a clear optical transition to be shown. As shown in table 2 stock solution of sodium persulfate (Na<sub>2</sub>S<sub>2</sub>O<sub>8</sub>, molar weight: 238.03 g/mol) and iron chloride hexa-hydrate (FeCl<sub>3</sub> 6 H<sub>2</sub>O, molar weight: 270.33 g/mol) was made with a concentration of 0.2 g/mL. This was done by weighing 2 grams of Na<sub>2</sub>S<sub>2</sub>O<sub>8</sub> or FeCl<sub>3</sub> in a 20 mL vial, then adding 10 mL of DI water. Finally, the closed vials were heated under warm water to ensure rapid dissolution of the chemicals; this procedure was used for all

stock solutions. The stock solutions were used to make the samples listed in table 3, 4. The measurements were done by first adding the Deionized (DI) water (Conductivity 18.2 M $\Omega$  at 25°C) and Ludox TMA if required to a container, then the EDOT was added. This was to ensure no polymerization was happening before the timelapse was started. After this the timelapse was started and the oxidizers were added.

**Table 2** Composition of Na<sub>2</sub>S<sub>2</sub>O<sub>8</sub>, FeCl<sub>3</sub> 6 H<sub>2</sub>O stock solutions that were used for timelapse and SEM experiments.

Stock solution	Amount (g)	DI water (mL)	Concentration (mg/mL)
Na <sub>2</sub> S <sub>2</sub> O <sub>8</sub>	0.2	1	200
FeCl <sub>3</sub> 6 H <sub>2</sub> O	0.2	1	200

**Table 3** Composition of samples that were used in the timelapse experiments consisting of the Ludox TMA, DI water, EDOT (table 1) and Na<sub>2</sub>S<sub>2</sub>O<sub>8</sub>, FeCl<sub>3</sub> 6 H<sub>2</sub>O stock solutions (table 2).

Sample	Total volume (mL)	Ludox TMA (mL)	DI water (mL)	EDOT ( $\mu$ L)	Na <sub>2</sub> S <sub>2</sub> O <sub>8</sub> stock solution (mL)	FeCl <sub>3</sub> 6 H <sub>2</sub> O stock solution (mL)
1	10	0.0	10	40	0.0	0.0
2	10	0.0	9.8	40	0.1	0.1
3	10	0.5	9.3	40	0.1	0.1
4	10	0.0	9.8	40	0.2	0.0
5	10	0.0	9.8	40	0.0	0.2
6	5	0.0	4.8	40	0.1	0.1
7	5	0.25	4.55	40	0.1	0.1

**Table 4** Concentrations of Na<sub>2</sub>S<sub>2</sub>O<sub>8</sub> and FeCl<sub>3</sub> (mmol/L) in the samples of table 3. With the corresponding ratio of Na<sub>2</sub>S<sub>2</sub>O<sub>8</sub>, FeCl<sub>3</sub> and EDOT in mmol.

Sample	Na <sub>2</sub> S <sub>2</sub> O <sub>8</sub> (mmol/L)	FeCl <sub>3</sub> (mmol/L)	Ratio Na <sub>2</sub> S <sub>2</sub> O <sub>8</sub> : FeCl <sub>3</sub> : EDOT (mmol)
1	0.0	0.0	0.000 : 0.000 : 0.380
2	8.4	7.4	0.084 : 0.074 : 0.380
3	8.4	7.4	0.084 : 0.074 : 0.380
4	16.8	0.0	0.168 : 0.000 : 0.380
5	0.0	14.8	0.000 : 0.148 : 0.380
6	8.4	7.4	0.084 : 0.074 : 0.380
7	8.4	7.4	0.084 : 0.074 : 0.380

### 3.2.2 Zeta-potential

In the zeta-potential measurements, the effect of PEDOT on the zeta-potential of the Ludox TMA was studied. First, CTAB, Na<sub>2</sub>S<sub>2</sub>O<sub>8</sub> and FeCl<sub>3</sub> stock solutions were made according to table 5. These stock solutions were used to make the samples for the zeta-potential measurements according to table 6,7. A stirring bar was added to the 20 mL vial after all the chemicals were added for samples 1-10. The vial was closed with a screw on cap and vigorously stirred at 1500 rpm for 7 days, this ensured that the polymerization was fully completed. For samples 11 and 12, the LUDOX TMA particles were added after 6 days of vigorous stirring with the other chemicals. After 1 day the samples were all stirring at room

temperature (ca. 19 C°) for 7 days total. Before the measurement, all the samples were heated at 40-50 C° for 2 hours in a water bath, this ensured that the polymerization was fully completed. The samples were left at room temperature for 1 hour before 5 mL was taken from the sample vial to measure the zeta-potential. To this 5 mL of sample 1-2 droplets of 1M NaOH were added to ensure the pH was around 11. All samples measured were visually stable and showed no visual sedimentation.

**Table 5** Composition of stock solutions that were used for zeta-potential experiments.

Stock solutions	Amount (g)	DI water (mL)	Concentration (mg/mL)
Na <sub>2</sub> S <sub>2</sub> O <sub>8</sub>	0.2	1	200.0
FeCl <sub>3</sub> 6 H <sub>2</sub> O	0.005	1	5.0
CTAB	0.100	1	100.0

**Table 6** Composition of samples that were measured in the zeta-potential experiments consisting Ludox TMA, DI water and EDOT (table 1) and Na<sub>2</sub>S<sub>2</sub>O<sub>8</sub>, FeCl<sub>3</sub> and CTAB stock solutions (table 5).

Sample	Total volume (mL)	Ludox TMA (mL)	DI water (mL)	EDOT (μL)	Na <sub>2</sub> S <sub>2</sub> O <sub>8</sub> stock solution (μL)	FeCl <sub>3</sub> 6 H <sub>2</sub> O stock solution (μL)	CTAB stock solution (μL)
1	10	0.15	9.850	0	0	0	0
2	10	0.15	9.818	0	32	0	0
3	10	0.15	9.813	5	32	0	0
4	10	0.15	9.814	0	0	0	36
5	10	0.15	9.845	5	0	0	0
6	10	0.15	9.845	0	0	5	0
7	10	0.15	9.787	0	63	0	0
8	10	0.15	9.782	0	63	5	0
9	10	0.15	9.745	0	63	5	36
10	10	0.15	9.740	5	63	5	36
11	10	0.15	9.777	5	63	5	0
12	10	0.15	9.740	5	63	5	36
13	10	0.15	9.840	5	0	5	0



**Table 7** Concentrations of  $\text{Na}_2\text{S}_2\text{O}_8$  and  $\text{FeCl}_3$  (mmol/L) in the samples of table 6. With the corresponding ratio of  $\text{Na}_2\text{S}_2\text{O}_8$ ,  $\text{FeCl}_3$  and EDOT in mmol.

Sample	$\text{Na}_2\text{S}_2\text{O}_8$ (mmol/L)	$\text{FeCl}_3$ (mmol/L)	Ratio $\text{Na}_2\text{S}_2\text{O}_8$ : $\text{FeCl}_3$ : EDOT (mmol)
1	0	0	0 : 0 : 0
2	2.7	0	0.027 : 0 : 0
3	2.7	0	0.027 : 0 : 0.050
4	0	0	0 : 0 : 0
5	0	0	0 : 0 : 0.050
6	0	0.00925	0 : 9.25E-05 : 0
7	5.3	0	0.053 : 0 : 0
8	5.3	0.00925	0.053 : 9.25E-05 : 0
9	5.3	0.00925	0.053 : 9.25E-05 : 0
10	5.3	0.00925	0.053 : 9.25E-05 : 0.050
11	5.3	0.00925	0.053 : 9.25E-05 : 0.050
12	5.3	0.00925	0.053 : 9.25E-05 : 0.050
13	5.3	0.00925	0.000 : 9.25E-05 : 0.050

### 3.2.3 Scanning Electron Microscope (SEM) Energy Dispersive X-ray (EDX)

These experiments were based on the second model. This was to visually investigate the PEDOT distribution around the silica. SEM samples were prepared according to table 8, 9 using the stock solutions from table 2. The components of samples 1-8 were all added sequentially after each other. After this a stir bar was added to the 20 mL vial and vigorously stirred for 24 hours at room temperature. Sample 9 DI water, EDOT,  $\text{Na}_2\text{S}_2\text{O}_8$  and  $\text{FeCl}_3$  were added with a stir bar to the vial. This solution was vigorously stirred for 24 hours, after this 24 hours, the Stöber silica particles were added to the solution. The solution was allowed to stir for another 24 hours with the particles. To prepare the samples for the SEM analysis, the samples were washed with DI and ethanol. This was done by letting the sample sediment, after which ca. 3 mL was taken from the bottom of the vial and transferred into a new vial with DI water. The sample was then again allowed to sediment and the DI water was taken out of the vial. The particles were then washed with ethanol and again allowed to sediment. After this, the ethanol was taken out and the particles were dried on a hot plate in an aluminium basket to around 200 C°. This ensured no oxidizer salt was left present in the sample.

**Table 8** Composition of samples that were measured in the zeta-potential experiments consisting Ludox TMA, DI water and EDOT (table 1) and  $\text{Na}_2\text{S}_2\text{O}_8$ ,  $\text{FeCl}_3$  and CTAB stock solutions (table 2).

Sample	Total volume (mL)	Stöber Silica dispersion (mL)	DI water (mL)	EDOT ( $\mu\text{L}$ )	$\text{Na}_2\text{S}_2\text{O}_8$ stock solution (mL)	$\text{FeCl}_3$ 6 H <sub>2</sub> O stock solution (mL)
1	20	0.2	19.800	0	0	0
2	20	0.2	17.800	0	1	1
3	20	0.2	18.800	0	0	1
4	20	0.2	18.800	0	1	0
5	20	0.2	19.795	5	0	0
6	20	0.2	17.795	5	1	1
7	20	0.2	18.795	5	1	0
8	20	0.2	18.795	5	0	1

**Table 9** Concentrations of  $\text{Na}_2\text{S}_2\text{O}_8$  and  $\text{FeCl}_3$  (mmol/L) in the samples of table 8. With the corresponding ratio of  $\text{Na}_2\text{S}_2\text{O}_8$ ,  $\text{FeCl}_3$  and EDOT in mmol.

Sample	$\text{Na}_2\text{S}_2\text{O}_8$ (mmol/L)	$\text{FeCl}_3$ (mmol/L)	Ratio $\text{Na}_2\text{S}_2\text{O}_8$ : $\text{FeCl}_3$ : EDOT (mmol)
1	0	0	0.000 : 0.000 : 0.000
2	42.0	36.9	0.840 : 0.739 : 0.000
3	0	36.9	0.000 : 0.739 : 0.000
4	42.0	0	0.840 : 0.000 : 0.000
5	0	0	0.000 : 0.000 : 0.050
6	42.0	36.9	0.840 : 0.739 : 0.050
7	42.0	36.9	0.840 : 0.739 : 0.050
8	0	36.9	0.000 : 0.739 : 0.050

### 3.3 Bijel system

#### 3.3.1 Precursor dispersion preparation

100 grams of Ludox TMA was evaporated using rotary evaporator at 60 degrees, 240 mbar. The bottom flask was weighed every 10 minutes and evaporated until the concentration of the particles was around 50 wt %. After this the particles were centrifuged at 3700 rpm for 15 minutes to ensure the aggregates are sedimented off and the pH was brought to 2.89. After this, the NaCl concentration was increased from 27 mM to 50 mM by adding NaCl directly to the particles. The pH was measured again and adjusted to 2.89 if needed. The weight fraction and density were also measured. This was done with an aluminium tray which was heated to 100 C° until no water was visible. After this the temperature was increased to 300 C° to make sure no water was left. Finally, after the tray had cooled down, the dried silica was weighed again, which resulted in a weight fraction of around 46.4 wt%.

A glycerol stock solution was made by mixing 50:50 v% glycerol with 1-propanol in a glass vial. Secondly a 200 mM CTAB stock solution was made by weighing 0.7289 grams of CTAB in a vial and pipetting 10 mL of 1-propanol. This solution was mixed and heated under hot tap water, this was repeated until the surfactant completely dissolved. While pipetting the CTAB solution was stored in a warm water bad to ensure it stays dissolved.

The precursor dispersion with 63 mM CTAB was made according to table 10, the other CTAB precursor dispersions were made according to appendix A. An oxidizer, either  $\text{Na}_2\text{S}_2\text{O}_8$  or  $\text{FeCl}_3$  was added to the precursor dispersion according to table 12. The other precursor dispersions with various concentrations of oxidizers were made according to appendix B.

**Table 10** Precursor composition of DEP, 1-propanol, LUDOX TMA and MiliQ (DI water) chemicals (table 1) and CTAB and glycerol stock solutions.

Pipet the following solutions sequentially in an Eppendorf using a pipet:	Type of chemical	Amount (mL)
DEP	Oil	0.070
CTAB Stock Solution	Surfactant	0.135
Glycerol Stock Solution	Solvent 2	0.241
1-propanol	Solvent	0.053
Aqueous Stock LUDOX TMA dispersion	nanoparticles	0.479
MilliQ	DI water	0.021
Total volume		1.000

**Table 11** Precursor composition with the addition of oxidizer.

	Amount (mL)
Oxidizer stock solution concentration g/ml	0.01
Amount oxidizer stock solution added ( $\mu\text{L}$ )	10.00
Amount of 1-propanol added ( $\mu\text{L}$ )	10.00
Precursor dispersion (mL)	0.18
Concentration oxidizer in precursor dispersion (mg/mL)	0.5

### 3.3.2 Microfluidic devices

A quick fiber device can be made by gluing a 50  $\mu\text{m}$  glass capillary in a 1 mL pipette tip using UV glue. And then the pipette tip was put under the UV lamp for 10 minutes. After this another drop of the UV glue was put on the end of the pipette tip to ensure a complete seal with the pipette and capillary.

To ensure the bijel formed is consistent through the formation, a microfluidic device was used. The device was built on a microscope slide. A round 50  $\mu\text{m}$  glass capillary was checked under the microscope to ensure that the end has a smooth round edge. The round capillary was glued into a 100  $\mu\text{m}$  square capillary using UV glue. This was put into a round 300  $\mu\text{m}$  capillary and checked under a microscope to ensure that the 50  $\mu\text{m}$  capillary is in the center. A flushing channel was made from the metal cylinder from a needle. A flushing channel was glued onto a microscope slide with the capillaries. On top of inlet 1 and inlet 2 needles were glued onto as shown in figure 10.

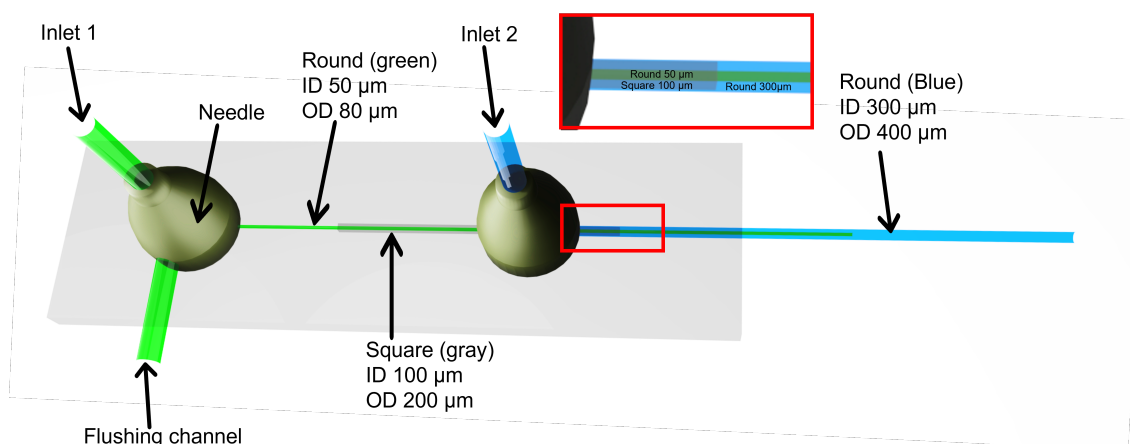


**Fig. 10:** Schematic representation of a flow device made using: needles, three types of capillary with various Inner Diameters (ID) and epoxy.

### 3.3.3 Device coating

The microfluidic device was coated using 3 wt% OTS solution in mineral oil. 300 mg of OTS was weighed and 10 g of mineral oil was added to the OTS. The microfluidic device was taped to a metal lift and the OTS solution was pumped through the device. This was done by using a glass syringe and tubing connected to inlet 1 while the flushing channel was blocked with a needle that was epoxied closed. While the pumping was happening the device and tubing were heated with a hair dryer. After 2-3 minutes the pump was stopped and hexane was flushed through inlet 1 and 2. This was flushed out again with ethanol and finally the device was dried with nitrogen.

### 3.3.4 Bijel fiber printing

A coated micro fluidic device was used, here a 1 mL syringe with a precursor dispersion was connected to inlet 1. A 20 mL syringe with water-saturated toluene was connected to inlet 2. The syringes were put in syringe pumps, here the flow of precursor dispersion was 0.95 mL/hour, the flow of the continuous phase was 3.9 mL/hour. This was to ensure continuous fiber was coming out of the flow device. After this the Lego printer was started. LEGO<sup>®</sup> Mindstorms<sup>®</sup> software was used for this as shown in figure 11. Finally, when finished the device was flushed with ethanol and dried with nitrogen.

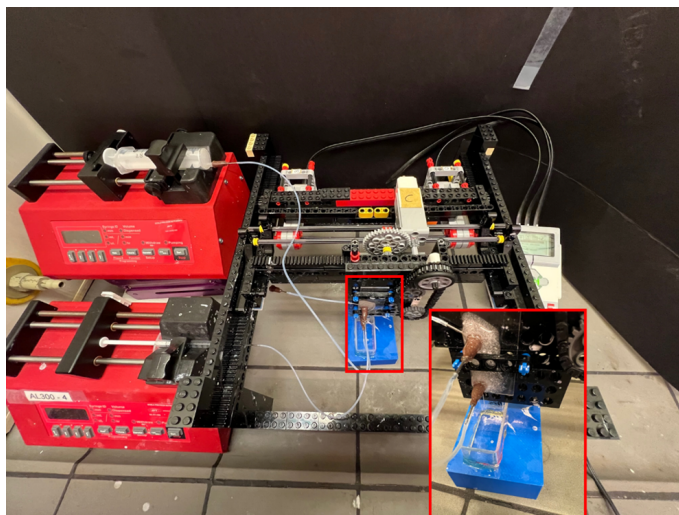


**Fig. 11:** Picture of lego printer used to print sequential uniform bijels in a container. Two pumps connect the continuous phase and the precursor dispersion to the flow device. The container is raised on a 3D printed cube that raises the container.

### 3.3.5 TEOS treatment

A TEOS solution was made by weighing 300 mg of TEOS in a vial in the glove box. The vial was closed and transferred outside the glove box. 10 g of mineral oil was added to the TEOS making a 3 wt% solution. The continuous phase of the fibers was changed from water-saturated toluene to water-saturated mineral oil. After 3 washing steps, 5 mL of the 3 wt% solution of TEOS was added. They were allowed to react with the TEOS for 24 hours. Finally, the continuous phase was replaced back again to water-saturated toluene.

### 3.3.6 Polymerization EDOT to PEDOT in bijel fibers for confocal analysis

The method to polymerize EDOT to PEDOT was done according to schematic figure 12. The continuous phase toluene was swapped by water saturated EDOT. Or the continuous phase was swapped out with water saturated EDOT were 0.05 mg of Iron chloride hexa-hydrate was mixed in. This EDOT was dispensed in the container without taking the iron chloride granules with it. The fibers were allowed to lay in the EDOT for various amount of days.

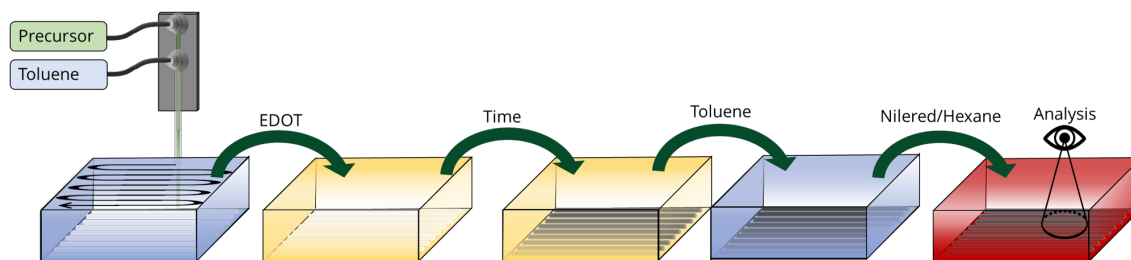


**Fig. 12:** Flow chart for bijel polymerization in the container it is printed in. The continuous phase is swapped for EDOT. After the polymerization is finished the continuous phase is swapped out for toluene to ensure the EDOT is washed out. Finally the container can be analyzed under the confocal with Nile red and hexane as the continuous phase.

### 3.3.7 Conductivity measurement

#### 3.3.7.1 Pre-polymerized EDOT

The PEDOT was polymerized mixing  $\text{FeCl}_3$  and EDOT together. Here the solution was stirred and ultrasonication was used until the mixture looked completely black. The remaining  $\text{FeCl}_3$  was centrifuged out of the solution at 14500 rpm for 2 minutes. A glass square was cut to size, using epoxy and UV glue it was glued to a microscope slide. Two copper electrodes were cut from the flat copper sheet. The electrodes were sanded with sand paper to ensure no residue or protecting layer is on the copper electrode. The electrodes were glued in the container using epoxy glue, using a 3D printed guide to ensure the electrodes are consistent through the containers. In between the electrodes a cut microscope slide is glued into place to ensure a flat underground for the fibers as shown in figure 13

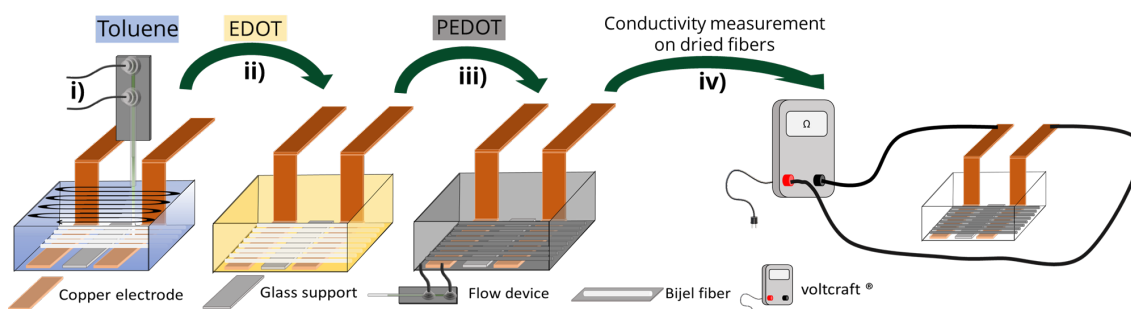


**Fig. 13:** Schematic representation of the work flow using pre-polymerized EDOT for the conductivity measurements. **i)** With between the copper electrodes a glass support for the fibers to lay on when printed in a zig zag pattern by the flow device and lego printer. **ii)** The continuous phase toluene was swapped by water saturated EDOT. **iii)** After this pre-polymerized EDOT in EDOT is added. **iv)** Finally, after 48 hours the fibers were washed with toluene and ethanol multiple times and air-dried for several hours before the conductivity measurement was done.

#### 3.3.7.2 Polymerization in continuous phase

A mixture of Toluene, 1-pentanol and Iron(III) p-toluenesulfonate hexahydrate ( $\text{Fe(III)(OTs)}_3$ , molecular weight: 677.5 g/mol) was made according to table 12. The chemicals were mixed in a vial and sonicated until the mixture was clear. The continuous phase was exchanged out with the oxidizer mixture and 0.2 mL of EDOT mixed with 0.2 mL of toluene making a 50/50% volume mixture, which was finally added afterwards. After 48 hours the fibers were washed with toluene and ethanol and dried to ensure the conductivity measurement could be done as schematically shown in figure 14.

**Table 12** Samples of  $\text{Fe(III)(OTs)}_3$  with increasing concentration in toluene with the addition of 3 volume percent 1-pentanol.

Sample	Toluene (mL)	1-pentanol (mL)	$\text{Fe(III)(OTs)}_3$ (mg)	Concentration (mg/mL)	Concentration (mmol/L)
1	19.4	0.6	100	5.0	7.5
2	19.4	0.6	50	2.5	3.7
3	19.4	0.6	25	1.25	1.8

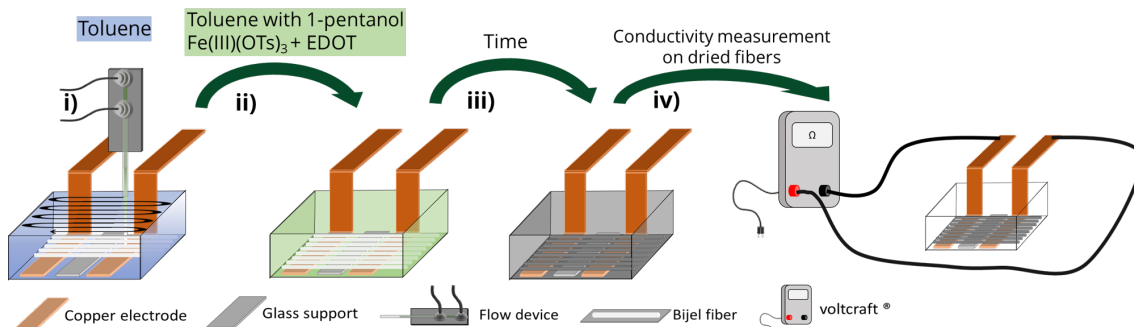


**Fig. 14:** Schematic representation of the work flow polymerizing PEDOT in the continuous phase for the conductivity measurements. **i)** With between the copper electrodes a glass support for the fibers to lay on when printed in a zig zag pattern by the flow device and lego printer. **ii)** The continuous phase toluene was swapped by a mixture of toluene, 1-pentanol and  $\text{Fe(III)(OTs)}_3$ . After this a 50/50% volume mixture of EDOT and toluene was added. **iii)** The fibers and the oxidizers were let to stand for 48 hours. This ensured that the EDOT could polymerized completely and all oxidizers available could be used. **iv)** Finally, the fibers were washed with toluene and ethanol multiple times and air dried for several hours before the conductivity measurement was done.

## 3.4 Characterization

### 3.4.1 Timelapse experiments

A leica M205 C with a back light was used to observe the samples with picture automatically being taken with various intervals.

### 3.4.2 Zeta-potential experiments

The zetasizer (Malvern Zetasizer Nano ZS) connected to a titration unit was used to determine the zeta potential of the LUDOX TMA particles. Here the titration unit has a solution of 1 M, 0.1 M and 0.01 M HCl solution connected. The sample is in a container containing a stirring bar an inlet to the zetasizer and an outlet. And a pH meter with three tubes connecting to a pump with the HCl solutions. This allows for every pH point the zetasizer takes three measurement points of the zeta potential at 25 C°.

### 3.4.3 Scanning electron microscope (SEM) - Energy Dispersive X-ray (EDX) experiments

After the bijel fibers or the 400 nm silica particles were retrieved, they were prepared for characterization with the SEM-EDX (Phenom ProX). For the 400 nm silica particles was done by taking a SEM holder and putting a carbon tape on it and pressing this on the sample that wants to be retrieved. For the fibers, a 3D-printed cube was wrapped in carbon tape and fibers were stuck to the sides to get a cross-section. This was then carefully stuck onto a sample holder with carbon tape on it. The top of the wrapped cube was then again stuck onto a sample to get a surface image of the fibers. The images

retrieved from the SEM were taken at 10 kV or 15 kV and later processed with ImageJ if that was needed. The EDX data was automatically composed by the software of the Phenom ProX.

### 3.4.4 Confocal microscope experiments

The fibers were imaged using a confocal microscope (Nikon Eclipse Ti-U, Leica Stellaris 5). The fibers were retrieved and were washed with hexane 2 times. This was to ensure all the toluene was washed out and the reflective index of the fibers matched the surroundings. After this the hexane was replaced with Nile red dissolved in hexane. The samples were looked at with a 63x water immersion objective. A laser 488 & 561nm laser were used to excite the Nile red and detect the signal from 400-800 nm with a detector.

### 3.4.5 Conductivity experiments

A voltcraft<sup>®</sup> VC190 SE was used to measure the ampere and resistance of a sample. Here one or two 9 volt VATRA LONGLIFE power batteries were used to measure the ampere through a set number of fibers. These batteries could be linked up to deliver 18 V in series as shown in figure 15. In the chapter that follows the results obtained will be discussed.

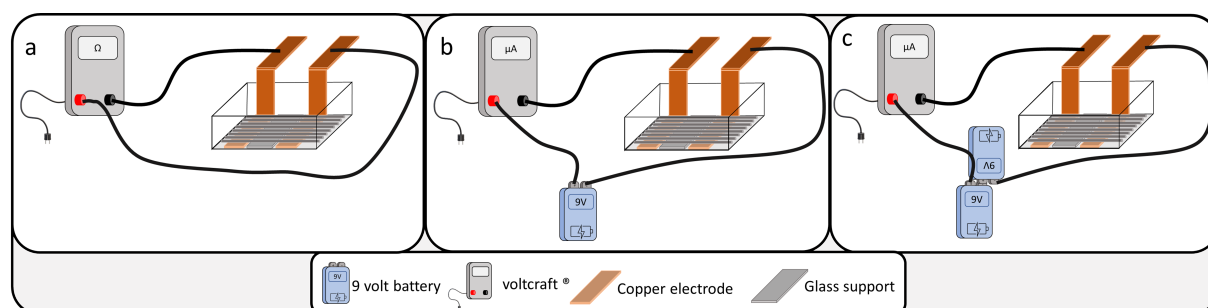


**Fig. 15:** Schematic representation of set up to measure conductivity of bijel fibers. **a)** The voltcraft<sup>®</sup> can measure the resistivity without an external power source. **b)** Set up to measure amperage at 9V. **c)** Set up to measure amperage at 18V.

## 4 Results and discussion

### 4.1 Model system

In this section we will discuss the results obtained from the model system. This model system is based around two silica nanoparticles and looked at with timelapses, zeta-potentials and SEM-EDX. The object was to get a better understanding of the PEDOT polymerization and the interaction of it with silica.

#### 4.1.1 Timelapse

In this section the timelapse results will be discussed. First, it was confirmed that EDOT could not polymerize without oxidizer. The polymerization rate with  $\text{Na}_2\text{S}_2\text{O}_8$  and/or  $\text{FeCl}_3$  was looked at. This was done by visually looking at an EDOT droplet in a continuous phase of water. Based on the principle that the PEDOT is very dark and easy to visually see being formed. Finally, Ludox TMA particles were added to see if this had any significant effect on the migration of PEDOT through the water phase. This could give an indication of the interaction between the two.

Timelapse intervals when no oxidizers are added is shown in figure 16. The full images taken with their correlating sample number and additional timelapse intervals are shown in appendix C.

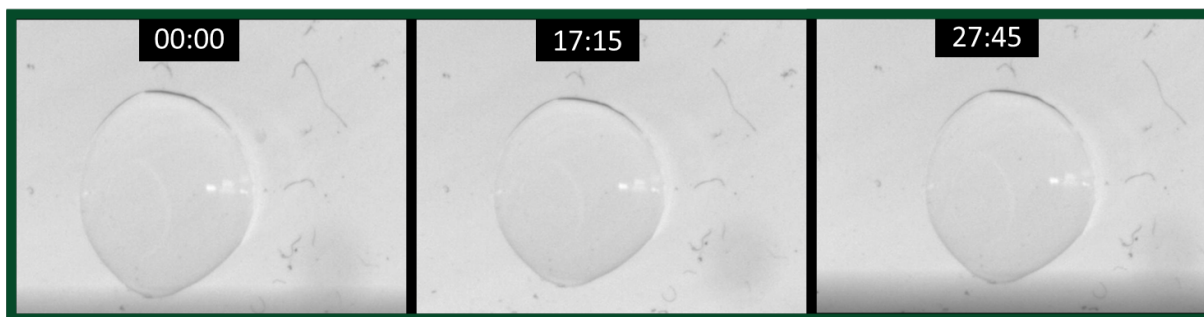


**Fig. 16:** Time intervals taken at  $t = 00:00, 17:15$  &  $27:45$  (minutes:seconds) from the timelapse of an EDOT droplet in the continuous water phase with no oxidizer

As shown in figure 16 we can see a clear droplet of EDOT in a clear continuous phase of water at  $t = 00:00$  (minutes:seconds). At  $t = 27:45$  the droplet is still clear and shows no change in colour and/or change in clarity. This indicates that over this chosen time period, no polymerization has visibly taken place. There still could be some small polymerization which is not visible. However, the PEDOT that should be formed is clearly black and all other smaller formed chains are not of interest. Overall, these results indicate that when no oxidizers are added no visible polymerization takes place. After this, the effect of  $\text{Na}_2\text{S}_2\text{O}_8$  and  $\text{FeCl}_3$  was looked at (see figure 17).



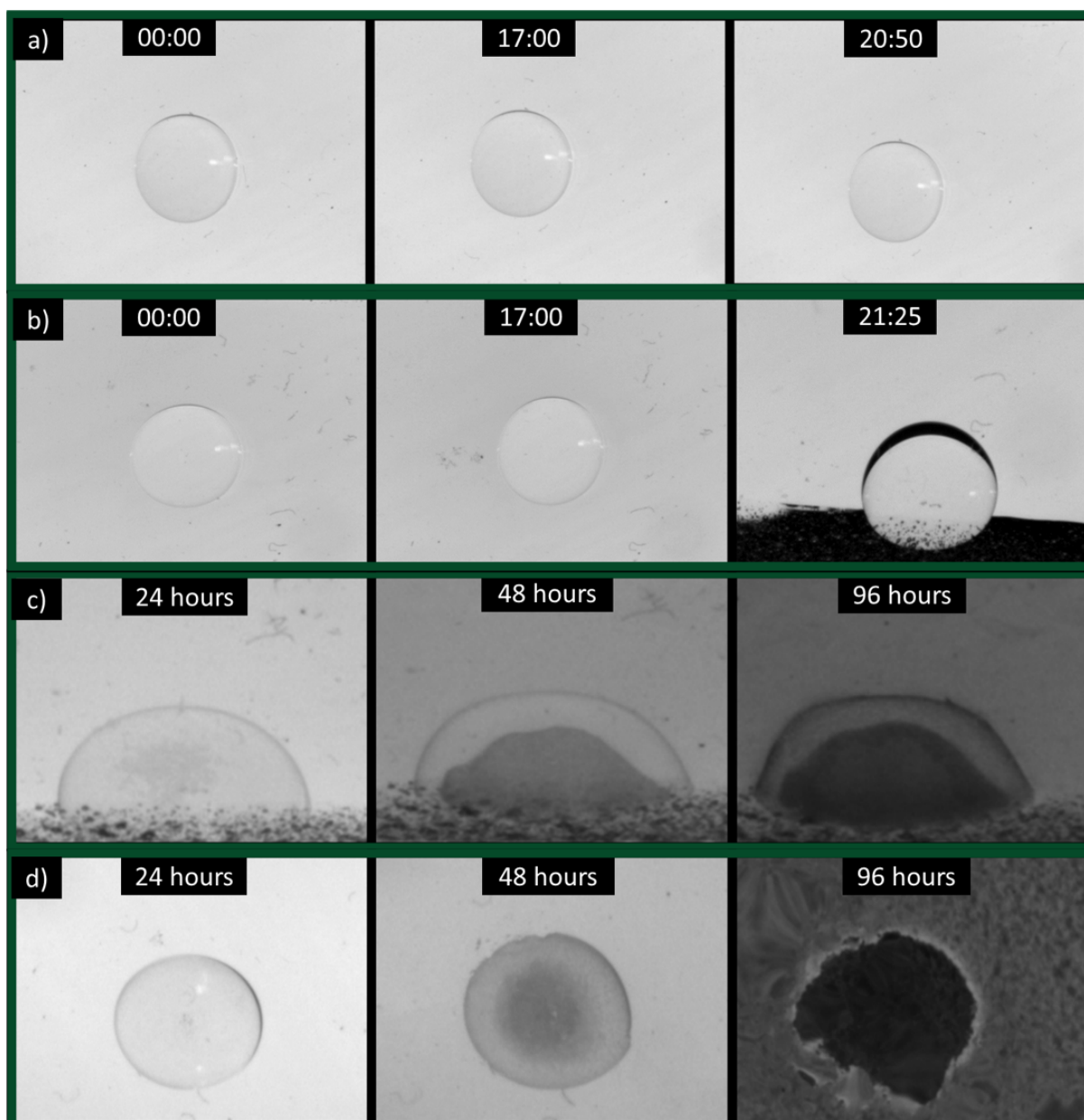


**Fig. 17:** **a)** Time intervals taken at  $t = 00:00$ ,  $17:00$  &  $20:50$  (minutes:seconds) from the timelapse of an EDOT droplet in the continuous water phase with  $\text{Na}_2\text{S}_2\text{O}_8$  added. **b)** Time intervals taken at  $t = 00:00$ ,  $17:00$  &  $21:25$  (minutes:seconds) from the timelapse of an EDOT droplet in the continuous water phase with  $\text{FeCl}_3$  added. Here, at  $t = 21:25$ , the droplet moved to the side of the container because of experimental error. **c)** Time intervals taken at  $t = 24$ ,  $48$  &  $96$  hours from the timelapse of an EDOT droplet in the continuous water phase with  $\text{Na}_2\text{S}_2\text{O}_8$  added. **d)** Time intervals taken at  $t = 24$ ,  $48$  &  $96$  hours from the timelapse of an EDOT droplet in the continuous water phase with  $\text{FeCl}_3$  added.

As shown in figure 17a from  $t = 00:00$  to  $t = 20:50$  the droplet is clear and has not changed visually with the addition of  $\text{Na}_2\text{S}_2\text{O}_8$ . The addition of this oxidizer should create PEDOT, it could be that the time scale chosen is too short. These results suggest that with the addition of  $\text{Na}_2\text{S}_2\text{O}_8$  no polymerization has taken place over the chosen time intervals. From  $t = 00:00$  to  $t = 21:25$ , the droplet is clear and has not changed visually with the addition of  $\text{FeCl}_3$  (see figure 17b). The addition of this oxidizer should create PEDOT, it could be that the time scale chosen is too short. These results suggest that here also no polymerization has taken place over the chosen time intervals. To see if the chosen intervals were too short the same samples were let to stand for a few days. The same droplet with  $\text{Na}_2\text{S}_2\text{O}_8$  at  $t =$

24 hours, there is a very small amount of colour change in the center of the droplet (see figure 17c). At  $t = 48$  hours there is a clear change in colour at the interface. At  $t = 96$  hours the droplet has become completely black and the continuous phase has also become significantly darker. The formation of PEDOT is mostly on the EDOT water interface. There is some formation from the EDOT dissolved in the water phase. This is not very clear from this image, but will be showed more clearly in appendix C. The results also indicate that the polymerization can happen on mostly the interface over a longer time period. The same droplet with  $\text{FeCl}_3$  at  $t = 24$  hours there is a very small amount of colour change in the center of the droplet (see figure 17d). At  $t = 48$  hours there is a clear change in colour at the interface. At  $t = 96$  hours, the interface of the droplet has become darker but not completely covered. The formation of PEDOT is mostly on the EDOT water interface as compared to the  $\text{Na}_2\text{S}_2\text{O}_8$  were there is some formation from the EDOT dissolved in the water phase. The polymerization rate of also looks to be slower compared to the  $\text{Na}_2\text{S}_2\text{O}_8$ , with their molar concentration being fairly similar. The results also indicate that polymerization can happen on the interface over a longer time period.

After this the two oxidizers were combined and the effect of the Ludox TMA particles was studied as shown in figure 18.

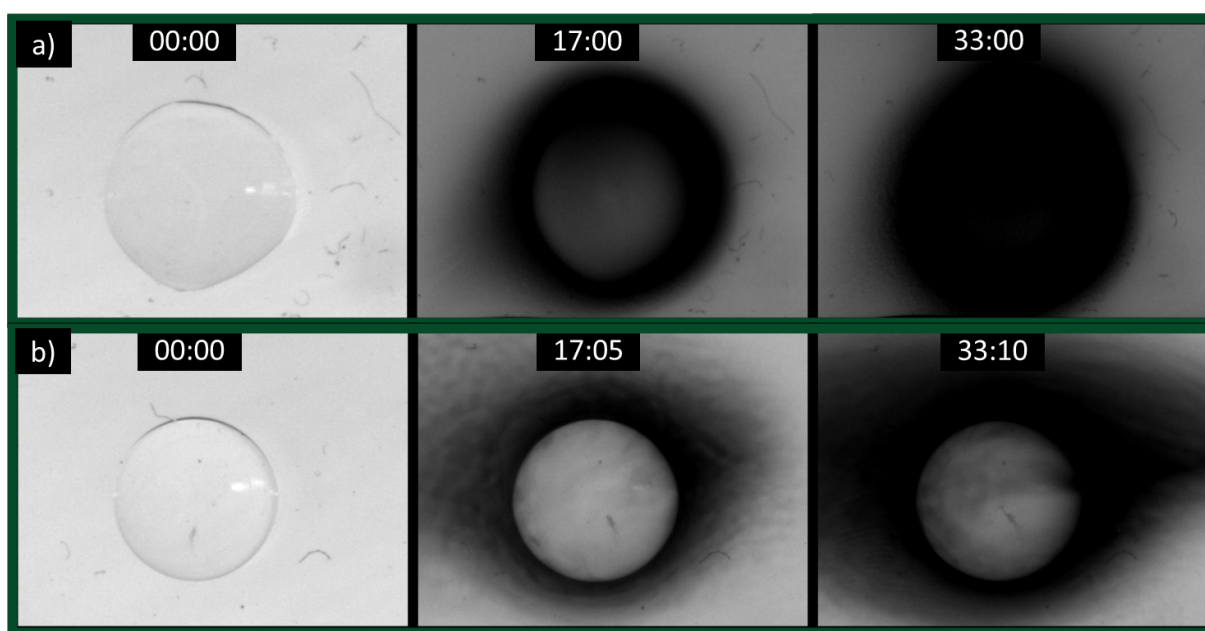


**Fig. 18:** a) Time intervals taken at  $t = 00:00$ ,  $17:00$  &  $33:00$  (minutes:seconds) from the timelapse of an EDOT droplet in the continuous water phase with  $\text{FeCl}_3$  and  $\text{Na}_2\text{S}_2\text{O}_8$  added. b) Time intervals taken at  $t = 00:00$ ,  $17:05$  &  $33:10$  (minutes:seconds) from the timelapse of an EDOT droplet in the continuous water phase with  $\text{FeCl}_3$ ,  $\text{Na}_2\text{S}_2\text{O}_8$  and Ludox TMA particles added.

As shown in figure 18a at  $t = 00:00$  there is a clear EDOT droplet in the a clear continuous phase. At  $t = 17:00$  the droplet has become much darker, and at  $t = 33:00$  the droplet has become completely black. This indicates that after 17 minutes there is already PEDOT created on the interface, which is significantly faster compared to the oxidizers separated. This is in agreement with the theory, which states that combining these two oxidizers creates faster free radicals. Overall, these results indicate that the combination of  $\text{FeCl}_3$  and  $\text{Na}_2\text{S}_2\text{O}_8$  results in the faster polymerization of PEDOT on the interface of EDOT. When particles are added (see figure 18b) there is a clear EDOT droplet in the a clear continuous phase at  $t = 00:00$ . At  $t = 17:05$  the surroundings of the droplet has become much darker, and at  $t = 33:10$  the surroundings of the droplet has become completely black. This indicates that the PEDOT polymerization is still at the interface but does move away from the interface faster compared to when no particles are added as in figure 18. This could be because of the possible electrostatic interaction between PEDOT and silica. To see this effect more clearly the timelapse was done again with and without particles but after each time interval the continuous phase was mixed as shown in figure 19.

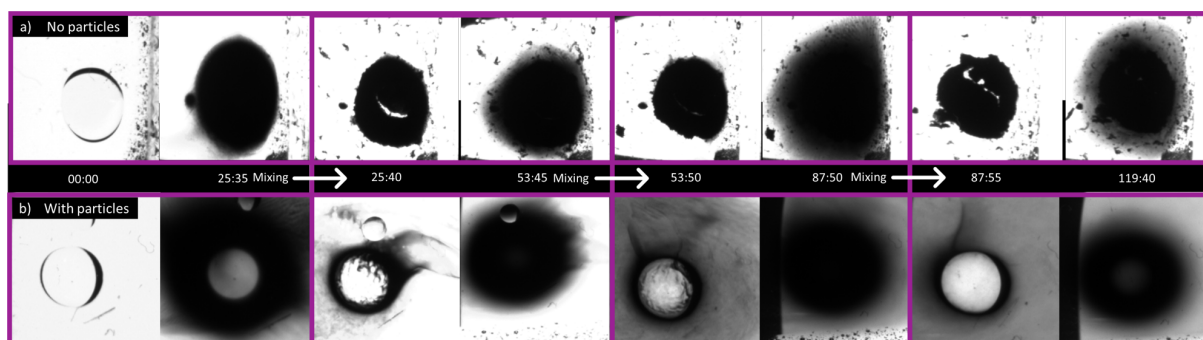


**Fig. 19:** Time intervals taken at  $t = 00:00, 25:35, 25:40, 53:45, 53:50, 87:50, 87:55$  &  $119:40$  (minutes:seconds) from the timelapse of an EDOT droplet in the continuous water phase with  $\text{FeCl}_3, \text{Na}_2\text{S}_2\text{O}_8$ . After certain time intervals, the continuous phase was mixed as indicated by the white arrow. **a)** no particles added. **b)** Ludox TMA particles added.

As shown in figure 19a when no particles are added at  $t = 25:35$  PEDOT is again formed around the interface. After mixing indicated by the white arrow at  $t = 25:40$ , most of the PEDOT is at the interface. This is repeated multiple times showing that this shell around the EDOT droplet stays intact and some bigger chunks break off this shell. It also shows from  $t = 53:50$  to  $87:50$  if this shell is intact, that the PEDOT can still form from within the droplet and diffuse to the continuous phase. When Ludox TMA particles are added to the continuous phase (see figure 19b), the droplet is visible at  $t = 25:40$ . This was not the case when no particles were added at  $t = 25:40$  in figure 19a. After the mixing the droplet is again clearly visible, indicating that the PEDOT does not form this shell around the droplet. After this mixing is repeated two more times, the droplet keeps being visible while the continuous phase keeps getting darker. This indicates that the black polymer adsorbs onto the particles and gets brought into the continuous phase. How this adsorption happens can not be concluded from these results. Because of the small size of the particles, the adsorption mechanism could not be determined.



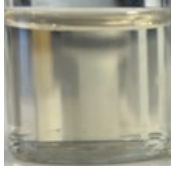

The results in this chapter indicate that when particles are added the PEDOT does not form this shell, and if this shell is formed it can still diffuse through this shell. And that the particles facilitate the movement of PEDOT away from the interface. How this happens could not be concluded from these experiments. The next chapter, therefore, moves on to discuss the interactions between PEDOT and silica using zeta-potential measurements.

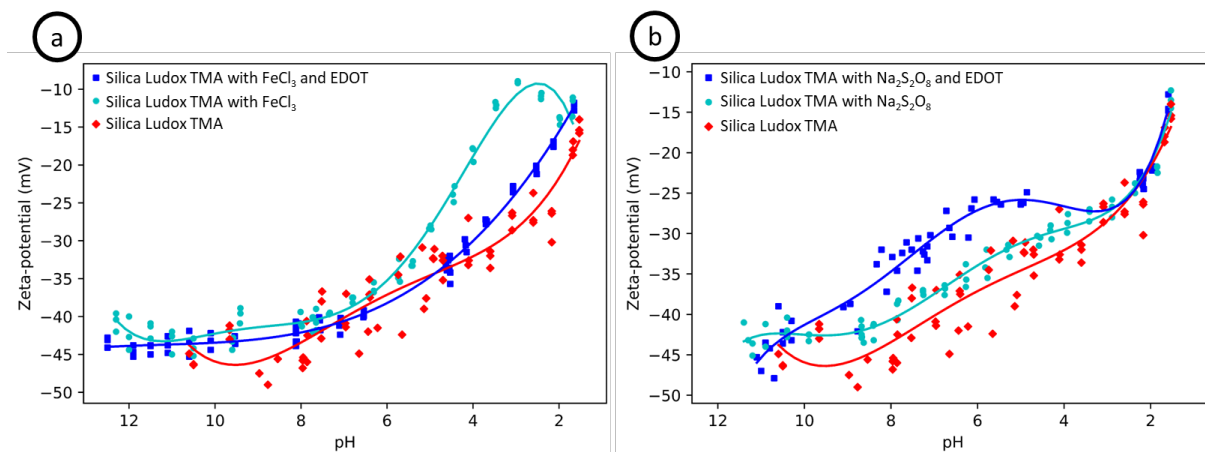
### 4.1.2 Zeta-potential

In this section the objective was to get a better understanding of the PEDOT silica interaction. This objective was looked at by polymerizing EDOT with various oxidizers in the presence or Ludox TMA particles. The effects of  $\text{FeCl}_3$  and  $\text{Na}_2\text{S}_2\text{O}_8$  without EDOT was looked at also the effect of EDOT without oxidizers was looked at. The results show that EDOT without oxidizers has no effect on the zeta-potential. The oxidizers have each their own effect on the zeta-potential, which will be discussed in appendix D. The pre-polymerization of PEDOT resulted in a significant amount of aggregation resulting in the particles to sediment and not being able to be measured (see appendix D).

Selective samples are shown in table 13 with the corresponding oxidizer concentration, CTAB concentration, mean particle size and images of the sample used for the zeta-potential measurement. The effect of polymerization of EDOT with  $\text{FeCl}_3$  (see figure 20a) or  $\text{Na}_2\text{S}_2\text{O}_8$  was looked at as shown in figure 20b. Here the X-axis is from basic to acidic following the titration sequence.

**Table 13** Table with samples used for zeta-potential measurements with  $\text{FeCl}_3$ ,  $\text{Na}_2\text{S}_2\text{O}_8$  and CTAB (mmol/L) with corresponding mean particle size (nm).

Sample	$\text{FeCl}_3$ (mmol/L)	$\text{Na}_2\text{S}_2\text{O}_8$ (mmol/L)	CTAB (mmol/L)	Mean particle size (nm)	Image of sample
Ludox TMA	0	0	0	$26.00 \pm 3.00$	
Ludox TMA with $\text{FeCl}_3$ and EDOT	9.25E-03	0	0	$29.47 \pm 1.43$	
Ludox TMA with $\text{Na}_2\text{S}_2\text{O}_8$ and EDOT	0	2.7	0	$27.55 \pm 1.52$	
Ludox TMA with $\text{Na}_2\text{S}_2\text{O}_8$ , $\text{FeCl}_3$ and EDOT	9.25E-03	5.3	0.1	$94.58 \pm 30.88$	

**Fig. 20:** Zeta-potential measurements as function of the pH for: **a)** Ludox TMA ( $\blacklozenge$ ), Ludox TMA and  $\text{FeCl}_3$  ( $\bullet$ ) & Ludox TMA,  $\text{FeCl}_3$  and EDOT ( $\blacksquare$ ). **b)** Ludox TMA ( $\blacklozenge$ ), Ludox TMA and  $\text{Na}_2\text{S}_2\text{O}_8$  ( $\bullet$ ) & Ludox TMA,  $\text{Na}_2\text{S}_2\text{O}_8$  and EDOT ( $\blacksquare$ ).

As shown in figure 20a the zeta-potential measurement of the Ludox TMA particles shows an upward trend as the pH gets increased as expected. This is because silica oxide surface charge changes with increasing pH. When  $\text{FeCl}_3$  there is a significant difference in zeta-potential compared to only the Ludox

TMA particles. This significant difference could be because of the solubility of Fe(III) which is not soluble at high pH but is soluble at low pH. When EDOT is added with the FeCl<sub>3</sub> there is no significant difference with the Ludox TMA particles. However, compared to when only the oxidizer is added, the zeta-potential decreases when EDOT is added. This is very contradicting to the expected results, which is when PEDOT is formed, the zeta-potential increases. The addition of the EDOT somehow, does not see this radical change in zeta-potential. It could be that some of the iron is reduced preventing this aggregation and change in zeta-potential, but does not form enough charged PEDOT to increase the zeta-potential. These results suggest that the addition is not enough to polymerize a significant amount of PEDOT to increase the zeta-potential. When sodium Na<sub>2</sub>S<sub>2</sub>O<sub>8</sub> is added the zeta-potential increased slightly but not significantly (see figure 20b). This could be because of the minimal added (2.7 mmol/L) Na<sub>2</sub>S<sub>2</sub>O<sub>8</sub> is not significant within the experimental error to make a difference. If the EDOT and Na<sub>2</sub>S<sub>2</sub>O<sub>8</sub> are added together, the increase in zeta-potential is more significant. There is a small plateau from pH 6 to pH 2 suggesting aggregation. Even though, that aggregation cannot increase the zeta-potential it can change the curve of the measurement often resulting in this plateau. From DLS measurements there was no significant change in particle size (see table 13), suggesting that this plateau is artificially formed due to the titrator skipping a few measurement points, resulting in the polynomial to show this plateau. This indicates that the PEDOT that is formed electrostatically adsorbs onto the silica and thus increasing the zeta-potential. These results suggest that PEDOT electrostatically adsorbs onto the silica. However, the method used to polymerize EDOT which is not soluble in water can result in very heterogeneous samples resulting in non-conforming zeta-potential data.

The bijel system also contains CTAB which electrostatically adsorbs onto the silica. Even though the 0.1 mM CTAB will probably not completely cover the surface of all the silica. It is still important to see if this affects the possible interaction between PEDOT and silica. The CTAB also helped with the polymerization allowing for the EDOT to be suspended in the water phase. FeCl<sub>3</sub> was added to speed up the polymerization as shown in figure 21.

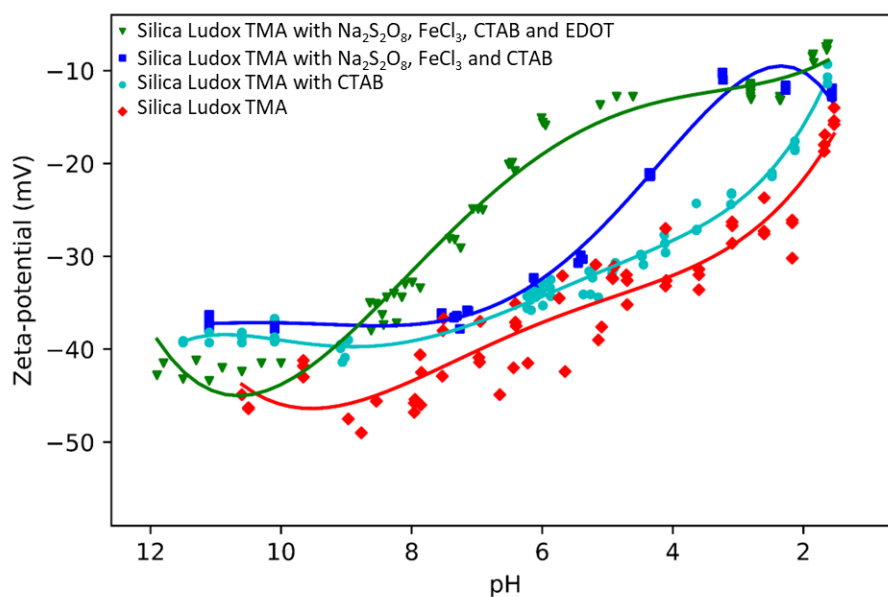


**Fig. 21:** Zeta-potential measurements as function of the pH for: Ludox TMA (♦), Ludox TMA and 0.1 mM CTAB (●), Ludox TMA, Na<sub>2</sub>S<sub>2</sub>O<sub>8</sub>, FeCl<sub>3</sub> and 0.1 mM CTAB (■) & Ludox TMA, Na<sub>2</sub>S<sub>2</sub>O<sub>8</sub>, FeCl<sub>3</sub>, 0.1 mM CTAB and EDOT (▼).

When the concentration is brought up to 0.1 mM CTAB, the particles there is a slight increase in zeta-potential because of the surfactant adsorption. The concentration was kept below the critical micelle concentration. This was to ensure that the silica particles were the only one being measured and not the micelles of the surfactant. When the oxidizers are added there is again an increase in zeta-potential.

When EDOT is added the increase in zeta-potential is more significant. Here a plateau is seen suggesting that the sample has aggregated from DLS measurements (see table 13) there is a significant increase particle size. The error shows a very heterogenous sample with various particle sizes. However, the zeta-potential is measured by measuring the electrophoretic mobility which is solely governed by the potential at their surface and does not depend on the size or shape of the particle. The aggregation does affect the shape of the curve, explaining why there is a plateau from pH 5 to pH 3. The results in this chapter indicate that PEDOT electrostatically adsorbs onto the silica with CTAB in the system. However, the method used to polymerize EDOT which is not soluble in water can result in very heterogenous samples resulting in non-conforming zeta-potential data. The next chapter, therefore, moves on to discuss the visual implications and confirm the electrostatic adsorption.

### 4.1.3 SEM-EDX

The final experiments were done with Stöber silica (400 nm), this was done to confirm that the PEDOT actually adsorbs onto a silica particle. And to visualize this, the 400 nm silica particles are needed because the LUDOX TMA particles are too small to observe with the SEM. First the particles were looked at with no EDOT present and with EDOT present and no oxidizers as shown in figure 22.

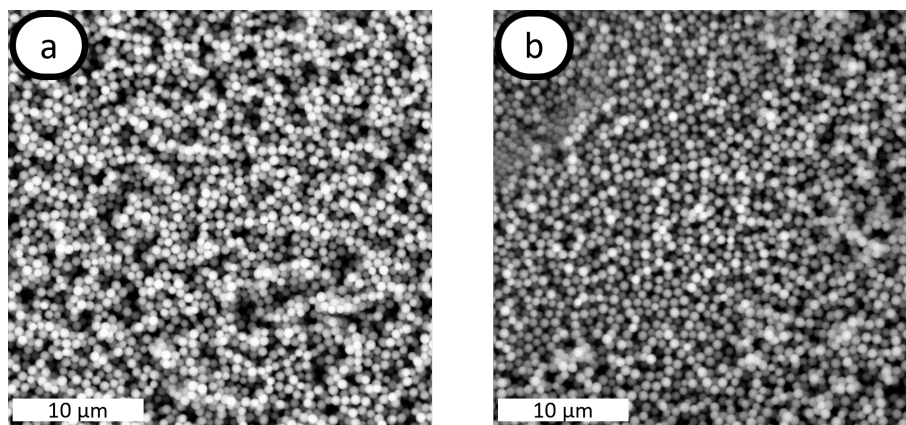


**Fig. 22:** a) Stöber silica stock solution imaged at 10kV. b) Stöber silica stock solution with EDOT imaged at 10kV.

The particles are clearly visible under the SEM as shown in figure 22a and addition of EDOT without oxidizers has no visual effect on the particles (see figure 22b). The EDX is also confirming this with showing a sulphur amount of 0.3 wt% and an error of 0.4% (see appendix F). Even though, PEDOT has also a lot of carbon and oxygen, it cannot be used to identify it. The sample is taped to carbon tape making the carbon atom not an accurate way to identify it. Oxygen is also in the silica particles present, making it hard to make a distinction between the particles and the PEDOT. Therefore, the most reliable atom to measure and use to identify is sulphur. Everything below 1 wt% is not significant to say it is present in the sample. After this, EDOT and the  $\text{FeCl}_3$  and  $\text{Na}_2\text{S}_2\text{O}_8$  were added separately as shown in figure 23.

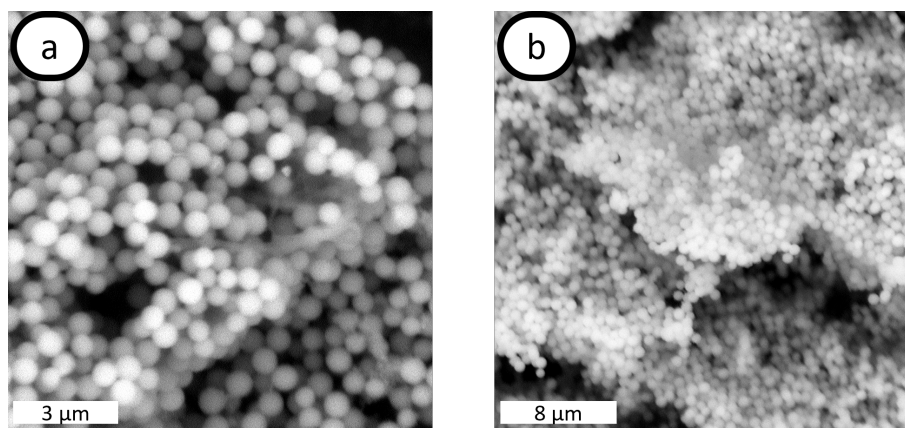


**Fig. 23:** a) Stöber silica stock solution with EDOT and  $\text{Na}_2\text{S}_2\text{O}_8$  imaged at 10kV. b) Stöber silica stock solution with EDOT and  $\text{FeCl}_3$  imaged at 10kV.

As shown in figure 23a the  $\text{Na}_2\text{S}_2\text{O}_8$  shows growth of a material on the silica particles, thus could indicate the PEDOT on the silica particles. The EDX shows a 2.3 wt% sulfur with an error of 0.1% on the particles, which is enough to say that there is PEDOT. However, the sulfur of the persulfate acts as a counter ion of the PEDOT which also contains sulfur. The sulfur signal could thus be from PEDOT or the counter ion of the PEDOT. Either way, the sulfur signal clearly shows that PEDOT is adsorbed onto the particles. The polymerization with  $\text{FeCl}_3$  (see figure 23b) shows a 1.0 wt% sulfur content with an error of 0.2%, however, here there is no visual material on the particles (see appendix F). This is not surprising considering the timelapse experiments, were the polymerization time with the oxidizers separated takes very long. And the samples have only had the time to polymerize for 24 hours.

Next the combination of oxidizers was looked at, here is a significant change shown compared to the other samples as shown in figure 24

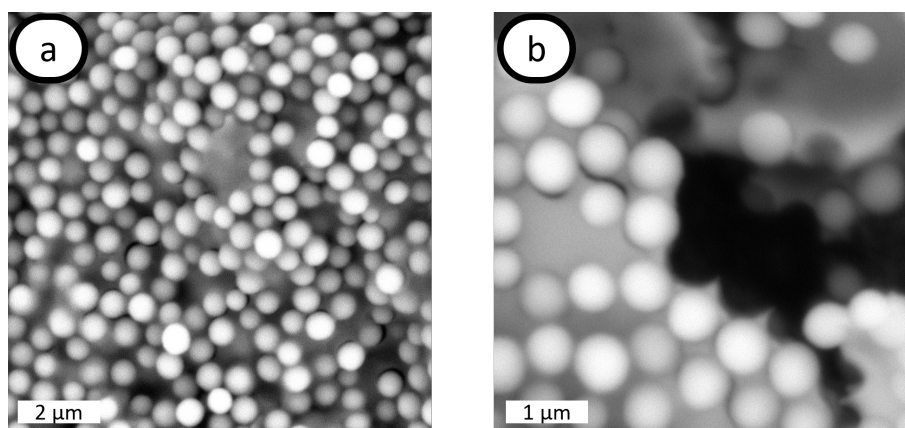


**Fig. 24:** a) b) Stöber silica stock solution with EDOT,  $\text{Na}_2\text{S}_2\text{O}_8$  and  $\text{FeCl}_3$  imaged at 10kV.

The particles as shown in the figure 24a and figure 24b are surrounded by a material. This is growing over and around the particles in a sheet configuration. This could be because the drying of the sample was done on a flat hotplate. The particles during drying sediment and are allowed to lay on the flat surface while drying. This could result in the spacial distribution of the particles and the PEDOT in flat sheets. Why and how this forms a sheet around the particles could not be concluded from these experiments. Even if the particles are ripped away from the PEDOT, the structure stays intact. This shows that PEDOT has some structural integrity even if the particles are taken away. To confirm that the material

‘grown’ around the particles is indeed PEDOT, EDX was performed as shown in figure 25 & table 14.

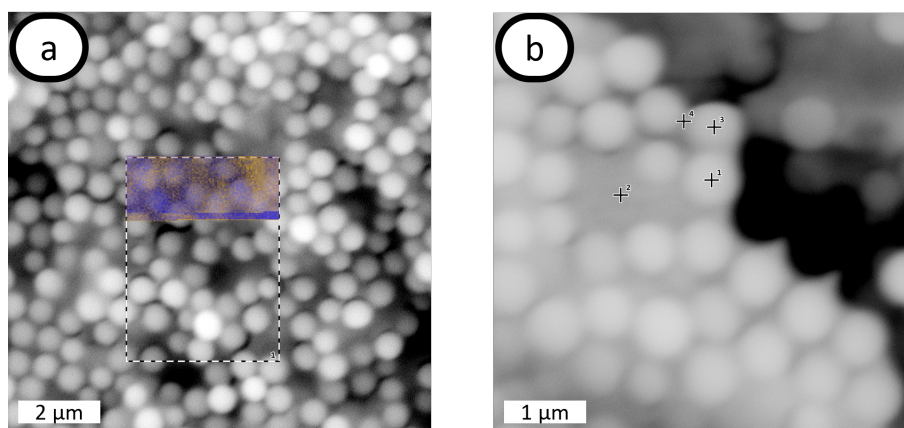


**Fig. 25:** Stöber silica stock solution with EDOT,  $\text{Na}_2\text{S}_2\text{O}_8$  and  $\text{FeCl}_3$  map EDX spectrum taken at 15kV. **a)** Here orange is the sulphur signal and blue is the silica signal. **b)** 4 EDX points taken at different places in the sample.

First a map EDX was taking of the sample in figure 25a here in orange we can see that sulphur is mostly around the particles and the particles are mostly silica as expected. The measurement was stopped after it showed that it had moved. The sample in figure 25b the mapping was not possible to do because of the movement of the sample. Instead, points were taken as shown in table 14.

**Table 14** Sulphur weight percent taken from figure 25 for both the map and point EDX measurement, full EDX spectrum shown in appendix F

Measurement	Weight concentration sulphur (%)	Error (%)
Map	6.3	0.0
Point 1	1.7	0.0
Point 2	3.9	0.0
Point 3	1.7	0.1
Point 4	1.8	0.0

Table 14 clearly shows an above 1 wt% sulphur content in all the measurements. This is a clear indication that PEDOT is on the silica particles and between the particles. Overall, these results indicate that PEDOT is formed and does adsorb onto the silica and is strong enough to keeps it shape even though the particles are torn away.

To see if pre-polymerized results in the same adsorption onto the silica particles, the EDOT was polymerized first and then the particles were added (see figure 26).



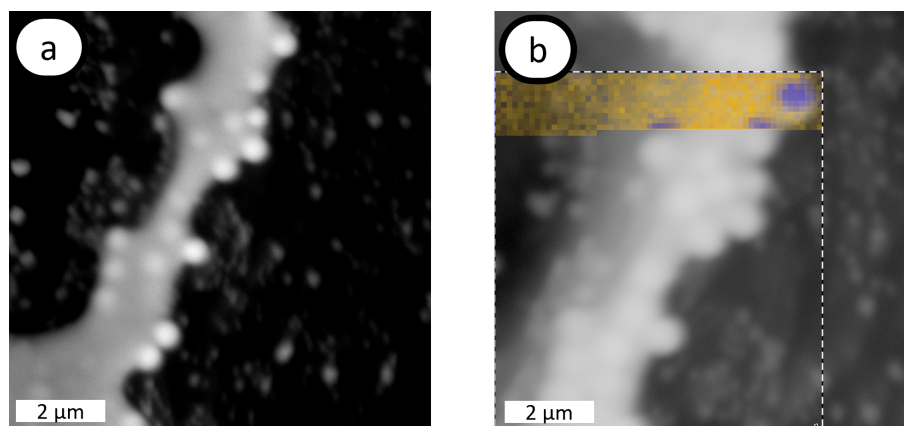


**Fig. 26:** **a)** Pre-polymerized EDOT and Stöber silica SEM image at 10kV. **b)** Pre-polymerized EDOT and Stöber silica SEM-EDX image at 15kV. With the silica (blue) particles surrounded by sulphur (orange) from the PEDOT.

As shown in figure 26a the particles are encapsulated by the PEDOT. Compared to the figure 25 the particles look less like a sheet. The material on and around the particles show a strong sulfur signal (see figure 26b) here 1.4 wt% with an error of 0.1% (see appendix F). It is not clear how this sample progresses during the polymerization and after the particles are added. The effect of the drying on the hot plate is not known and could affect the final spatial distribution of the particles and the PEDOT. From this it could be concluded that PEDOT even though not soluble in water can electrostatically interact with silica particles and thus adsorb onto the particles.

## 4.2 Bijel system

In this section the results of the bijel system are shown and discussed. The objective here was to introduce PEDOT into a bijel and get a better understanding of this process. The first hypothesis was; the introduction of EDOT into the precursor dispersion will be a viable way to introduce PEDOT into a bijel, however, this did not result in any promising results and will be discussed in appendix G.

The second hypothesis was; the introduction of PEDOT after the bijel has already been formed will be a viable way to introduce PEDOT into the bijel. Which was investigated using a small domain precursor dispersion made with a different oil. And then replacing the continuous phase with EDOT. The first way to polymerize the EDOT was by adding oxidizers to the water phase of the bijel. The second way the introduction of PEDOT was investigated was by pre-polymerizing EDOT and then introducing it in the continuous phase. Finally, the polymerization from the continuous oil phase was investigated. This was investigated with the confocal microscope, SEM-EDX and conductivity measurements.

### 4.2.1 Confocal microscope

In this section the results of the confocal microscope will be discussed, which consists of: the bijel formation and the effect of the oxidizer to its structure. The effect of the polymerization on the spectral shift of Nile red. The polymerization and adsorption of the PEDOT onto the silica particles should change the spectral shift of the Nile red and thus give an idea of the polymerization in the bijel. To understand what can happen when the oxidizers are added the bijel without oxidizers needs to be looked at (see figure 27).

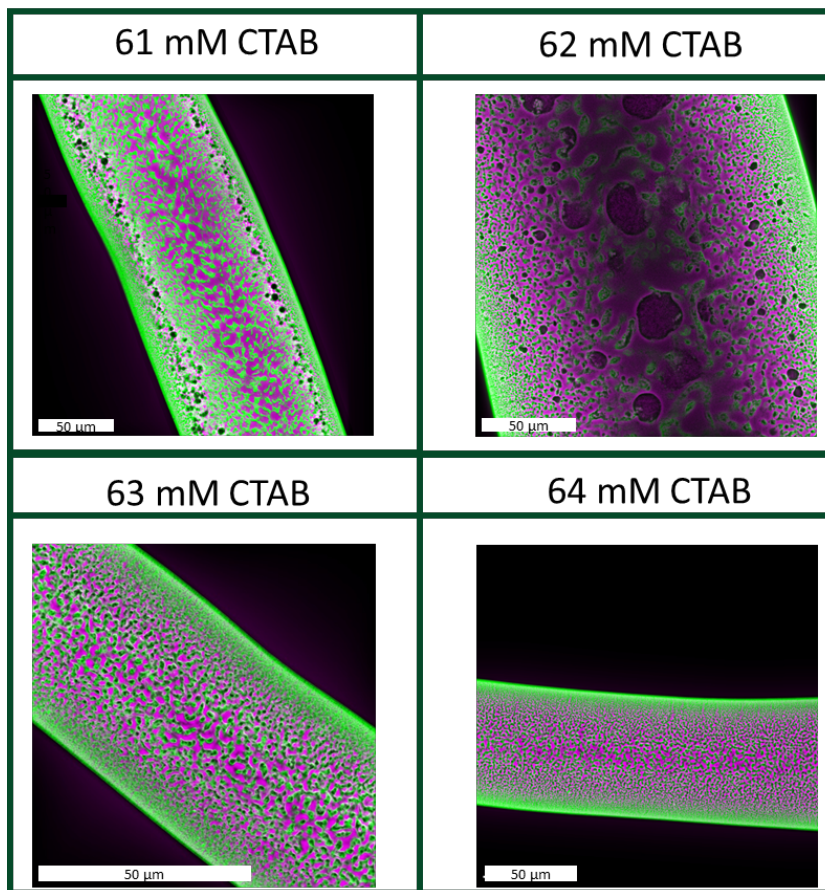


**Fig. 27:** Bijel fiber printed in continuous oil phase (black) with the precursor dispersion with no oxidizers and 61, 62, 63 and 64 mM CTAB. Containing water (magenta) and surface active Ludox TMA particles (green) at the interface.

As shown in figure 27 the increase in CTAB concentration changes the structure because of the change of wettability of the particle. The structure shown with 61 and 62 mM CTAB show no open oil (black) channels filled with oil but show the particles (green) inside the water (magenta) phase. The 62 mM is quite larger compared to the wanted  $50 \mu\text{m}$  which could influence the structure because of the long diffusion path. However, no bicontinuous structure is seen and thus indicating that the particle is still too hydrophilic. The 63 and 64 mM CTAB concentration shows that the oil channels in the water separated by the particles. Therefore, it can be said that this structure is bicontinuous with a concentration of 63 and 64 mM. The 64 mM CTAB shows the formation of radial channels in on the edges indicating that the particles are too hydrophobic thus forming these radial channels. From this parameter study it was concluded that 63 mM CTAB was the optimal concentration to form a bicontinuous structure. After this the  $\text{Na}_2\text{S}_2\text{O}_8$  (see figure 28) and  $\text{FeCl}_3$  (see figure 29) was added to the ternary with various concentrations.

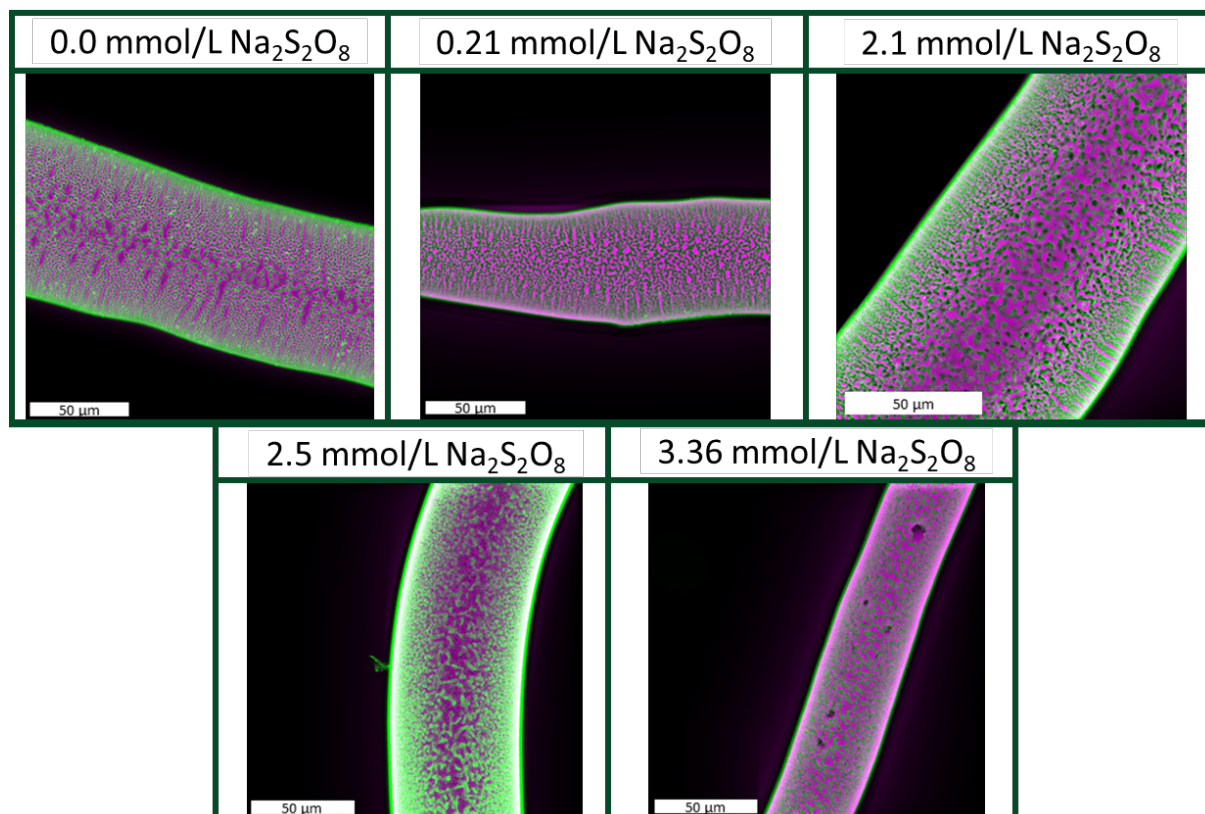


**Fig. 28:** Bijel fiber printed in continuous oil phase (black) with the 63 mM CTAB precursor dispersion with 0.0, 0.21, 2.1, 2.5 and 3.36 mmol/L (0.0, 0.05, 0.5, 0.6 and 0.8 mg/mL)  $\text{Na}_2\text{S}_2\text{O}_8$ . Containing water (magenta) and surface active Ludox TMA particles (green) at the interface.

As shown in figure 28 the 0.0, 0.21 and 2.1 mmol/L of  $\text{Na}_2\text{S}_2\text{O}_8$  show a bicontinuous structure. The oxidizer was added after the ternary was thus resulting in some aggregation in the 0.0 and 0.05 mg/mL samples. With the increase of concentration to 2.5 and 3.36 mmol/L the bicontinuous structure is lost because of the charge screening of the sodium. There could be an optimum concentration between 2.1 and 2.5 mmol/L however, the gain in this increase of concentration should not result in drastic increase in PEDOT formation. The results indicate that the maximum concentration of  $\text{Na}_2\text{S}_2\text{O}_8$  is 2.1 mmol/L without losing its bicontinuous structure.

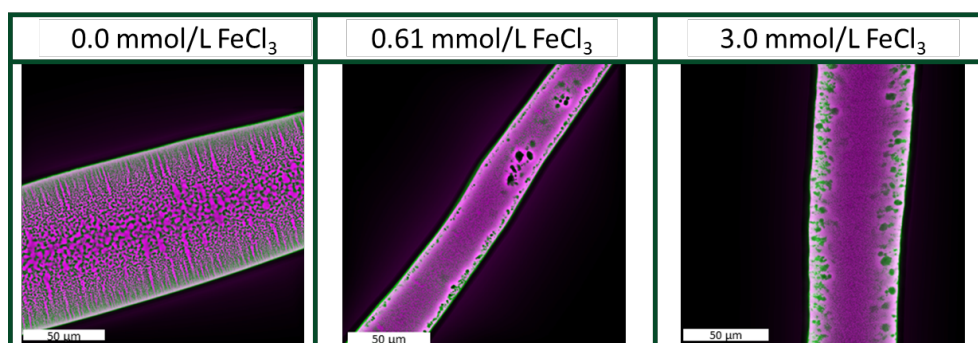


**Fig. 29:** Bijel fiber printed in continuous oil phase (black) with the precursor dispersion with 0.0, 0.61 and 3.0 mmol/L (0.0, 0.1 and 0.5 mg/mL)  $\text{FeCl}_3$ . Containing water (magenta) and surface active Ludox TMA particles (green) at the interface. The magenta in the black continuous phase is an artificial effect from the image processing.

As shown in figure 29 the addition of  $\text{FeCl}_3$  with a concentration of 0.61 mmol/L the bijel lost its bicontinuous structure. Because of the triple charge on the iron the screening potential it has on the nanoparticles is very significant compared to the  $\text{Na}_2\text{S}_2\text{O}_8$ . If the concentration would have been reduced a bicontinuous structure could have been obtained. However, this would not theoretically be enough to polymerize a substantial amount of EDOT. Combined with the apparent slower reaction rate found in timelapse experiments it was concluded that  $\text{Na}_2\text{S}_2\text{O}_8$  would be the more promising oxidizer to use in the following experiments.

The bijel was looked at under the confocal microscope, the sampling was done over period of days. Here the two peaks which shift with polarity are compared to each other over a time period. There are two samples one sample contained only 2.1 mmol/L  $\text{Na}_2\text{S}_2\text{O}_8$  (see figure 31a) the second sample the continuous phase of EDOT was pre-polymerized EDOT with a small amount of  $\text{FeCl}_3$  (see figure 31b).

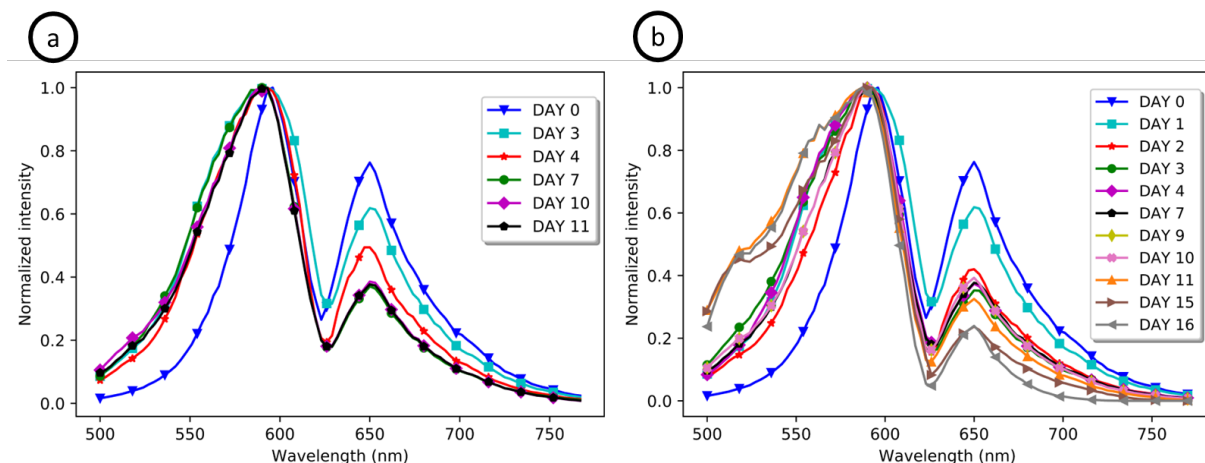


**Fig. 30:** Normalized confocal spectrum of Nile red adsorbed onto the particles of the bijels over a period of days. **a)** Bijels polymerized with 2.1 mmol/L (0.5 mg/mL)  $\text{Na}_2\text{S}_2\text{O}_8$  from the water phase. **b)** Bijels polymerized with 0.5 mg/mL  $\text{Na}_2\text{S}_2\text{O}_8$  from the water phase and pre-polymerized EDOT.

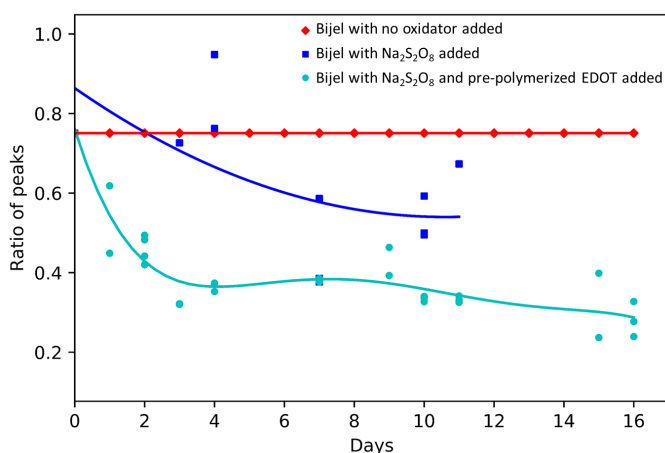


**Fig. 31:** The peak ratio's of the Nile red spectrum on the particles of the bijel as function of time (days) (see figure 30 for the spectrum's used). Peak ratio's of a bijel with no oxidizers added to it ( $\blacklozenge$ ), 2.1 mmol/L (0.5 mg/mL)  $\text{Na}_2\text{S}_2\text{O}_8$  added to the water phase of the bijel ( $\blacksquare$ ) over a period of 10 days. Peak ratios of a bijel with 2.1 mmol/L (0.5 mg/mL)  $\text{Na}_2\text{S}_2\text{O}_8$  and pre-polymerized EDOT mixed with the continuous phase of EDOT ( $\bullet$ ) over a period of 16 days.

As shown in figure 30a the spectrum is normalized with the 600 nm peak and the change in spectral shift is observed with the 650 nm peak. At day 0 the bijel has the highest 650 nm peak indicating the highest polarity. At day 11 the peak is the lowest indicating the decrease in polarity of the particles. When the EDOT is pre-polymerized added to the system (see figure 30b) the same is seen were the day 0 shows the highest 650 nm peak and day 16 shows the lowest peak. To translate this into a trend the peak ratio can be taken and plotted over the days (see figure 31). The red line shows the ratio of the spectrum of a bijel that did not undergo polymerization. When  $\text{Na}_2\text{S}_2\text{O}_8$  was added to the water phase and the continuous phase was swapped to EDOT, the peak ratio decreases to around 0.6. Looking at the bijel system were pre-polymerized EDOT was added to the continuous phase, the peak ratio decreases to 0.3 at day 10. And when let stand for longer, it continues to decrease even further. The bijel were no oxidator was added, stays on average consistent compared to when oxidators were added. The PEDOT formed with the oxidizers adsorbs onto the surface of the nanoparticles and thus changing the polarity. The peak ratio decreases rapidly with  $\text{Na}_2\text{S}_2\text{O}_8$  and pre-polymerized EDOT compared to only  $\text{Na}_2\text{S}_2\text{O}_8$ . Here the pre-polymerizes the EDOT and thus could increase the adsorbed amount on the surface. However, the addition of the pre-polymerized EDOT is a very heterogeneous to introduce more PEDOT to the bijel system. It was expected that the peak ratio increases because of the positive charge of PEDOT and thus increasing the polarity. This would result in a line that would go up in peak ratio instead of showing a downwards trend. However, the PEDOT could rearrange itself, only exposing the positive charges to the silica surfaces. These results suggest that, the polymerization of EDOT in bijels changes the polarity of the surface of the silica nanoparticles of the bijels over time.

#### 4.2.2 SEM-EDX

The confocal results give an indication of the change of polarity. However, it cannot conclude if there is any PEDOT formed. To see if the adsorption was significant enough to keep the fragile porous bijel structure open when dried SEM was done. If the bijel structure can be reinforced by this polymerization, something can be said about the formation of PEDOT. In this chapter, SEM images of the same samples for the confocal analysis are looked at. The addition of pre-polymerized EDOT to the continuous phase was investigated with the SEM. EDX could not be preformed unfortunately, because of the porous nature and size of the silica nanoparticles the EDX measurement would not result in any viable results.

##### 4.2.2.1 Refrence bijels SEM analysis

To understand when the enough EDOT was polymerized to keep the structure of the bijel intact the a bijel fiber with no treatment and TEOS treatment was looked at as shown in figure 32.

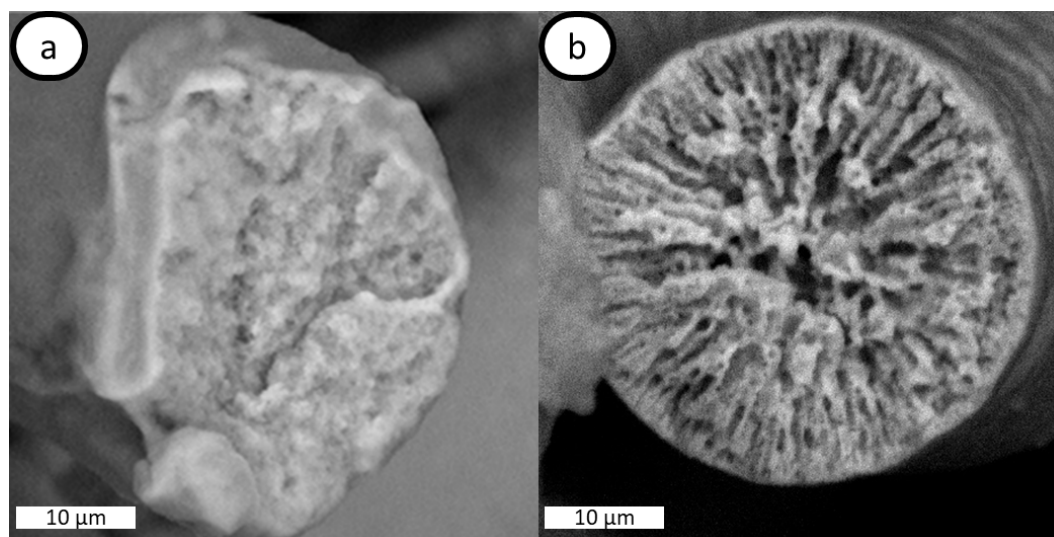


**Fig. 32:** Cross section SEM images of bijel fibers. **a)** Bijel fiber with no treatment completely collapsed with no open oil channels. **b)** TEOS treated fiber with open oil channels.

As shown in figure 32a the bijel fiber shows no porous resemblance of a bijel image. All the channels shown in the confocal images are collapsed. This is because the nanoparticles have no support and are not strong enough to keep the channels open. When looking at a TEOS treatment (see 32b) the structure of the bijel is open en porous. Here the oil channels are clearly visible and are open because of the extra silanes that reinforce the structure. The TEOS treated fiber is slightly different compared to the confocal image this could be because the time between fiber formation and or batch error. In summary, these results show that if no treatment is done the fiber is completely collapsed and when the structure is reinforced with TEOS the oil channels are clearly visible and open.

#### 4.2.2.2 Confocal microscope bijels SEM analysis

All the SEM images of confocal fibers are shown in appendix H. Here the starting day and end day SEM images will be discussed.

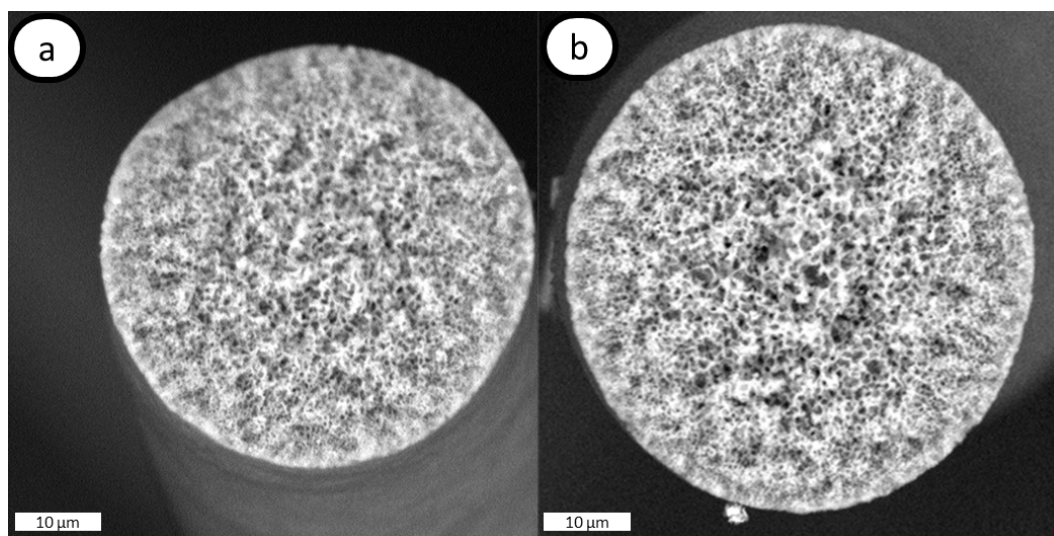


**Fig. 33:** Cross section SEM images of bijel fibers from the confocal analysis with only  $\text{Na}_2\text{S}_2\text{O}_8$ . **a)** Bijel fiber at day 3 of the confocal experiment. **b)** Bijel fiber at day 10 of the confocal experiment.

As shown in figure 33a the bijel is not collapsed and looks to be porous at day 3. However, when compared to a TEOS-treated fiber the structure looks to be more homogeneous. And does not show distinct channels that are open. The channels look to be collapsed, but the fiber is not completely collapsed. The fiber is not completely collapsed compared to the no treatment fiber. At day 10 (see figure 33b) the structure does not look much different compared to the bijel at day 3. In summary, these results show that when only using  $\text{Na}_2\text{S}_2\text{O}_8$  and letting the polymerization happen for 3 to 10 days is not enough to reinforce the structure.

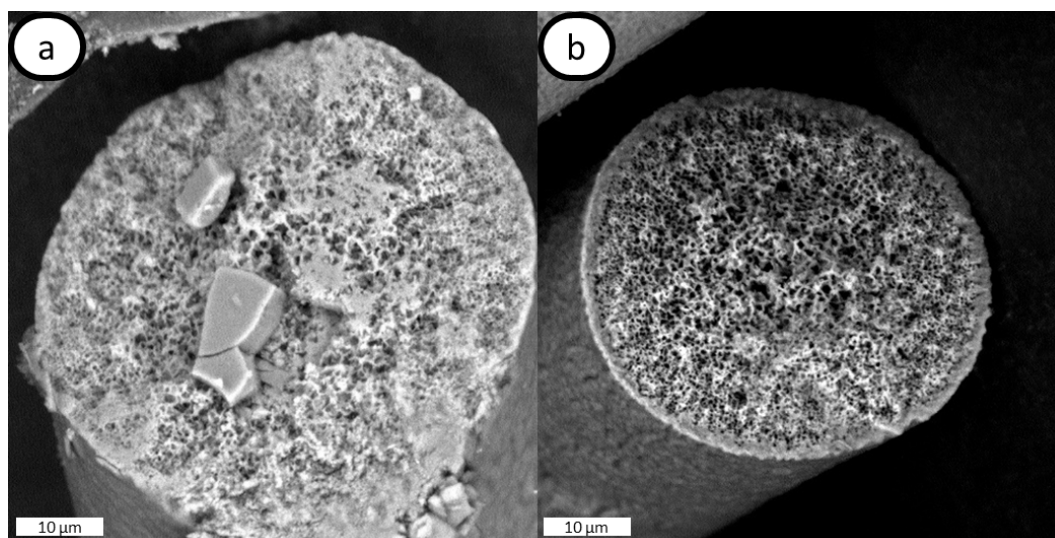


**Fig. 34:** Cross section SEM images of bijel fibers from the confocal analysis with  $\text{Na}_2\text{S}_2\text{O}_8$  and pre-polymerized EDOT. **a)** Bijel fiber at day 1 of the confocal experiment. **b)** Bijel fiber at day 16 of the confocal experiment.

As shown in figure 34a at day 1 the bijel is collapsed in various places and still look somewhat porous on the inside. There are collapsed bijel pieces stuck in the middle of the bijel obstructing a complete view of the structure. However, the bijel is not completely collapsed and only the oil channels are collapsed. At day 16 (see figure 34b) the bijel looks porous and the surface pores also look to be open and not collapsed. However, when looking at the cross section, no open oil channels are seen and they again seem to be collapsed. EDX was not able to be performed on the fibers because of their movement. Even though, that there are no EDX measurements confirming the presence of PEDOT, the porous structure does indicate the presence of some PEDOT. In summary, these results show that even though there might be PEDOT formed on the interface, it is not enough to reinforce the structure.

#### 4.2.2.3 Pre-polymerized EDOT bijels SEM analysis

Because of the limited amount of oxidizer that could be added to the ternary, the formation of the PEDOT was not substantial enough to keep oil channels open of the bijel. Therefore, instead of waiting for the polymerization, pre-polymerized EDOT was added to the system. This in theory should work the same because of the positive charge it contains. It should eventually cover the entire surface of the negatively charged silica. It was added to the continuous phase allowing for diffusion to transport it through the container and into the oil channels of the fibers. Because the continuous phase is the monomer of the polymer, it was allowed to diffuse through and did not precipitate as it did with toluene, as shown in appendix I.

To get an idea if the substantial amount of PEDOT added could in fact keep the oil channels open the fibers were looked at under the SEM (see figure 35).

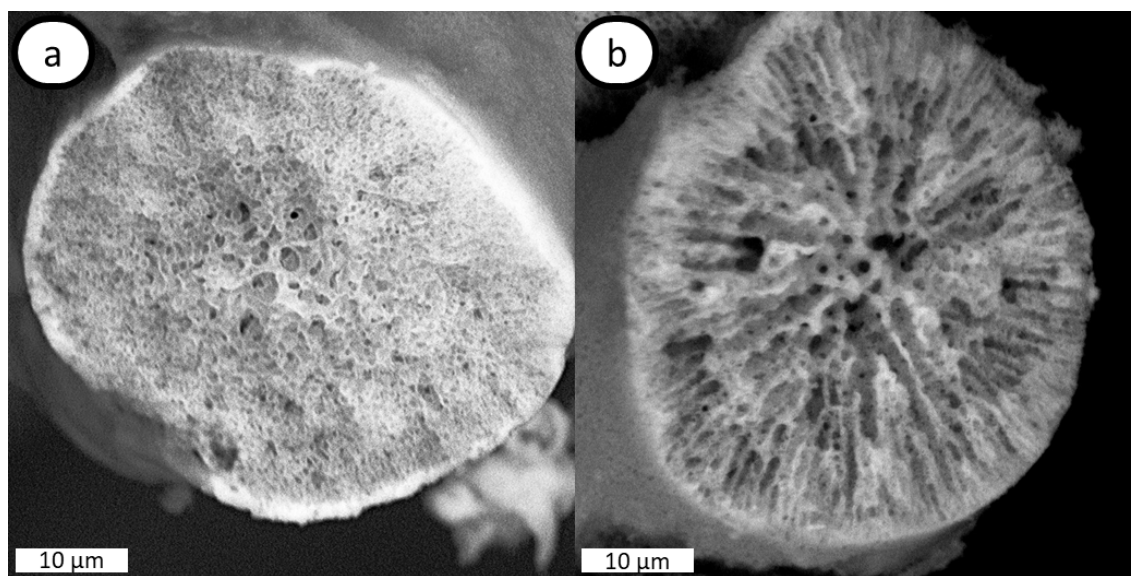


**Fig. 35:** Cross section SEM images of bijel fibers with different treatments. **a)** Bijel fiber with pre-polymerized EDOT added to the continuous phase of the bijels. **b)** TEOS treated bijel fiber for comparison

As shown in figure 35a the channels look porous and the oil channels are still open. The same structure is seen in the TEOS treated fiber (see figure 35b). When the amount of PEDOT is significant enough, the oil channels are being kept open. Here 0.5 mL of EDOT was polymerized using  $\text{FeCl}_3$  which was added in excess, the remaining crystals were removed from the solution and the PEDOT was added to the continuous phase consisting of 3 mL EDOT. Finally, after 48 hours the fibers were washed with toluene and ethanol and let dry resulting in the dried fibers shown in figure 35. This ensured all the EDOT and PEDOT that had no interaction with the fibers was removed. These results also reinforces the results found in the model system which showed that the PEDOT could adsorb onto the silica. Comparing the images it looks somewhat different. This could be because of the different properties of the coatings. The results also indicate that when PEDOT is added in a significant amount to the continuous phase, the structure was reinforced and prevented the oil channels from collapsing.

### 4.2.3 Conductivity measurement

In this section the results of the conductivity measurements of bijel fibers will be discussed. Here there are two methods used to introduce PEDOT into the bijel fibers. In the first section, the method of introducing pre-polymerized EDOT to the continuous phase was used. The second section, the method of polymerizing PEDOT in the continuous phase was used. The conductivity calculations were done according to equations shown in appendix I. The goal of these sections was to see if various methods could be used to introduce PEDOT into the bijel system to increase the conductivity compared to TEOS-treated fibers.

#### 4.2.3.1 Pre-polymerized EDOT

The fibers were treated with TEOS and PEDOT in the conductivity container as shown in figure 36.



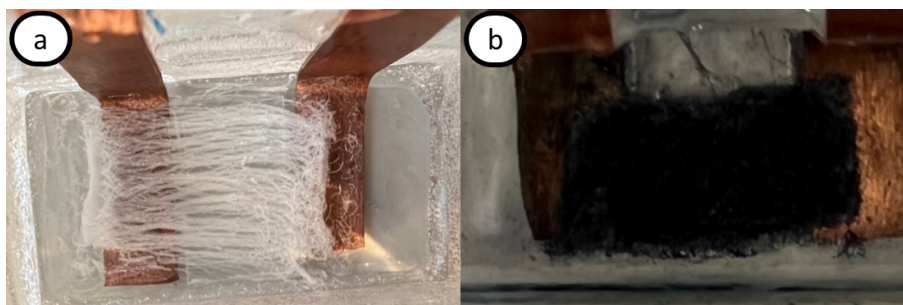


**Fig. 36:** Image taken of the printed fiber with various treatments in a conductivity measurement container  
 a) White fiber treated with TEOS b) Black fibers treated with pre-polymerized EDOT.

As shown in figure 36a the fibers are still white and not broken, making full contact with the electrode. And the PEDOT-treated fibers have turned completely black from the treatment (see figure 36b). It is a good indication that the PEDOT has adsorbed onto the fibers and have turned completely black even after washing. The conductivity of the bijel fibers were measured three different ways as shown in figure 37.

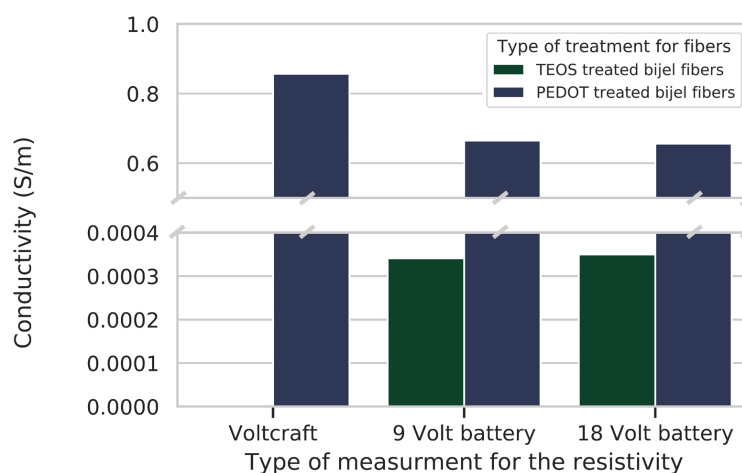


**Fig. 37:** Conductivity (S/m) measured of TEOS-treated fibers (green) and pre-polymerized EDOT bijel fibers (blue). Measured by the voltcraft<sup>®</sup> with out external power source, with a 9-Volt battery and two 9-volt batteries making 18 volts.

As shown in figure 36 the voltcraft<sup>®</sup> could not read any resistivity of the TEOS treated fibers, the 9 volt and 18 volt battery measured a conductivity of around  $3.5 \times 10^{-4}$  S/m. The voltcraft<sup>®</sup> measured a conductivity of 0.85 S/m and the 9 volt and 18 volt battery measured a conductivity of 0.65 S/m. The first measurement was done with just the voltcraft<sup>®</sup> directly measuring the resistance, which it does by applying a very small current and measuring the voltage. The other two were measured using external batteries which required more cables and thus introduced more resistance lowering the conductivity a bit. The TEOS-treated fiber measurement is so small that it could be in the range of error of the measurement method. The PEDOT-treated fibers were only made once, which does not allow for an error to be shown. Because of the method used for introducing PEDOT, it could be that there is an error. Overall, these results indicate that the introduction of pre-polymerized EDOT significantly increases the conductivity of the bijel fibers.

#### 4.2.3.2 Polymerization in continuous phase

The addition method of pre-polymerized EDOT is even though, effective, is very uncontrolled. If the oxidizer could be introduced to the continuous phase it should give more control of the PEDOT deposition. Using  $\text{Fe(III)(OTs)}_3$  and 3% v/v of 1-pentanol allows for Fe(III) to be dissolved in toluene. Without the

addition of 1-pentanol the  $\text{Fe(III)(OTs)}_3$  could not be dissolved (see appendix I). The polymerization after 48 hours resulted in the fibers shown in figure 38. The increase in concentration of  $\text{Fe(III)(OTs)}_3$  resulted in the fibers visibly changing from yellow the oxidizer to more black from the PEDOT as shown in figure 38. After being washed with toluene and ethanol, the current was measured giving a resistivity. Here the concentration of the oxidizer was increased to see if this would correlate to the increase in conductivity as shown in figure 39.

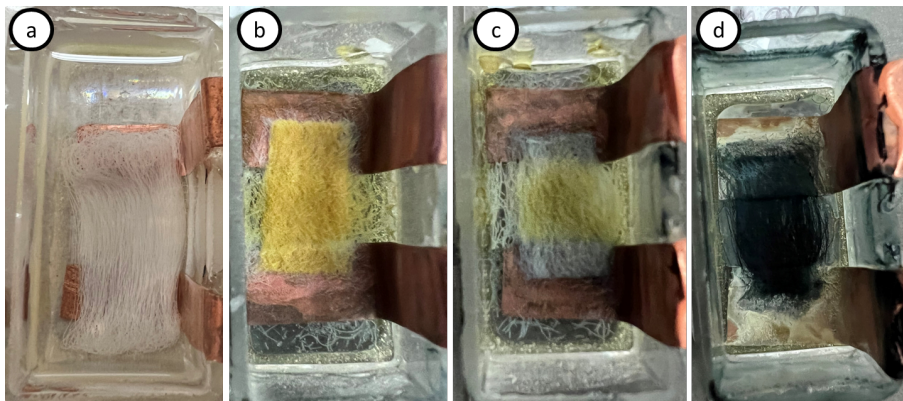


**Fig. 38:** Fibers after polymerization with various  $\text{Fe(III)(OTs)}_3$  concentrations. **a)** 0.0 mg/mL (0.0 mmol/L) **b)** 1.25 mg/mL (1.8 mmol/L) **c)** 2.5 mg/mL (3.7 mmol/L) **d)** 5.0 mg/mL (7.5 mmol/L).

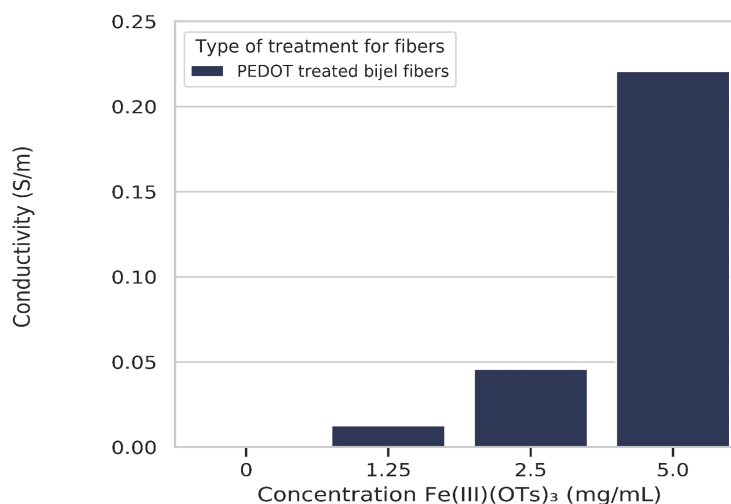


**Fig. 39:** Conductivity (S/m) measured of bijel fibers with PEDOT polymerized in the continuous phase toluene with increasing  $\text{Fe(III)(OTs)}_3$  concentration (mg/mL). The conductivity was measure using the voltcraft<sup>®</sup> without external power source.

As shown in figure 39 when no oxidizers are added the resistivity could not be measured. When the concentration of  $\text{Fe(III)(OTs)}_3$  is increased the conductivity also increases. With the maximum being at 5.0 mg/mL (7.5 mmol/L) with a conductivity of 0.22 S/m. This also came with an increase of black fibers indicating more PEDOT was polymerized thus facilitating the increase in conductivity (see appendix I). The EDOT concentration was kept constant and was added in excess thus making the polymerization oxidizer dependent. The oxidizer concentration could be increased. However, the maximum solubility was reached at 5.0 mg/mL (7.5 mmol/L). Increasing the 1-pentanol concentration could increase this. However, the effect of 1-pentanol and the EDOT polymerization to the bijel is not known. Overall, these results indicate that when the concentration of  $\text{Fe(III)(OTs)}_3$  is increased the conductivity of the bijel fibers is also increased.

## 5 Conclusions and outlook

The research question was: to which extent can we introduce Poly(3,4-ethylenedioxythiophene) (PEDOT) into a silica bijel system forming a conductive bijel? The introduction of EDOT into the precursor dispersion was not a viable way to introduce PEDOT into a bijel. This research showed that introduction of PEDOT after the bijel has already been formed was a viable way to introduce PEDOT into the silica bijel system forming conductive bijels.

The research question was investigated by setting up a model system where the silica PEDOT interaction was investigated. Which was done by timelapse, zeta-potential measurements and SEM-EDX analysis. It was concluded from the timelapse results that the EDOT is polymerized relatively fast at the EDOT-water interface with  $\text{Na}_2\text{S}_2\text{O}_8$  and  $\text{FeCl}_3$  combined. Separating these oxidizers increases the polymerization time from 17 minutes to several days. The polymerization of EDOT with  $\text{Na}_2\text{S}_2\text{O}_8$  increased the zeta-potential of the silica particles, which was not the case with  $\text{FeCl}_3$ . The addition of EDOT, CTAB and the oxidizers increases the zeta-potential of the silica particles. Confirming that the PEDOT can electrostatically adsorb onto the surface of the particles with or without CTAB. However, the method of polymerization results in very heterogeneous samples and thus non-conforming data. The SEM-EDX results show that structurally strong PEDOT is formed and can adsorb onto the silica. The addition of pre-polymerized EDOT resulted into the same visual characteristics.

Finally, the bijel system was investigated to see what the introduction of PEDOT does to the bijel system. Which was done by confocal microscope analysis, SEM-EDX and conductivity measurements. From the confocal analysis it could be concluded that to 1 mL of the chosen precursor dispersion, 0.5 mg of  $\text{Na}_2\text{S}_2\text{O}_8$  could be added without losing the bicontinuous characteristic of the bijel. The addition of 0.1 mg  $\text{FeCl}_3$  does not allow for the bicontinuous structure to remain. And any lower concentration is not theoretically worth investigating for polymerization from the water phase. The addition of  $\text{Na}_2\text{S}_2\text{O}_8$  reduces the polarity of the silica particles in the bijels. The addition of pre-polymerized to the continuous phase reduces the polarity even more. However, the method of using pre-polymerized EDOT is very heterogeneous. The SEM analysis of these fibers showed that over a certain time frame there is not enough PEDOT polymerized to keep the bijel structure open.

From the SEM analysis it was concluded that with the addition of excess pre-polymerized EDOT could keep the structure of the bijel open. With the conductivity measurements showing significant increase in the conductivity of the bijel fibers compared to TEOS-treated bijel fibers. The addition of 1-pentanol and  $\text{Fe(III)(OTs)}_3$  to the continuous phase allowed for a more controlled way to polymerize PEDOT. Here the increase in oxidizer concentration increases the conductivity of the fibers because more PEDOT is formed.

The most important limitation of this study lies in the fact that two systems that are complex and sensitive are combined. However, this research extends our knowledge of the introduction of PEDOT into the bijel system and is an experimental stepping stone for future fundamental research. If the research is to be moved forward, a better understanding of the polymerization through time for EDOT in the model needs to be developed. Also the method used in the model system to investigate the zeta-potential needs to be reconsidered if more work is to be done. Considerably more work will need to be done to determine the effects of PEDOT to the bijel system. Here the effects of the polymerization conditions can affect the conductivity or the bijel structure and should thus be studied in detail separately. Finally, the method of measuring conductivity leaves a lot of space for error if all fibers are not touching the electrode the measurement is understating the conductivity. This could be solved using conductive glue to connect all the fibers resulting in a more accurate measurement.

## 6 Acknowledgements

Firstly, I want to thank Martin for his constant advice, guidance and his endless optimism. I am very grateful for receiving this project from him and being able to extend my knowledge within this project. Most of all, I would like to give my special thanks to Matthijs for his constant support, patience and supervision during this project. They truly have taught me so much in the endless realms of science and I will be eternally grateful for that.

Secondly, I would like to thank Alex, Bonny and Dominique for their deep insights in various subjects and helping me become a better and more organized scientist. I am also very grateful for all the people in the Haase research group for their insightful discussions and very much appreciated feedback. I am particularly grateful for all the people at FCC for the warm welcome and making the long journey to the beautiful Hugo R. Kruyt building worth while. Most of all, I would like to thank all the FCC master students for the never ending jokes and high-yielding discussions during my challenging but fun project.

Finally, I would like to thank my family and friends for endlessly listening to me talking about the research I was doing and supporting me each and every day.

### *Standing on the shoulders of giants*



*Jacobus Henricus van 't Hoff*

*"It is sometimes easier to circumvent prevailing difficulties [in science] rather than to attack them"*



*Maria Salomea Skłodowska-Curie*

*"I am among those who think that science has great beauty. A scientist in his laboratory is not only a technician: he is also a child placed before natural phenomena which impress him like a fairy tale."*

## References

- [1] IEA: Renewables 2019 (2019 <https://www.iea.org/reports/renewables-2019>)
- [2] IEA: Global supply chains of ev batteries (2022 <https://www.iea.org/reports/global-supply-chains-of-ev-batteries>)
- [3] IEA: Grid-scale storage (2022 <https://www.iea.org/reports/grid-scale-storage>)
- [4] Tian, H., Gardner, J., Edvinsson, T., Pati, P.B., Cong, J., Xu, B., Abrahamsson, M., Cappel, U.B., Barea, E.M.: Dye-sensitised solar cells, 89–152 (2019)
- [5] Matsumura, M., Matsudaira, S., Tsubomura, H., Takata, M., Yanagida, H.: Dye sensitization and surface structures of semiconductor electrodes. *Industrial & Engineering Chemistry Product Research and Development* **19**(3), 415–421 (1980)
- [6] Ahmad, M.S., Pandey, A.K., Abd Rahim, N.: Advancements in the development of tio<sub>2</sub> photoanodes and its fabrication methods for dye sensitized solar cell (dssc) applications. a review. *Renewable and Sustainable Energy Reviews* **77**, 89–108 (2017)
- [7] Padbury, R., Zhang, X.: Lithium–oxygen batteries—limiting factors that affect performance. *Journal of Power Sources* **196**(10), 4436–4444 (2011)
- [8] Balbuena, P.B., Wang, Y.X.: Lithium-ion batteries: solid-electrolyte interphase (2004)
- [9] Stratford, K., Adhikari, R., Pagonabarraga, I., Desplat, J.-C., Cates, M.E.: Colloidal jamming at interfaces: A route to fluid-bicontinuous gels. *Science* **309**(5744), 2198–2201 (2005)
- [10] Cates, M.E., Clegg, P.S.: Bijels: a new class of soft materials. *Soft Matter* **4**(11), 2132–2138 (2008)
- [11] Haase, M.F., Stebe, K.J., Lee, D.: Continuous fabrication of hierarchical and asymmetric bijel microparticles, fibers, and membranes by solvent transfer-induced phase separation (strips). *Advanced Materials* **27**(44), 7065–7071 (2015)
- [12] D’Apolito, R., Perazzo, A., D’Antuono, M., Preziosi, V., Tomaiuolo, G., Miller, R., Guido, S.: Measuring interfacial tension of emulsions in situ by microfluidics. *Langmuir* **34**(17), 4991–4997 (2018)
- [13] Schramm, L.L.: *Emulsions, foams, suspensions, and aerosols: microscience and applications* (2014)
- [14] Tadros, T.F.: *Interfacial phenomena and colloid stability: basic principles* **1** (2015)
- [15] Wilde, P.: Interfaces: their role in foam and emulsion behaviour. *Current Opinion in Colloid & Interface Science* **5**(3-4), 176–181 (2000)
- [16] Israelachvili, J.N.: *Intermolecular and surface forces* (2011)
- [17] Aveyard, R., Binks, B.P., Clint, J.H.: Emulsions stabilised solely by colloidal particles. *Advances in Colloid and Interface Science* **100**, 503–546 (2003)
- [18] Abbott, S.: *Surfactant science: principles and practice. Update* **1**, 2–26 (2016)
- [19] CXCVI, P.S.: Emulsions. *J. Chem. Soc. Trans* **91**, 2001–2021 (1907)
- [20] Ramsden, W.: Separation of solids in the surface-layers of solutions and ‘suspensions’ (observations on surface-membranes, bubbles, emulsions, and mechanical coagulation).—preliminary account. *Proceedings of the royal Society of London* **72**(477-486), 156–164 (1904)
- [21] Boakye-Ansah, S., Khan, M.A., Haase, M.F.: Controlling surfactant adsorption on highly charged nanoparticles to stabilize bijels. *The Journal of Physical Chemistry C* **124**(23), 12417–12423 (2020)

- 
- [22] Binks, B.P., Horozov, T.S.: Colloidal particles at liquid interfaces (2006)
- [23] Levine, S., Bowen, B.D., Partridge, S.J.: Stabilization of emulsions by fine particles i. partitioning of particles between continuous phase and oil/water interface. *Colloids and surfaces* **38**(2), 325–343 (1989)
- [24] Haase, M.F., Jeon, H., Hough, N., Kim, J.H., Stebe, K.J., Lee, D.: Multifunctional nanocomposite hollow fiber membranes by solvent transfer induced phase separation. *Nature communications* **8**(1), 1–7 (2017)
- [25] Haase, M.F., Brujic, J.: Tailoring of high-order multiple emulsions by the liquid–liquid phase separation of ternary mixtures. *Angewandte Chemie* **126**(44), 11987–11991 (2014)
- [26] Khan, M.A., Sprockel, A.J., Macmillan, K.A., Alting, M.T., Kharal, S.P., Boakye-Ansah, S., Haase, M.F.: Nanostructured, fluid-bicontinuous gels for continuous-flow liquid–liquid extraction. *Advanced Materials*, 2109547 (2022)
- [27] Chiang, C., Fincher Jr, C., Park, Y., Heeger, A., Shirakawa, H., Louis, E., Gau, S., MacDiarmid, A.G.: Electrical conductivity in doped polyacetylene. *Physical Review Letters* **40**(22), 1472 (1978)
- [28] Heeger, A.J.: *Semiconducting and metallic polymers: the fourth generation of polymeric materials*. ACS Publications (2001)
- [29] Atkins, P., Atkins, P.W., de Paula, J.: *Atkins’ physical chemistry* (2014)
- [30] Nalwa, H.S.: *Handbook of organic conductive molecules and polymers* (1997)
- [31] Elschner, A., Kirchmeyer, S., Lovenich, W., Merker, U., Reuter, K.: *Pedot: principles and applications of an intrinsically conductive polymer* (2010)
- [32] Jonas, F., Heywang, G., Schmidtberg, W., Heinze, J., Dietrich, M.: *Polythiophenes, process for their preparation and their use*. Google Patents (1990)
- [33] Nie, S., Li, Z., Yao, Y., Jin, Y.: Progress in synthesis of conductive polymer poly (3, 4-ethylenedioxythiophene)(pedot). *Frontiers in Chemistry*, 1137 (2021)
- [34] Koizumi, Y., Shida, N., Ohira, M., Nishiyama, H., Tomita, I., Inagi, S.: Electropolymerization on wireless electrodes towards conducting polymer microfibre networks. *Nature communications* **7**(1), 1–6 (2016)
- [35] Wu, Y., Prulho, R., Brigante, M., Dong, W., Hanna, K., Mailhot, G.: Activation of persulfate by fe (iii) species: implications for 4-tert-butylphenol degradation. *Journal of hazardous materials* **322**, 380–386 (2017)
- [36] Liu, H., Bruton, T.A., Li, W., Buren, J.V., Prasse, C., Doyle, F.M., Sedlak, D.L.: Oxidation of benzene by persulfate in the presence of fe (iii)-and mn (iv)-containing oxides: stoichiometric efficiency and transformation products. *Environmental science & technology* **50**(2), 890–898 (2016)
- [37] Sakunpongpitiporn, P., Phasukom, K., Paradee, N., Sirivat, A.: Facile synthesis of highly conductive pedot: Pss via surfactant templates. *RSC advances* **9**(11), 6363–6378 (2019)
- [38] Mueller, M., Fabretto, M., Evans, D., Hojati-Talemi, P., Gruber, C., Murphy, P.: Vacuum vapour phase polymerization of high conductivity pedot: Role of peg-ppg-peg, the origin of water, and choice of oxidant. *Polymer* **53**(11), 2146–2151 (2012)
- [39] Johansson, T., Pettersson, L.A., Inganäs, O.: Conductivity of de-doped poly (3, 4-ethylenedioxythiophene). *Synthetic metals* **129**(3), 269–274 (2002)
- [40] Zuber, K., Fabretto, M., Hall, C., Murphy, P.: Improved pedot conductivity via suppression of

- 
- crystallite formation in fe (iii) tosylate during vapor phase polymerization. *Macromolecular rapid communications* **29**(18), 1503–1508 (2008)
- [41] Kim, J., Jung, J., Lee, D., Joo, J.: Enhancement of electrical conductivity of poly (3, 4-ethylenedioxythiophene)/poly (4-styrenesulfonate) by a change of solvents. *Synthetic Metals* **126**(2-3), 311–316 (2002)
- [42] Lövenich, W.: Pedot-properties and applications. *Polymer Science Series C* **56**(1), 135–143 (2014)
- [43] Park, T., Park, C., Kim, B., Shin, H., Kim, E.: Flexible pedot electrodes with large thermoelectric power factors to generate electricity by the touch of fingertips. *Energy & Environmental Science* **6**(3), 788–792 (2013)
- [44] Sun, K., Zhang, S., Li, P., Xia, Y., Zhang, X., Du, D., Isikgor, F.H., Ouyang, J.: Review on application of pedots and pedot: Pss in energy conversion and storage devices. *Journal of Materials Science: Materials in Electronics* **26**(7), 4438–4462 (2015)
- [45] Furcas, F.E., Lothenbach, B., Isgor, O.B., Mundra, S., Zhang, Z., Angst, U.M.: Solubility and speciation of iron in cementitious systems. *Cement and Concrete Research* **151**, 106620 (2022)

## Appendix A - Bijel formation

In this appendix the details of the formation of the bijel will be discussed and looked at the CTAB concentration. The precursor dispersions with various CTAB concentrations are made according to table A1,A2. All precursor dispersion have a NaCl concentration of 50 mM.

**Table A1** Precursor composition with increasing CTAB concentration with increments of 5 mM

Pipet the following solutions sequentially in an Eppendorf using a pipet:	Sample CTAB 50 mM	Sample CTAB 55 mM	Sample CTAB 60 mM	Sample CTAB 65 mM	Sample CTAB 70 mM
DEP (mL)	0.070	0.070	0.070	0.070	0.070
CTAB stock solution (mL)	0.108	0.118	0.129	0.140	0.151
Glycerol Stock Solution (mL)	0.241	0.241	0.241	0.000	0.000
1-propanol (mL)	0.081	0.070	0.060	0.290	0.280
Aqueous Stock Ludox TMA dispersion (mL)	0.479	0.479	0.479	0.479	0.479
MilliQ (mL)	0.021	0.021	0.021	0.021	0.021
Total volume (mL)	1	1	1	1	1

**Table A2** Precursor composition with increasing CTAB concentration with increments of 1 mM

Pipet the following solutions sequentially in an Eppendorf using a pipet:	Sample CTAB 61 mM	Sample CTAB 62 mM	Sample CTAB 63 mM	Sample CTAB 64 mM
DEP (mL)	0.070	0.070	0.070	0.070
CTAB stock solution (mL)	0.131	0.133	0.135	0.138
Glycerol Stock Solution (mL)	0.000	0.000	0.000	0.000
1-propanol (mL)	0.299	0.297	0.295	0.292
Aqueous Stock Ludox TMA dispersion (mL)	0.479	0.479	0.479	0.479
MilliQ (mL)	0.021	0.021	0.021	0.021
Total volume (mL)	1	1	1	1



To make a bijel a neutral wetting particle is needed, to get this, the right amount of CTAB is needed. To find the right concentration of CTAB a parameter scan was done to as shown in figure A2 and A3. The method of extraction was quick fiber, which is a 50  $\mu\text{m}$  capillary glued into a pipette tip containing the precursor dispersion which was printed in toluene (see figure A1).

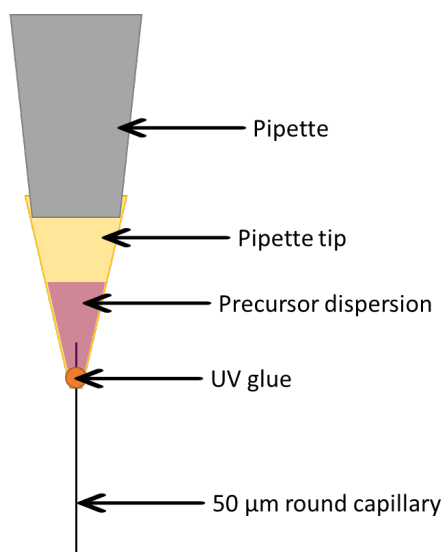


**Fig. A1:** Quick fiber method using the pressure from a pipette, here ternary is pushed from the pipette tip through the 50  $\mu\text{m}$  round capillary into the continuous phase.

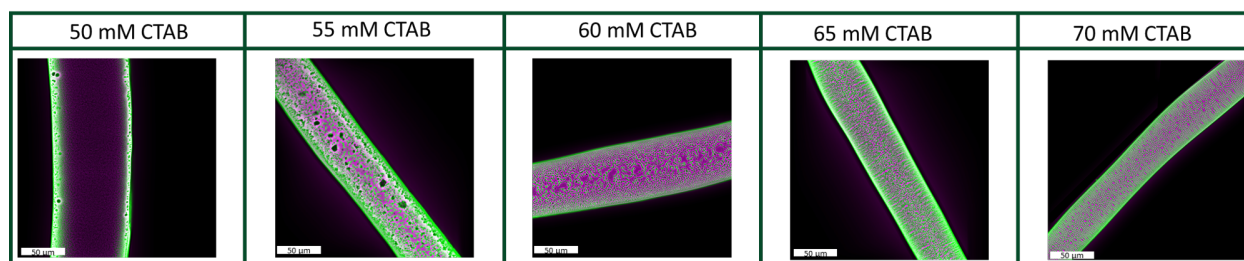


**Fig. A2:** Confocal images of bijel extruded in the continuous phase of oil (black). Here the bijel contains water (magenta) and the surface active Ludox TMA particles (green) which can be visually separated by the use of Nile red under the confocal. Here the CTAB concentration is increased with 5 mM increments (see table A1).

As shown in figure A2 the first broad scan was done with increments of 5 mM CTAB. Here there is no bicontinuous structure from 50 to 60 mM CTAB. From 65 mM there is a bicontinuous structure seen with some radial channels indicating that the CTAB concentration is too high. There for the close to optimal concentration is between 60 and 65 mM, which was investigated as shown in figure A3.

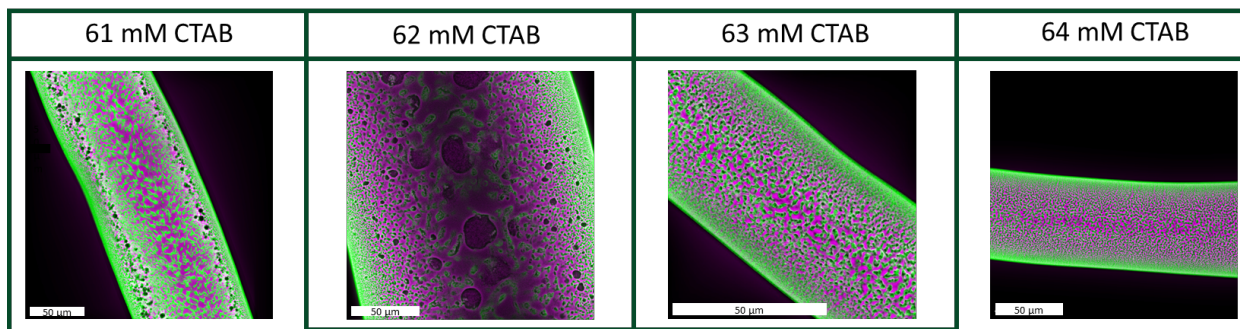


**Fig. A3:** Confocal images of bijel extruded in the continuous phase of oil (black). Here the bijel contains water (magenta) and the surface active Ludox TMA particles (green) which can be visually separated by the use of Nile red under the confocal. Here the CTAB concentration is increased with 1 mM increments (see table A2).

Here 63 mM CTAB showed the closest to optimal bicontinuous structure and was thus chosen to be the precursor dispersion used for the bijel creation. The script that was used to process the results of the bijel in ImageJ (version 2.9.0, Java 1.8.0 322) (see figure A4).

```

var A = "Insert here file name"
var B = "C1-" + A
var C = "C2-" + A
selectWindow("C1-" + A);
run("Bandpass Filter...", "filter_large=40 filter_small=3 suppress=None tolerance=5 autoscale saturate");
run("Enhance Contrast...", "saturated=0.35 equalize");
run("Invert");

run("RGB Color");
run("Color Balance...");
resetMinAndMax();
setMinAndMax(255, 255, 2);
run("Close");
run("Subtract Background...", "rolling=1000");

selectWindow("C2-" + A);
run("RGB Color");
run("Color Balance...");
resetMinAndMax();
setMinAndMax(255, 255, 5);
run("Close");

run("Merge Channels...", "c2=&C + c6=&B");

run("Set Scale...", "distance=Insert length of 1 pixel known=1 unit=micron");
run("Scale Bar...", "width=10 height=150 thickness=25 font=28 color=white background=Black location=[Lower Left] horizontal bold overlay");

```

**Fig. A4:** Code used in ImageJ to process bijels consistently

## Appendix B - Oxidator addition to bijel precursor dispersion

In this appendix the details for the formation of the oxidizers with the precursor dispersion are discussed. The samples with the  $\text{Na}_2\text{S}_2\text{O}_8$  were made according to table B3 and the samples with  $\text{FeCl}_3$  were made according to table B4.

**Table B3** Precursor dispersions (63 mM CTAB) with increasing  $\text{Na}_2\text{S}_2\text{O}_8$  concentration.

Precursor preparation increasing oxidizer concentration	0.00 mmol/L (0.00 mg/mL) $\text{Na}_2\text{S}_2\text{O}_8$	0.21 mmol/L (0.05 mg/mL) $\text{Na}_2\text{S}_2\text{O}_8$	2.1 mmol/L (0.5 mg/mL) $\text{Na}_2\text{S}_2\text{O}_8$	2.5 mmol/L (0.6 mg/mL) $\text{Na}_2\text{S}_2\text{O}_8$	3.36 mmol/L (0.8 mg/mL) $\text{Na}_2\text{S}_2\text{O}_8$
Oxidizer stock solution concentration g/ml	0.00	0.001	0.01	0.01	0.02
Amount oxidizer stock solution added ( $\mu\text{L}$ )	10.00	10.00	10.00	10.00	10.00
Amount of 1-propanol added ( $\mu\text{L}$ )	10.00	10.00	10.00	10.00	10.00
Precursor dispersion (mL)	0.18	0.18	0.18	0.18	0.18
Concentration oxidizer in precursor dispersion (mg/mL)	0.00	0.05	0.50	0.60	0.80

**Table B4** Precursor dispersions (63 mM CTAB) with increasing  $\text{FeCl}_3$  concentration.

Precursor preparation increasing oxidizer concentration	0.0 mmol/L (0.00 mg/mL) $\text{FeCl}_3$	0.61 mmol/L (0.1 mg/mL) $\text{FeCl}_3$	3.0 mmol/L (0.5 mg/mL) $\text{FeCl}_3$
Oxidizer stock solution concentration g/ml	0.00	0.00	0.01
Amount oxidizer stock solution added ( $\mu\text{L}$ )	10.00	10.00	10.00
Amount of 1-propanol added ( $\mu\text{L}$ )	10.00	10.00	10.00
Precursor dispersion (mL)	0.18	0.18	0.18
Concentration oxidizer in precursor dispersion (mg/mL)	0.00	0.10	0.50

## Appendix C - Timelapse

In this appendix the images of the time intervals from the timelapse are shown in more detail. Figures C5,C6 are discussed in great detail in chapter 4. Figure C7 is discussed also discussed here until  $t = 119:40$  (minutes:seconds), after this time interval of figure C7a the interface was broken by experimental error. Because of this the results could not be compared to the results of C7b.

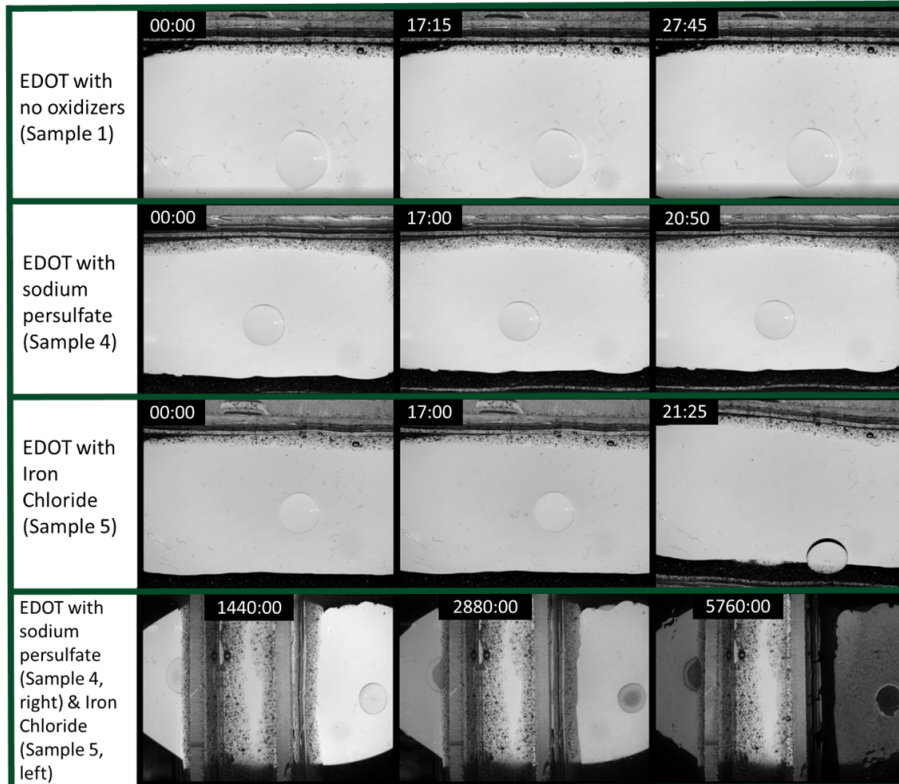


**Fig. C5:** Time intervals of a timelapse of an EDOT droplet in water with no oxidizers (sample 1), only  $\text{Na}_2\text{S}_2\text{O}_8$  (sample 4), only  $\text{FeCl}_3$  (sample 5).

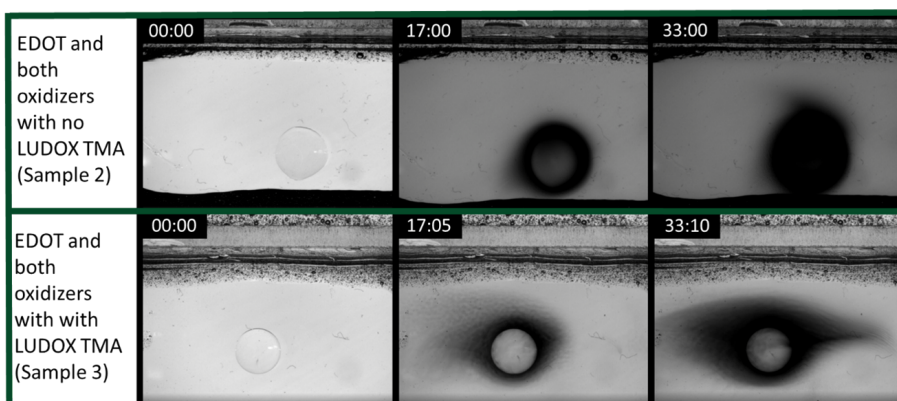


**Fig. C6:** Time intervals of a timelapse of an EDOT droplet in water with  $\text{Na}_2\text{S}_2\text{O}_8$  and  $\text{FeCl}_3$  (sample 2) no Ludox TMA and with Ludox TMA (sample 3).

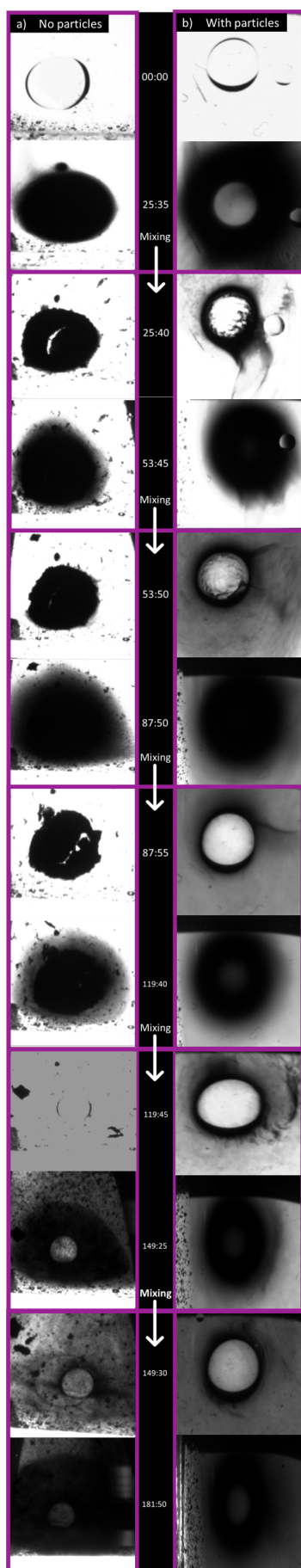


**Fig. C7:** Intervals taken of the time laps here at  $t = 00:00$  (minutes:seconds). After each time interval, the continuous phase is mixed as indicated by the white arrow. And finally new images are taken and the process is repeated. **a)** On the left, no particles are added (sample 6). **b)** On the right there are particles added (sample 7).

## Appendix D - Zeta-potential

The zeta-potential measurements were done with the LUDOX TMA particles and made according to table 6 in chapter 3. First the zeta-potential with the oxidizers were measured to see how these affect the zeta-potential as shown in figure D8. We can see that with only the particles we have, a zeta-potential that goes up when the pH is increased as expected. Here the silica groups get protonated and thus increasing the pH increases the zeta-potential. However, the zeta-potential does not increase to a positive value because of alumina oxide groups in the LUDOX TMA. With the addition of  $\text{Na}_2\text{S}_2\text{O}_8$  the zeta-potential doesn't really change compared to the particles. This could be because of the low amounts of sodium added to the system not having a significant effect on pH.

When the  $\text{FeCl}_3$  is added to the solution, the increase of zeta-potential is more significant. The effect is more significant because of the +3 oxidation state of the iron. The ionic strength here scales quadratically with the oxidation state of such ion thus having a more significant effect on the zeta-potential. This is because iron ions can change aqueous species and thus the oxidation state from soluble  $\text{FeO}_2^-$  (pH 4 - 11) to almost not soluble ( $\text{pH}$  8). And then again to soluble  $\text{FeO}^+$  (pH 5) to  $\text{Fe}^{3+}$  (pH 3 - 2) [45]. This sudden solubility causes aggregation and could explain the difference in curve compared to the Ludox TMA. This explains the significant difference in trend compared to  $\text{Na}_2\text{S}_2\text{O}_8$ .

When the  $\text{Na}_2\text{S}_2\text{O}_8$  and  $\text{FeCl}_3$  are combined, the zeta-potential is lower compared to only  $\text{FeCl}_3$ . This could be because of the decomposition mechanism of the  $\text{Na}_2\text{S}_2\text{O}_8$  and the iron. As mentioned in chapter 2 the iron can be reduced in this mechanism, resulting in charged iron with an oxidation number of +2. This iron ion is also more soluble at higher pH. Also the sodium ions add competition to for the iron ions and could act as a screening agent. Finally, EDOT was added with no oxidizers to confirm that it has no impact on the zeta-potential on its own. The difference compared to the particles is very minimal. There is a slight increase. However, this is not significant enough to say that the EDOT has an impact on the zeta-potential. The EDOT could become dimers and trimers due to an acid catalyzed reaction, which also could explain this increase. However, because of high pH initially and the slow rate constants, this dimer and trimer formation should be limited at lower pH measurements.

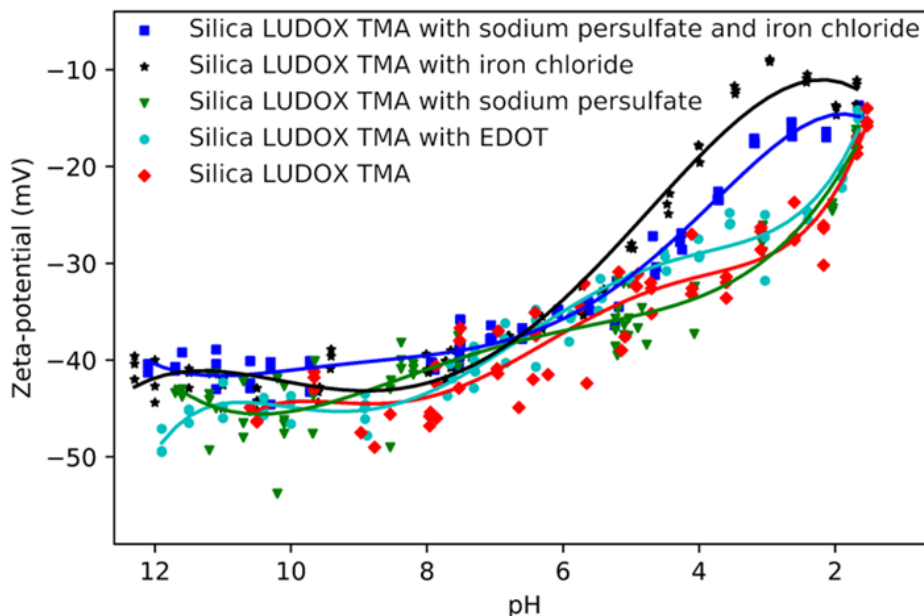


**Fig. D8:** Zeta-potential measurements in function of the pH for: sample 1 ( $\blacklozenge$ ), sample 5 ( $\bullet$ ), sample 6 ( $\star$ ), sample 7 ( $\blacktriangledown$ ) & sample 8 ( $\blacksquare$ ) from chapter 3 table 6.

Assuming the adsorption mechanism of PEDOT is electro-statically the same results could be measured by first polymerizing the EDOT and then adding the silica particles. Unfortunately, both samples with or without CTAB precipitated because of aggregation as shown in figure D9. Both the samples were precipitated, not allowing for a representative zeta-potential measurement. This did not happen to the other samples containing EDOT with (see figure D9a) and without (see figure D9b) CTAB. Here the it has the change to gradually polymerize and adsorb onto the particles. And because samples without particles initially, the EDOT can polymerize longer and thus coil up more and making it easier for nucleation of the particles to happen. This is also shown in the timelapse experiments when no particles are present these big chunks and a hard shell is formed around the droplet. The vigorous stirring might mitigate this a bit, but not as good as the particles can.

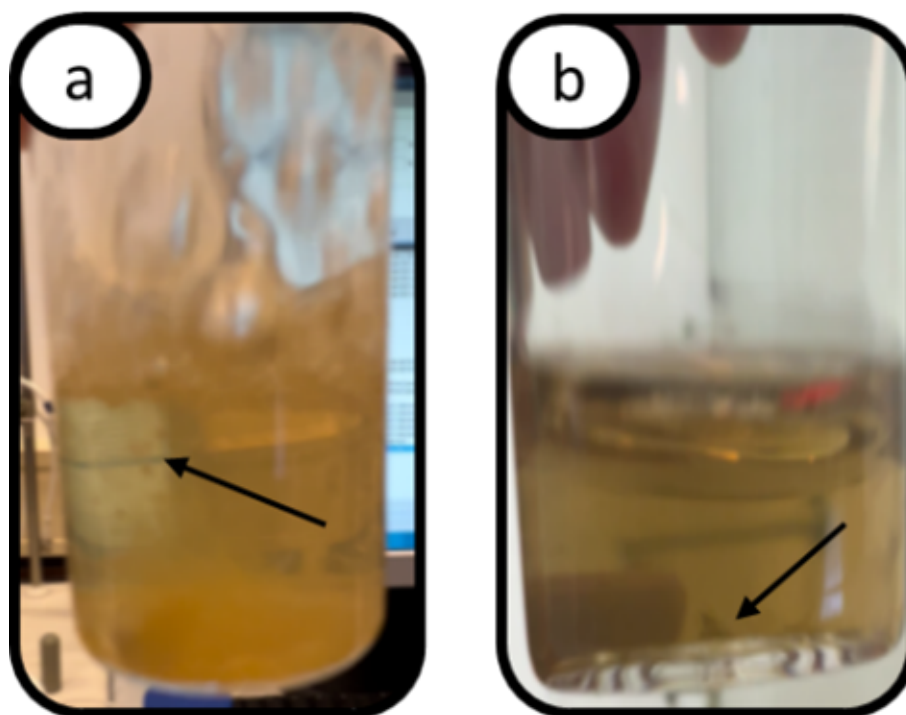


**Fig. D9:** a) Image taken from sample 12 with the arrow pointing to aggregated of particles b) Image taken from sample 11 with the arrow pointing to aggregated of particles

## Appendix E - Dynamic light scattering (DLS)

In this section, the DLS measurements of a few select zeta-potential samples are shown. The number percent value was chosen to show because the measurements of the Ludox TMA measurement are close to the reported value on the bottle. In the figures the mean of the samples are shown, however, these are just an indication because the system forms a bi-disperse system and are not correctly represented as shown in figure E10, E11, E12, E13 & E14. The figures show there is no aggeration outside of the error except for the sample with  $\text{Na}_2\text{S}_2\text{O}_8$  and  $\text{FeCl}_3$  and EDOT with CTAB. Here there is a significant increase of particle size thus verifying that there is aggregation. Unfortunately, not all samples could be measured. However, the most important samples were measured and showed that the salts did not cause significant aggregation and depending on the sample, the polymerization of EDOT did.

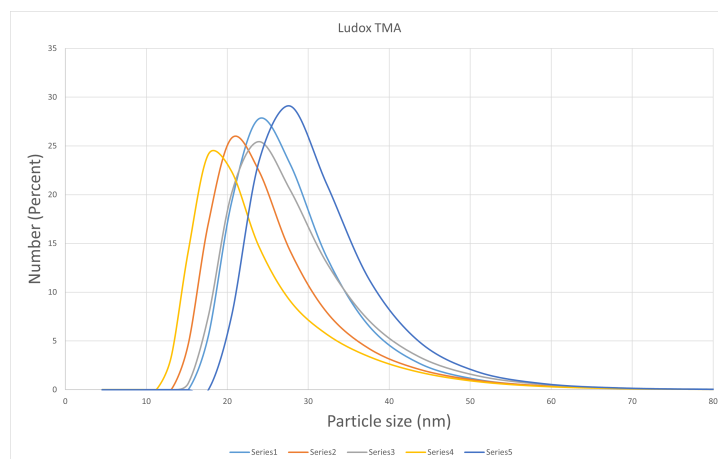


**Fig. E10:** DLS measurement of Ludox TMA with no oxidizers added (sample 1,5), number percentage as function of the particle size. With a mean particle size of  $26.00 \text{ nm} \pm 3.00$ .

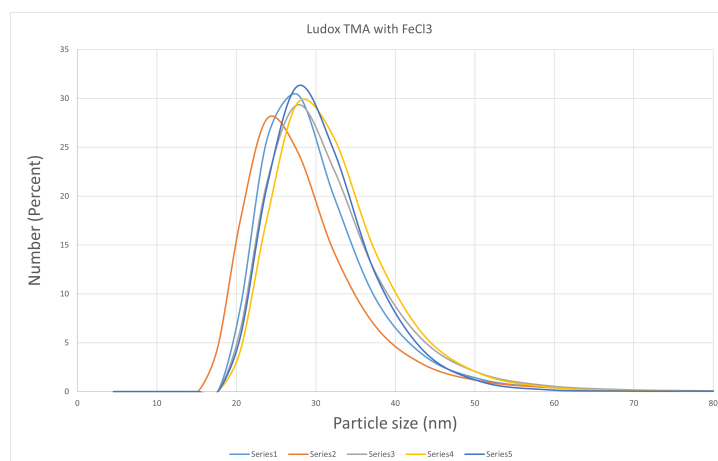


**Fig. E11:** DLS measurement of Ludox TMA with  $\text{FeCl}_3$  no EDOT added (sample 6), number percentage as function of the particle size. With a mean particle size of  $26.34 \text{ nm} \pm 5.35$ .



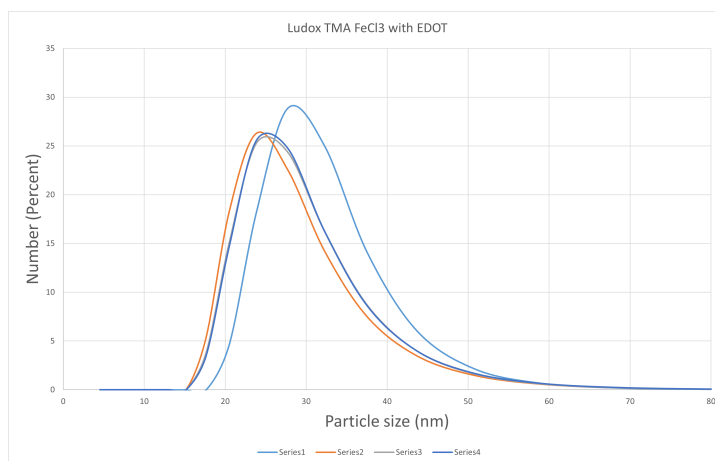


**Fig. E12:** DLS measurement of Ludox TMA with  $\text{FeCl}_3$  with EDOT added (sample 13), number percentage as function of the particle size. With a mean particle size of  $29.47 \text{ nm} \pm 1.43$ .

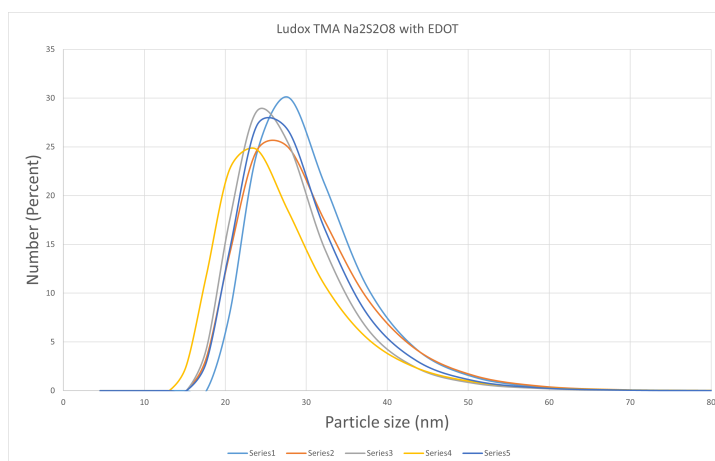


**Fig. E13:** DLS measurement of Ludox TMA with  $\text{Na}_2\text{S}_2\text{O}_8$  with EDOT (sample 3), number percentage as function of the particle size. With a mean particle size of  $27.55 \text{ nm} \pm 1.52$ .

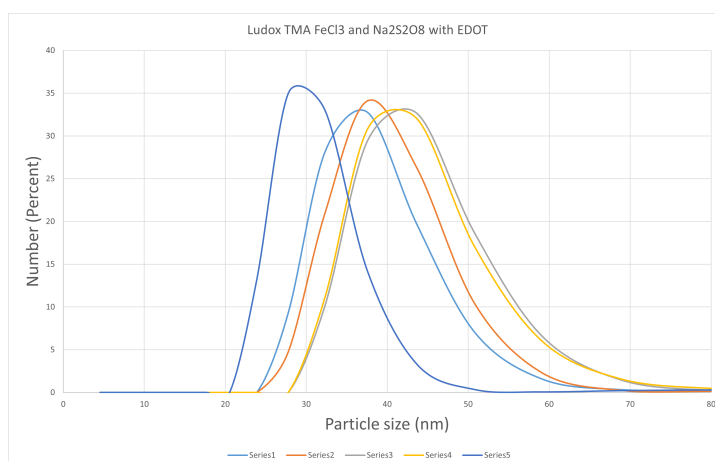


**Fig. E14:** DLS measurement of Ludox TMA with  $\text{Na}_2\text{S}_2\text{O}_8$  and  $\text{FeCl}_3$  with EDOT and CTAB (sample 10), number percentage as function of the particle size. With a mean particle size of  $94.58 \text{ nm} \pm 30.88$ .

## Appendix F - SEM-EDX model system

In this section the EDX spectrum's are shown of the various samples measured of the model system with Stöber Silica (400 nm). All the samples were washed other wise the possible oxidizer that is left crystallizes out after evaporating the water (see figure F15). Sometimes a unlabelled peak is seen at 1.486 keV is seen, this is from the aluminium tray that was used to evaporate the water. The applying of the sample on the carbon tape for the SEM measurement could have cause the aluminium to be transferred onto the sample. When no EDOT is introduced into the system there is no sulfur peak from the  $\text{Na}_2\text{S}_2\text{O}_8$ , confirming that the washing removes enough to not allow this sulfur peak to interfere with the sulfur peak of PEDOT. The sulfur peak is clearly shown in the samples were PEDOT should be polymerized using the oxidators. Here a clear  $\text{K}\alpha$  (2.307 keV) and  $\text{K}\beta$  (2.45 keV) from the sulfur is shown. The only peak that has the same keV as sulfur is Molybdenum peak which is not in the system.

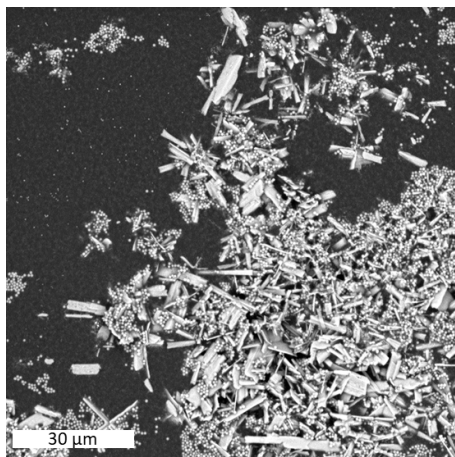


**Fig. F15:** EDX spectrum of Stöber Silica particles with  $\text{Na}_2\text{S}_2\text{O}_8$  not washed with water and ethanol (sample 2).

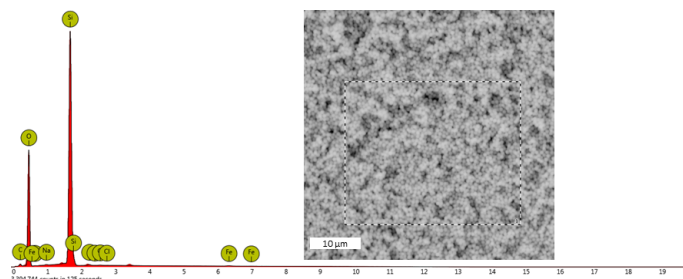


**Fig. F16:** EDX spectrum of Stöber Silica particles with  $\text{Na}_2\text{S}_2\text{O}_8$  and  $\text{FeCl}_3$  (sample 2).

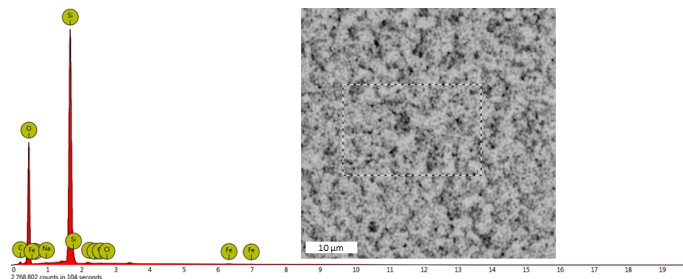


**Fig. F17:** EDX spectrum of Stöber Silica particles with  $\text{FeCl}_3$  (sample 3).

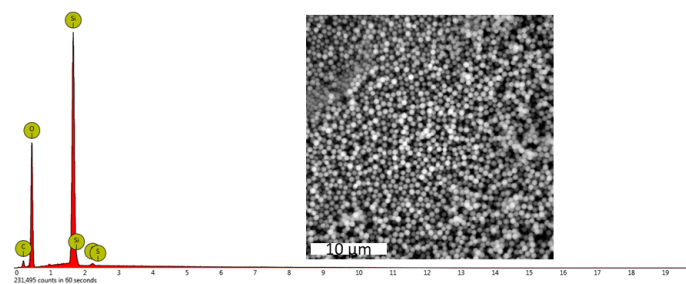


**Fig. F18:** EDX spectrum of Stober Silica particles with  $\text{Na}_2\text{S}_2\text{O}_8$  (sample 4).

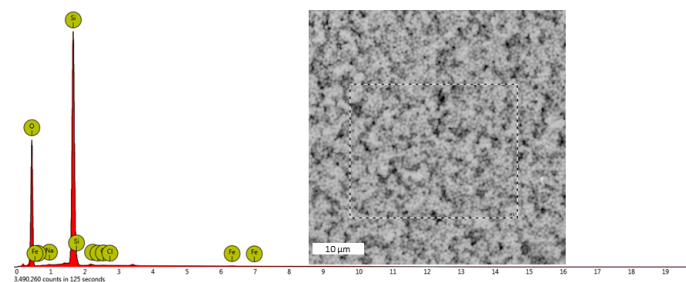


**Fig. F19:** EDX spectrum of Stober Silica particles (sample 1).

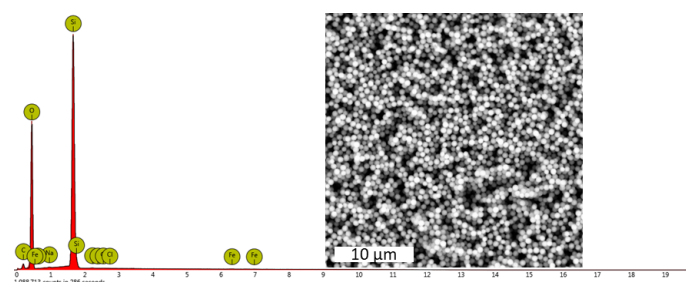


**Fig. F20:** EDX spectrum of Stober Silica particles with EDOT (sample 5).

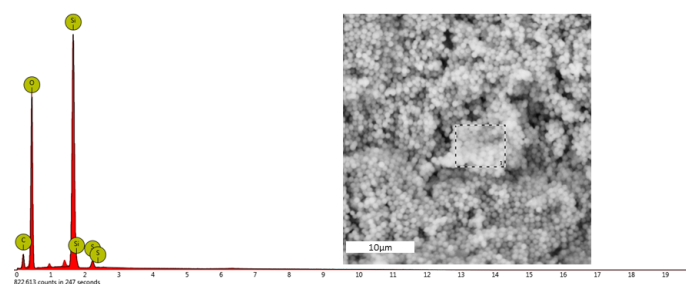


**Fig. F21:** EDX spectrum of Stober Silica particles with  $\text{FeCl}_3$  and EDOT (sample 8).

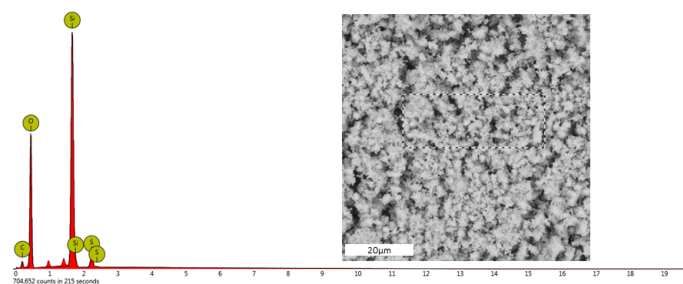


**Fig. F22:** EDX spectrum of Stober Silica particles with  $\text{Na}_2\text{S}_2\text{O}_8$  and EDOT (sample 7).

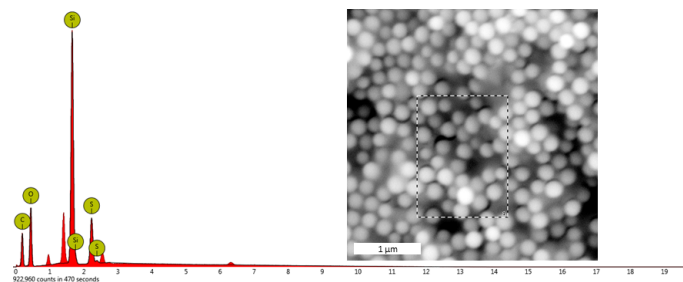


**Fig. F23:** EDX spectrum of Stober Silica particles with  $\text{Na}_2\text{S}_2\text{O}_8$  and  $\text{FeCl}_3$  and EDOT (sample 6).

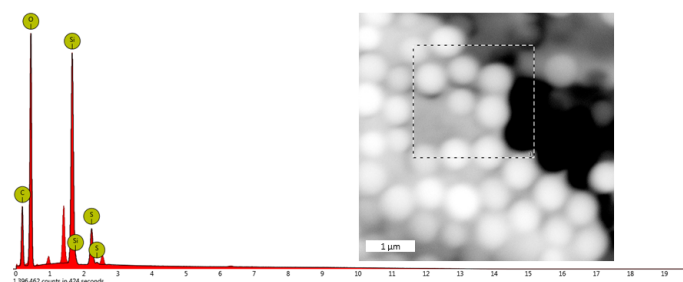


**Fig. F24:** EDX spectrum of Stober Silica particles with  $\text{Na}_2\text{S}_2\text{O}_8$  and  $\text{FeCl}_3$  and EDOT (sample 6).

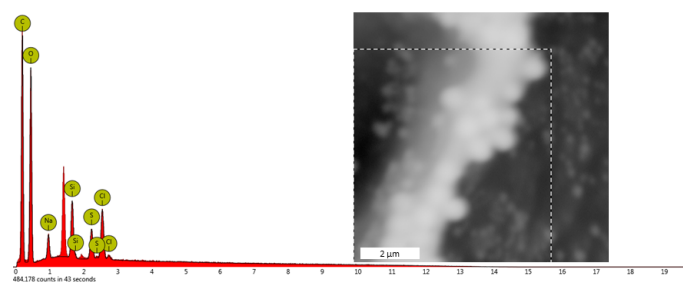


**Fig. F25:** EDX spectrum of Stober Silica particles with  $\text{Na}_2\text{S}_2\text{O}_8$  and  $\text{FeCl}_3$  and EDOT (sample 6). EDOT was polymerized first and the Stober Silica was added later.

## Appendix G - Initial results for PEDOT introduction

In this section the results that were found initially will be discussed. To introduce PEDOT into a bijel the first idea was to use EDOT as the oil component for the precursor dispersion. This would allow for a bijel to be formed with the water channels being surrounded by the EDOT oil. Because the monomer is already in the bijel it would in theory be very easy to polymerize and thus introduce PEDOT into a bijel. First, a ternary phase diagram was measured with 1-propanol, EDOT and water (see figure G26). The binodal was determined by changing the composition and seeing where the solution goes from clear to cloudy. To make a bijel the critical point has to be determined. Here the circles in figure G26 show the compositions that were investigated. This was done by making the compositions and adding Nile red allowing for the water (black) and oil (red) phase to be separated visually. The green circle shows that the oil is in the water and the water is in the oil suggesting that the composition is around  $\varphi_{\text{EDOT}} = 0.51$ ,  $\varphi_{\text{1-propanol}} = 0.43$  &  $\varphi_{\text{water}} = 0.06$ . This would not allow for a high weight percentage of Ludox TMA to be added to the precursor dispersion. The particles could be added to the solvent. Unfortunately, this is not possible with 1-propanol. Therefore, different solvents such as ethanol, 1-pentanol & 2-propanol were investigated (see figure G27). Here with 1-pentanol the ternary switches from oil in water to water in oil. This suggests that the critical point has shifted to a more water-rich phase. Unfortunately, 1-pentanol is not miscible with the continuous phase, which is water in this case. If the solvent is not miscible with the continuous phase spinodal decomposition could not take place and thus a bijel could not be formed.

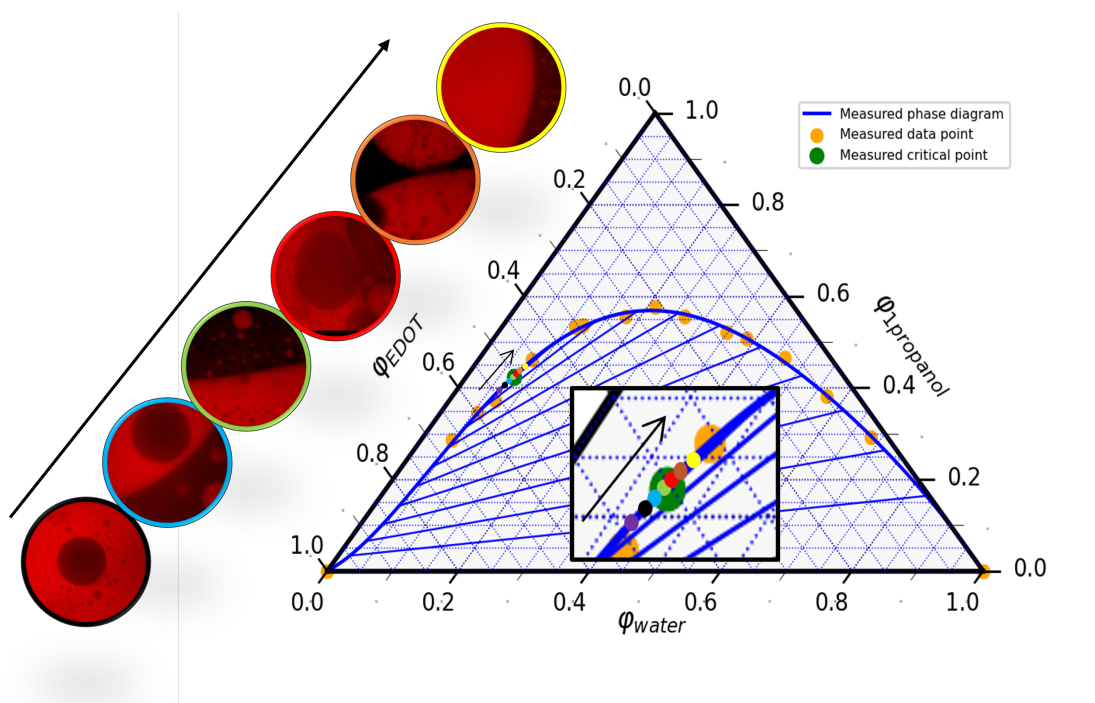


**Fig. G26:** Ternary phase diagram of EDOT, 1-propanol and water with the polynomial binodal line based on the measured points. The critical point was determined by the images shown in the circle which correspond to the circles on the binodal line in the insert.

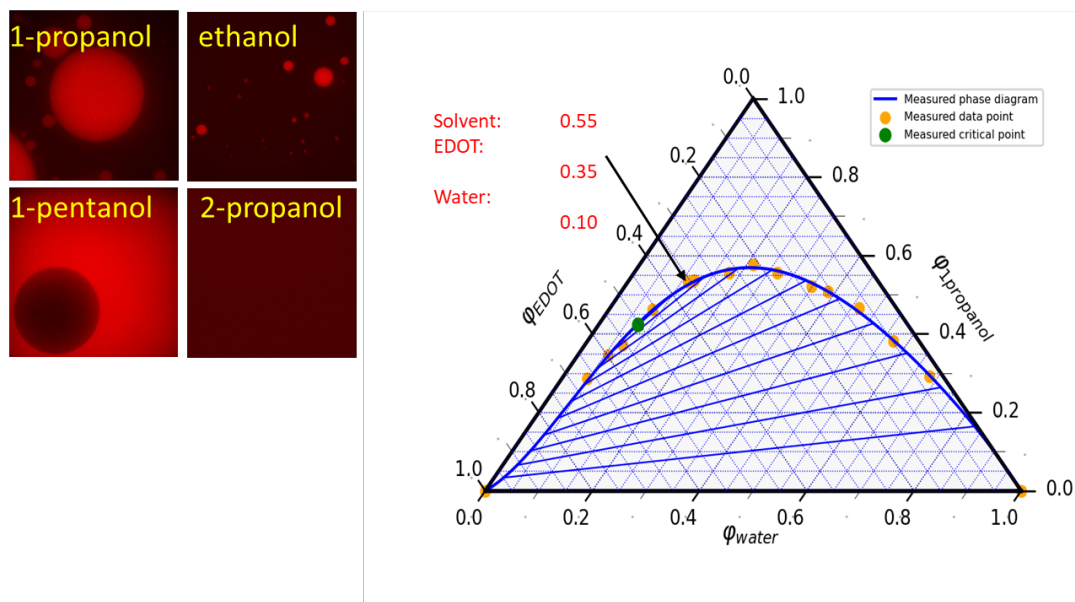


**Fig. G27:** Ternary phase diagram of EDOT, 1-propanol and water with the effect of ethanol, 1-pentanol, 2-propanol to the composition (indicated with the arrow and red text).

To add enough particles to precursor dispersion ethanol could be used. The particles were prepared in water and the water was swapped with ethanol through dialysis. First, the ternary phase diagram was measured with ethanol (see figure G28). The same procedure for 1-propanol was used to get this ternary phase diagram. As shown at the green dot the critical point is located at  $\varphi_{\text{EDOT}} = 0.60$ ,  $\varphi_{\text{ethanol}} = 0.35$  &  $\varphi_{\text{water}} = 0.05$ . Here the image associated with the critical point shows two images in two different z-axis locations. Because of the density it was not possible to show the oil in the water and the water in the oil in one picture. Because so limited water could be added without crossing the binodal line causing phase separation. The CTAB concentration parameter study was done with only EDOT and ethanol (see figure G29). From this it was determined that the optimal pH was 2 and that the CTAB concentration should be below 130 mM. There for, the CTAB concentration range of 60 mM - 120 mM was investigated (see figure G30). The bijel extrusion was done with two CTAB concentrations 100 mM and 120 mM and two coatings (see figure G31). This resulted in no clear bicontinuous structure the PDADMAC coating allowed for a homogeneous distribution of EDOT through the fiber. However, there are no indications of a bicontinuous structure. Because of the difficult challenge, this approach was abandoned and instead the approach in this research was chosen. Here using a precursor dispersion of a known system that works and then introducing the EDOT/PEDOT.

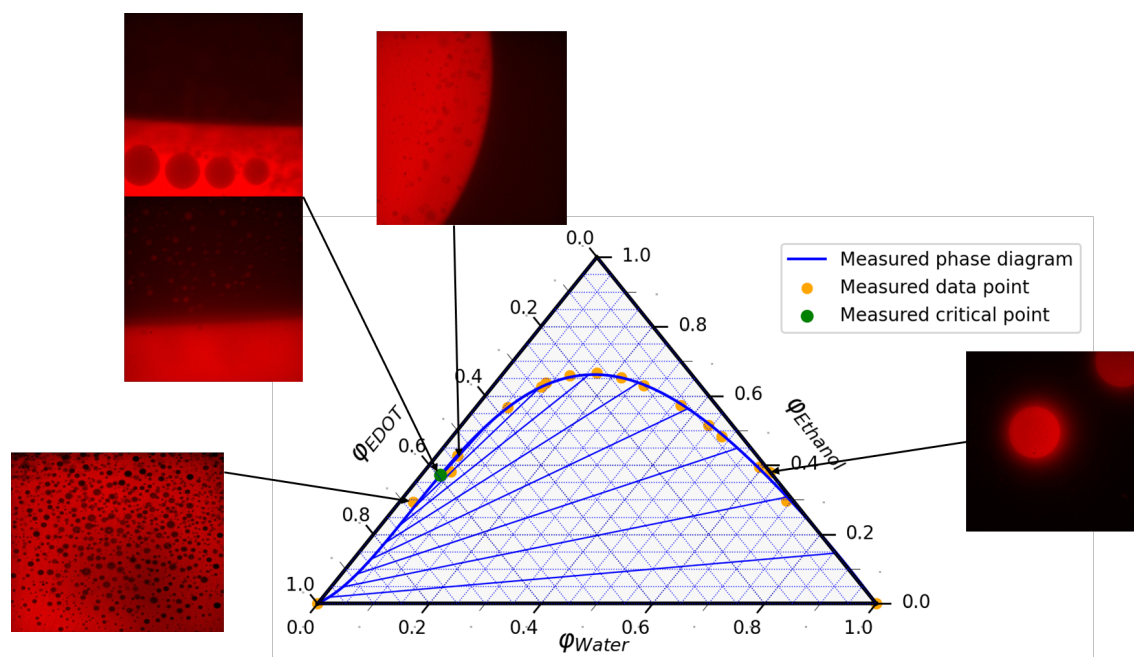


**Fig. G28:** Ternary phase diagram of EDOT, ethanol and water with the polynomial binodal line based on the measured points. With the images pointing to the compositions used.

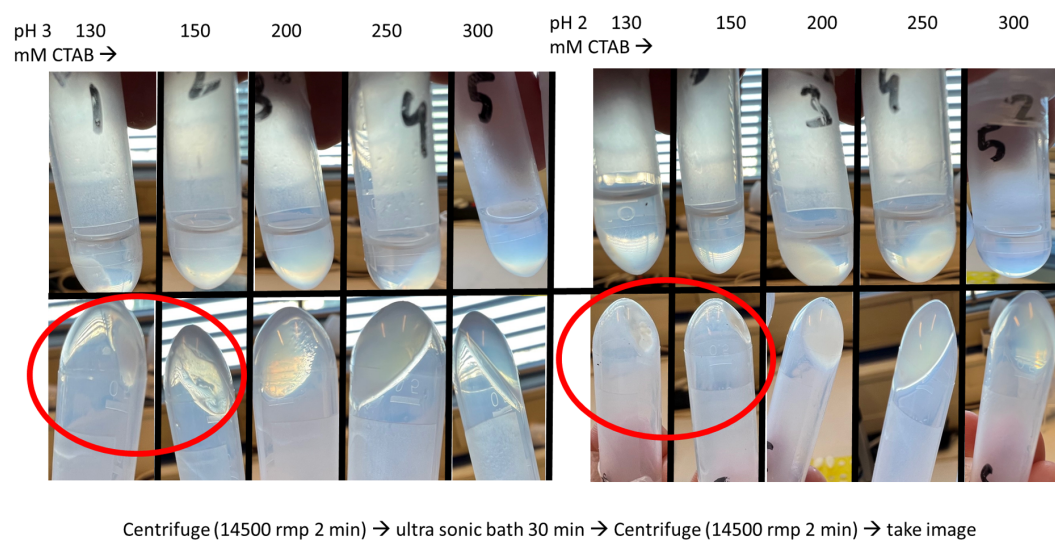


**Fig. G29:** Images of the critical point composition of EDOT, ethanol and water with various CTAB concentrations at pH 2 and 3.

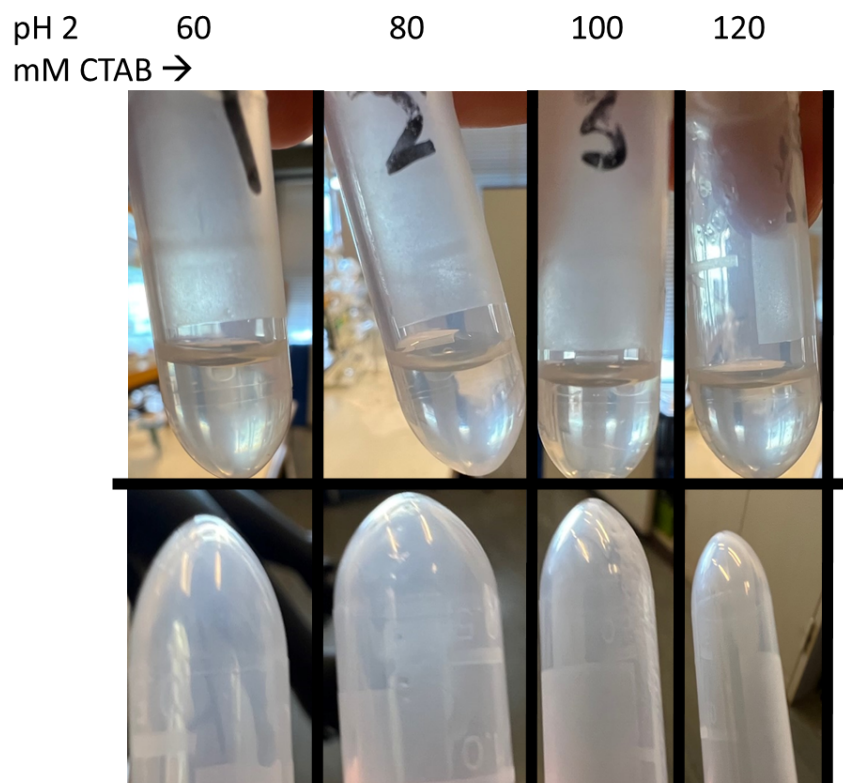


**Fig. G30:** Images of the critical point composition of EDOT, ethanol and water with various CTAB concentrations at pH 2.

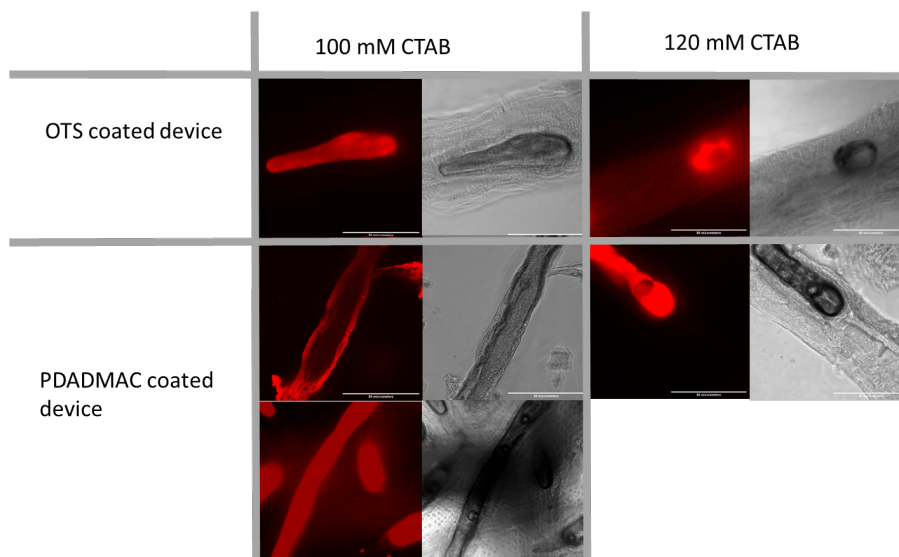


**Fig. G31:** Images of the critical point composition of EDOT (red), ethanol and water (black) with various CTAB concentrations at pH 2 and 3.



## Appendix H - SEM images of confocal bijel fibers

In this section all the SEM images of the confocal analyzed images are shown. All the bijels contain  $\text{Na}_2\text{S}_2\text{O}_8$  in the water phase. The bijel fibers without  $\text{FeCl}_3$  in the continuous phase are shown in figure H32. And the bijel fibers with  $\text{FeCl}_3$  in the continuous phase are shown in figure H32. Here the bijel shows no significant change over time for both figures. All samples show collapsed oil channels. Even though, the bijels are not completely collapsed, there was not enough PEDOT to keep the oil channels open.

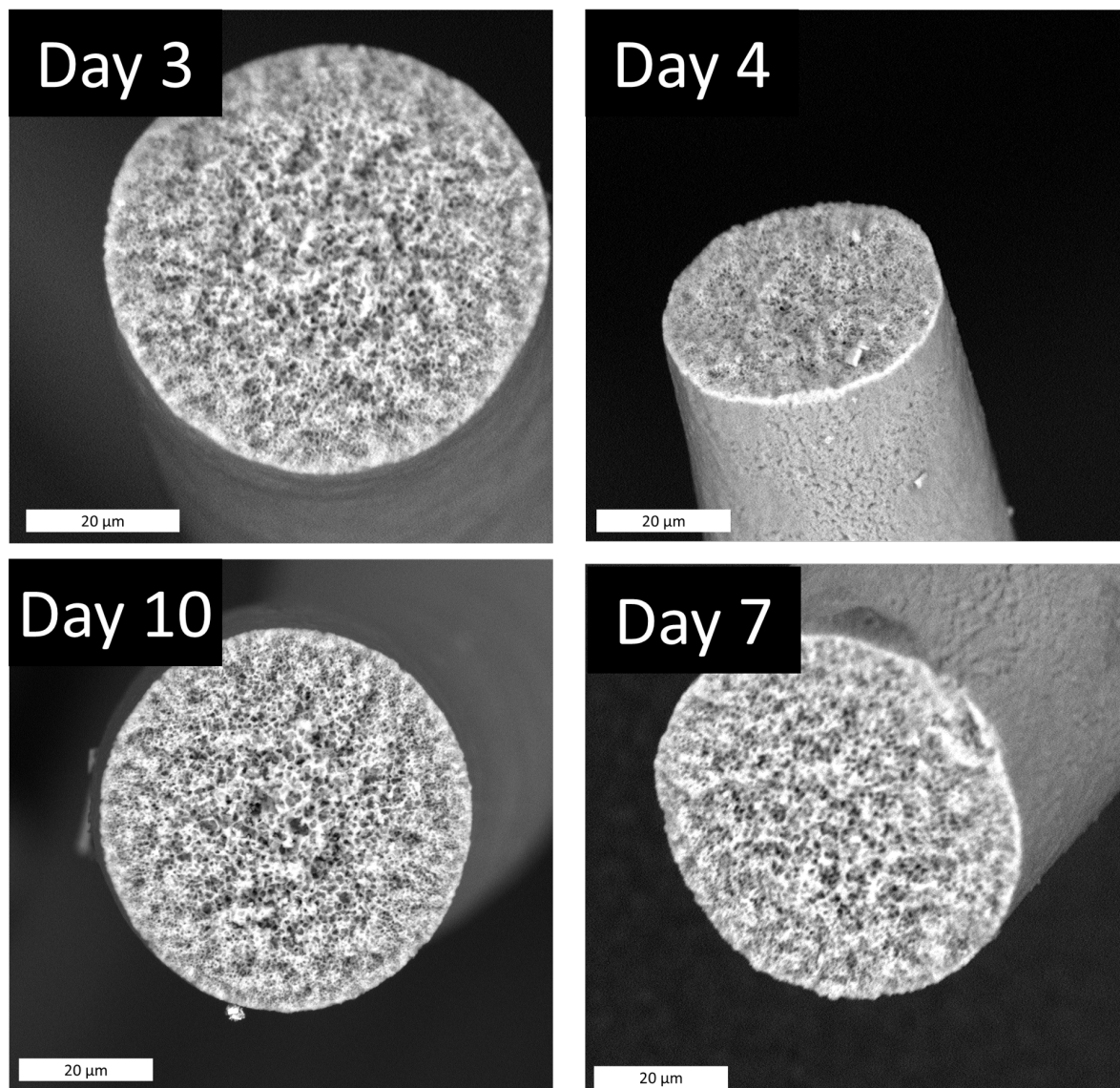


**Fig. H32:** Bijel fibers analyzed with SEM at 10 kV with the scale bar being 20 micrometers ( $\mu\text{m}$ ). The fibers were the same fibers analyzed under the confocal containing  $\text{Na}_2\text{S}_2\text{O}_8$  in the water phase of the bijel. (See chapter 4 figure 31).

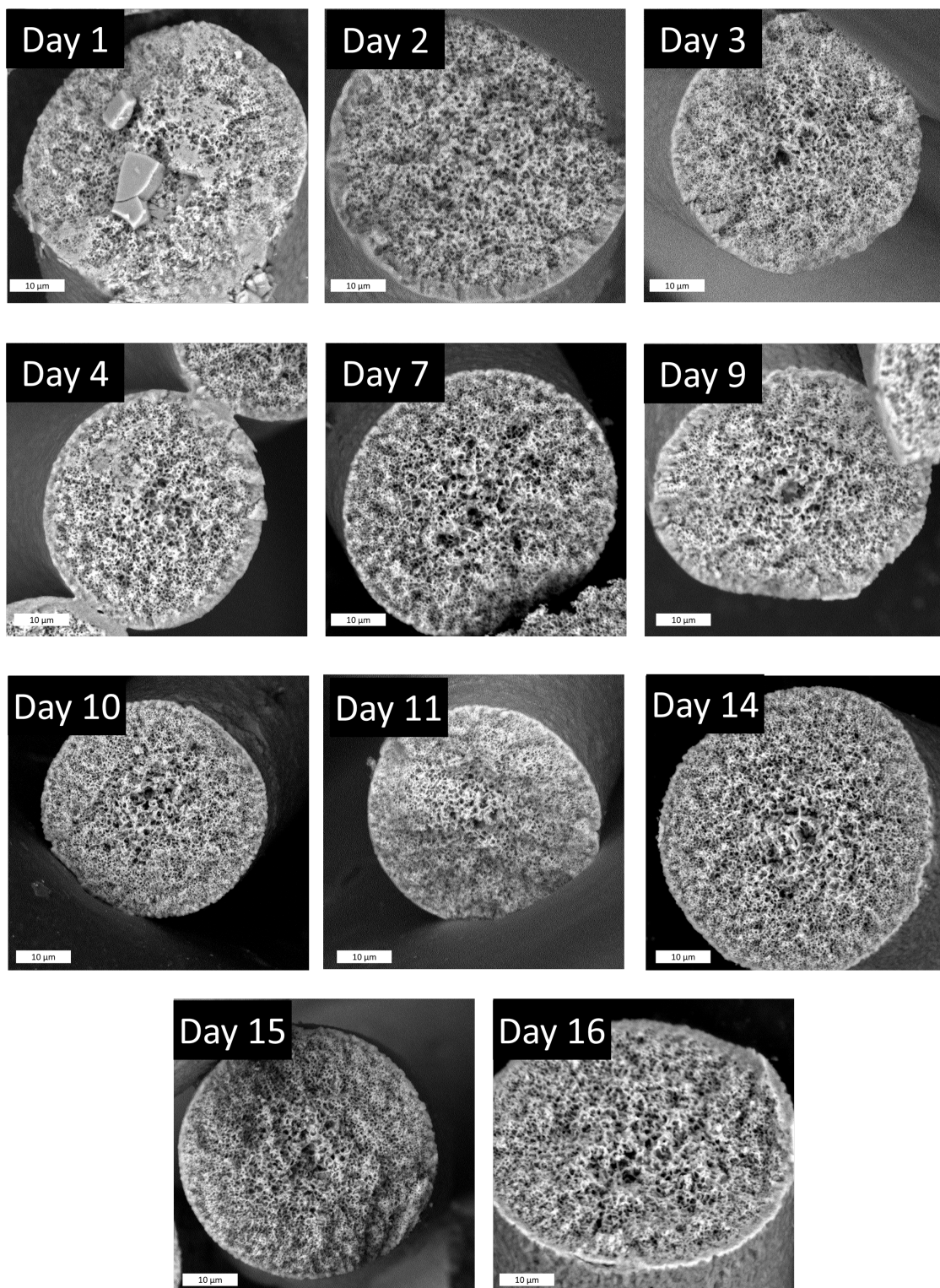


**Fig. H33:** Bijel fibers analyzed with SEM at 10 kV with the scale bar being 10 micrometers ( $\mu\text{m}$ ). The fibers were the same fibers analyzed under the confocal containing  $\text{Na}_2\text{S}_2\text{O}_8$  in the water phase of the bijel and  $\text{FeCl}_3$  in the continuous phase. (See chapter 4 figure 31).

## Appendix I - Conductivity measurements

In this section the calculations made for the conductivity measurements are discussed. Also, the solubility of the continuous phase polymerization of PEDOT is discussed. Finally, the pictures of the fibers after the polymerization with increasing  $\text{Fe(III)(OTs)}_3$  concentration in the continuous phase of toluene are shown (see figure I34a). The addition of  $600 \mu\text{L}$  allows the  $\text{Fe(III)(OTs)}_3$  to be soluble (see figure I34b). A higher concentration of  $\text{Fe(III)(OTs)}_3$  could not be achieved because of solubility restrictions. However, this could not be visually imaged further research would be needed to see how to reach the maximum solubility of  $\text{Fe(III)(OTs)}_3$  in toluene or any other oil.

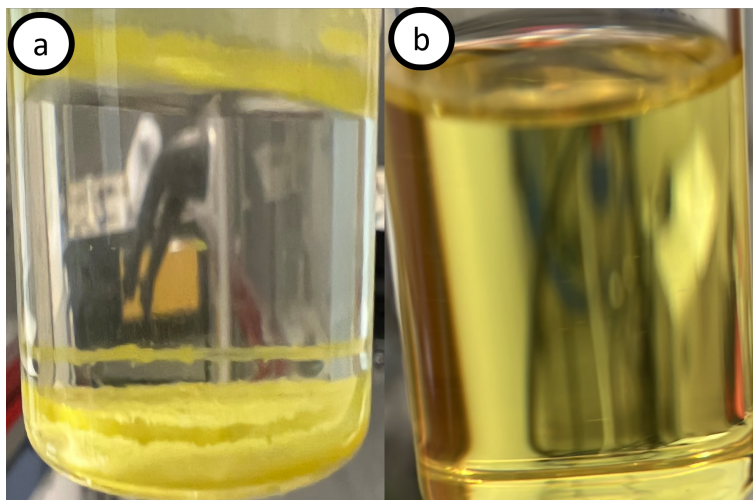


**Fig. I34:** a)  $100\text{mg Fe(III)(OTs)}_3$  in  $20\text{ mL}$  toluene stirred for 48 hours. b)  $100\text{mg Fe(III)(OTs)}_3$  in  $20\text{ mL}$  toluene with  $600 \mu\text{L}$  of 1-pentanol ( $5\text{ mg/ml}$ ).

If an external voltage ( $V$ ) was used such as a 9-volt battery the current ( $I$ ) could be measured and using equation I1 the resistance ( $R$ ) could be calculated. Here a second voltage meter was used to measure the actual voltage over the system, which is a bit higher than 9 volt. If the voltcraft<sup>®</sup> was used the resistance was read from the voltcraft<sup>®</sup> itself, which uses a small voltage to measure the current. The surface area of the fiber ( $A$ ) times the amount of fibers ( $x$ ) divided by the length ( $L$ ) between the electrodes times the resistance results in the electrical resistivity ( $\rho$ ) (see equation I2). The inverse of the electrical resistivity results in the electrical conductivity ( $\sigma$ ) (see equation I3).

$$R = VI \quad (\text{I1})$$

$$\rho = R \frac{xA}{L} \quad (\text{I2})$$

$$\sigma = \frac{1}{\rho} \quad (\text{I3})$$